Varsayımsal Bir Hücre Tipi Ofis İçin Farklı Uyarlanabilir Cephe Sistemlerinin Günışığı ve Enerji Performansının Değerlendirilmesi

Muhammed Kabir Musa

YÜKSEK LİSANS TEZİ

Mimarlık Anabilim Dalı

Haziran 2021

Evaluating the Daylight and Energy Performance of Different Adaptive Facade Systems for a Hypothetical Cell-Type Office Unit

Muhammed Kabir Musa

MASTER OF SCIENCE THESIS

Department of Architecture

June 2021

Evaluating the Daylight and Energy Performance of Different Adaptive Facade Systems for a Hypothetical Cell-Type Office Unit

A thesis submitted to the Eskişehir Osmangazi University
Graduate School of Natural and Applied Sciences in partial
fulfillment of the requirements for the degree of Master of Science
in Discipline of Building Science of the Department of Architecture
by

Muhammed Kabir MUSA

Supervisor: Assoc. Prof. Dr. Başak GÜÇYETER
June 2021

ETHICAL STATEMENT

I hereby declare that this thesis study titled “Evaluating the Daylight and Energy Performance of Different Adaptive Facade Systems for a Hypothetical Cell-Type Office Unit” has been prepared in accordance with the thesis writing rules of Eskişehir Osmangazi University Graduate School of Natural and Applied Sciences under academic consultancy of my supervisor Assoc. Prof. Dr. Başak Güçyeter. I hereby declare that the work presented in this thesis is original. I also declare that, I have respected scientific ethical principles and rules in all stages of my thesis study, all information and data presented in this thesis have been obtained within the scope of scientific and academic ethical principles and rules, all materials used in this thesis which are not original to this work have been fully cited and referenced, and all knowledge, documents and results have been presented in accordance with scientific ethical principles and rules. 23/06/2021

Muhammed Kabir MUSA

ÖZET

Ofis mekanlarında yeterli gün ışığı seviyesinin sağlanması son yıllarda önemli araştırma konularından biri olarak ele alınmaktadır. Yeterli gün ışığı, enerji verimliliği ve iyileştirilmiş kullanıcı konforuna yönelik olarak yapı kabuğunda farklı yaklaşım ve stratejiler önem kazanmaktadır. Yapı kabuğu iç ve dış ortamı birbirinden ayırmakta olan bir ara yüzdür ve mekandaki gün ışığı seviyelerini ve bina kullanıcılarının konforunu optimize etme amacıyla uyarlanabilir yaklaşımlarla donatılma yeteneğine sahiptir.

Bu tez çalışması, çeşitli geometri ve hareket türlerinden oluşan uyarlanabilir cephe sistemlerini varsayımsal hücre tipi bir ofis hacmi üzerinden simülasyon yöntemiyle değerlendirilmesine odaklanmaktadır. Tasarlanan uyarlanabilir cephe bileşenleri ile varsayımsal hücre tipi ofisin gün ışığı seviyeleri, görsel performansı ve enerji performansı simülasyon yöntemi ile değerlendirilmiştir. Simülasyondan elde edilen sonuçlar gün ışığı seviyeleri, görsel konfor ve enerji performansı bağlamında karşılaştırılmış ve analiz edilmiştir. Sekiz uyarlanabilir cephe sistemi (UCS) iki ve üç boyutlu geometrik konfigürasyonlar üzerinden sınıflandırılmış ve sümülasyon çalışmaları Rhino, Grasshopper, Energy Plus ve DIVA for Rhino aracılığıyla yürütülmüştür. Simülasyon sonuçları, dairesel üç boyutlu UCS hariç, üç boyutlu geometriye sahip UCS'lerin günışığı simülasyonları bakımından daha iyi performans gösterdiğini ortaya koymuştur. Hem iki hem de üç boyutlu UCS'nin parlama kontrolü bakımından etkin olduğu saptanmıştır. Ayrıca, tüm UCS'ler baz durum modelinin (referans ofisi) enerji kullanım yoğunluğunu indirgemiştir. Bu çalışmanın bulguları, uyarlanabilir cephe sistemlerinin (UCS) bina performansı ve kullanıcı konforu üzerindeki önemini ve tasarım aşamasında bina performans değerlendirmesinin önemine vurgu yapmaktadır.

Anahtar Kelimeler: Adaptif cephe sistemi, Gün ışığı aydınlatması, Güneş kazançları, Ofis birimi

SUMMARY

The quest for adequate daylight levels in office spaces is an advancing research domain of the last decades. Novel concepts and strategies for building envelopes were proposed to achieve adequate daylight levels, energy efficiency, and improved occupant comfort. The building envelope is the interface that links the indoor and outdoor environment and has the ability to be equipped with adaptive approaches to optimize the daylight levels and occupant comfort in the building.

The present study focuses on simulating a hypothetical cell-type office building that incorporates adaptive façade systems composed of several types of geometries and motion. Daylight levels, visual performance, and the energy performance of the hypothetical cell-type office with the designed adaptive façade components were investigated via simulation. The results retrieved from the simulations were compared and analyzed in the context of daylight levels, visual comfort, and energy performance. Eight adaptive façade systems (AFSs) were classified into 2D and 3D geometric configurations and were simulated via Rhino, Grasshopper, Energy Plus, and DIVA for Rhino. The simulation outcomes indicated that AFSs with 3D geometry performed better for Daylight simulations, except the 3D Circular AFS. Glare management was mostly efficient both for 2D and 3D AFSs. Furthermore, all AFSs reduced the energy use intensity (EUI) of the base case model (reference office). The findings of the present study highlighted the significance AFSs have on building performance and occupant comfort, and the importance of conducting building performance evaluations during the design phase.

Keywords: Adaptive façade systems, Daylighting, Solar gains, Office unit

LIST OF CONTENTS

Page

ÖZET …….. vi
SUMMARY ……... vii
ACKNOWLEDGEMENT …….. viii
LIST OF CONTENTS ……... ix
LIST OF FIGURES ……... xi
LIST OF TABLES ……... xiii
LIST OF ABBREVIATIONS and SYMBOLS ……... xv
1. INTRODUCTION AND PURPOSE …… 1
2. LITERATURE REVIEW …… 7
2.1 Adaptive Façades …… 7
2.1.1 Definitions of Adaptive Façades ……... 10
2.1.2 Emergence and Development ……... 12
2.1.3 Adaptive Façade Classifications ……... 17
2.1.4 Adaptive Facades for Energy Efficiency ……... 23
2.2. Daylighting …….. 26
2.2.1. Basic Daylight Characteristics …… 27
2.2.2. Daylighting for Commercial Office Buildings …… 32
2.3. Solar Gains in Buildings …….. 35
3. MATERIALS AND METHODS …… 37
3.1. Definition of the Hypothetical Model …… 38
3.1.1. Base Case Model Design …… 38
3.1.2. Boundary Conditions of the Base Case Model …… 40
3.1.3. Sample Climatic Condition …….. 42
3.2. Design of the Adaptive Façade Components …….. 43
3.2.1. 2D Geometry and Motion Characteristics for Adaptive Façade Components ..44
3.2.2. 3D Geometry and Motion Characteristics for Adaptive Façade Components ..46
3.3. Simulation Model Setup …….. 49
3.3.1. Script Development for Adaptive Façade Components in Grasshopper …….49
3.3.1.1. 2D Circular Adaptive Façade System …… 50

LIST OF CONTENTS (continued)

Page

3.3.1.2. 3D Circular Adaptive Façade System …… 51
3.3.1.3. 2D Triangular Adaptive Façade System …… 51
3.3.1.4. 3D Triangular Adaptive Façade System …… 52
3.3.1.5. 2D Diamond Adaptive Façade System ……... 52
3.3.1.6. 3D Diamond Adaptive Façade System ……... 53
3.3.1.7. 2D Square Adaptive Façade System ……... 54
3.3.1.8. 3D Square Adaptive Façade System ……... 54
3.3.2. Definition of the Operation Algorithms in DIVA for Rhino …… 55
3.3.3. Definition of Radiance Based Simulation Parameters …… 61
3.3.4. Definition of EnergyPlus Based Simulation Parameters …….. 63
3.4. Simulation of the Hypothetical Cell-Type Office Unit …… 64
3.4.1. Daylight Simulations ……... 64
3.4.2. Thermal Simulations …… 66
4. RESULTS AND DISCUSSION …… 67
4.1. Annual Glare Simulation Results …… 67
4.2. Daylight Autonomy Simulation Results ……. 79
4.3. Electric Lighting Simulation Results ……... 83
4.4. Shading Control Results …….. 87
4.5. Thermal Simulation Results …… 89
4.5.1. Monthly Energy Use …… 89
4.5.2. Heating and Cooling Energy Consumption …….. 92
4.5.3. Energy use intensity (EUI) ……... 94
5. CONCLUSION AND RECOMMENDATIONS …….. 98
REFERENCES ……..... 100

LIST OF FIGURES

Figure **Page**

1.1. Thesis structure ……... 5
2.1. Façade functions ……. 9
2.2. The interior of Rietveld Schröder House by Gerrit Thomas Rietveld …….. 11
2.3. MVRDV, Ypenburg 'VINEX' development …… 11
2.4. Aluminum louvers on south façade of Los Angeles County Hall of Records …….. 13
2.5. Buckminster Fuller's façade ……. 13
2.6. The Polyvalent Wall by Mike Davies ……... 14
2.7. Capricorn House, Düsseldorf. …….. 15
2.8. BIX Communicative Display Skin for the Kunsthaus Graz ……. 15
2.9. Kinetic façade that regulates sunlight and illumination in Arab World Institute, Jean Nouvel ……. 16
2.10. The responsive facade that reduces solar gain and glare, Aedas Architects …….. 16
2.11. Adaptive facades classification based on various control technologies …… 17
2.12. Kinetic Facades main and sub-Categories …….. 17
2.13. Typology of adaptive Façade systems …… 18
2.14. Overview of characterization concepts for envelope adaptivity ……. 19
2.15. The visible part of the electromagnetic spectrum ……... 27
2.16. The components of daylight …… 28
2.17. Schematic diagram showing the interaction between fenestration solar gains and daylighting……. 35
3.1. Steps of the thesis methodology …… 37
3.2. Shoebox geometry and heat transfer setup per surface ……. 39
3.3. The floor plan showing the furniture layout of the reference office ……. 39
3.4. South façade of reference office and sectional view of Reference office …… 40
3.5. Seven climate zones recognized by Building America in the continental US …….. 42
3.6. 2D circular adaptive façade system script developed in Grasshopper …….. 50
3.7. 3D circular adaptive façade system script developed in Grasshopper …….. 51
3.8. 2D Triangular adaptive façade system script developed in Grasshopper ……. 52
3.9. 3D Triangular adaptive façade system script developed in Grasshopper ……. 52

LIST OF FIGURES (continued)

Figure **Page**

3.10. 2D Diamond adaptive façade system script developed in Grasshopper ……. 53
3.11. 3D Diamond adaptive façade system script developed in Grasshopper ……. 53
3.12. 2D Square adaptive façade system script developed in Grasshopper ……. 54
3.13. 3D Square adaptive façade system script developed in Grasshopper ……. 54
3.14. Operation algorithm for the Adaptive Façade Systems ……. 55
3.15. Operation algorithm for Electrical Lighting ……. 57
3.16. Plan showing occupant work plane ……. 65
3.17. The geometry of reference office (a) Base case model (b) Energy model …….. 66
4.1. Base case (Reference office) Daylight autonomy simulation ……. 79
4.2. Reference Office Point in time visualization ……. 80
4.3. Reference Office false-color illuminance map ……. 80
4.4. Compiled results of Daylight autonomy and glare simulations ……. 83
4.5. Lighting strategies employed in the study, (a) single group lighting coverage, (b) split group lighting strategy ……. 84
4.6. Manual control on/off switch ……. 84
4.7. Office illumination through electric lights ……. 87
4.8. False color map of the office ……. 87
4.9. Heating, cooling, and lighting energy consumption ……. 94
4.10. Energy Use Intensity (EUI) of the AFSs ……. 97

LIST OF TABLES

Table **Page**

2.1. Examples for adaptive façade materials 20

2.2. Examples for adaptive façade components 21

2.3. Examples for adaptive façade systems 22

2.4. Adaptive façades for energy efficiency in buildings 24

2.5. Daylighting studies for office buildings as an energy-saving strategy 34

3.1. Shoebox cell-type office model materials and their properties 41

3.2. Materials used for thermal simulation 41

3.3. 2D Circle geometry and motion features 44

3.4. 2D Triangle geometry and motion features 45

3.5. 2D Diamond geometry and motion features 45

3.6. 2D Square geometry and motion features 46

3.7. 3D Circle geometry and motion features 47

3.8. 3D Triangle geometry and motion features 48

3.9. 3D Diamond geometry and motion features 48

3.10. 3D Square geometry and motion features 49

3.11. Shading control and shading states of 2D and 3D AFSs 58

3.12 Radiance simulation parameters 61

3.13 Electric lighting fixture details 61

3.14 Recommended light levels and lighting power density by space 62

3.15 Parameters for EnergyPlus based simulation 64

4.1 Glare study for all work planes 69

4.2 Annual glare simulation (2D Circular façade system) 70

4.3 Annual glare simulation (3D Circular Facade system) 71

4.4 Annual glare simulation (2D Triangular Facade system) 72

4.5 Annual glare simulation (3D Triangular Facade system) 73

4.6 Annual glare simulation (2D Diamond facade system) 74

LIST OF TABLES (continued)

Figure **Page**

4.7 Annual glare simulation (3D Diamond facade system) 75

4.8 Annual glare simulation (2D Square facade system) 76

4.9 Annual glare simulation (3D Square facade system) 77

4.10 Annual glare simulation with shading 78

4.11 Daylight autonomy simulations and glare percentages 81

4.12 Artificial lighting studies 85

4.13 Shading control schedule 88

4.14 Monthly energy use 90

4.15 Heating and cooling energy consumption 92

LIST OF ABBREVIATIONS and SYMBOLS

Symbols	**Descriptions**
E_v	Vertical eye illuminance
$L_{s, I}$	Luminance of source
ω_s, I	Solid angle of source l
P	Guth position index
°C	Degree Celsius

Abbreviations	**Descriptions**
3D	Three-Dimensional
2D	Two-Dimensional
AF	Adaptive Façade
AFC	Adaptive Façade Component
AFS	Adaptive Façade System
ASHRAE	American Society of Heating, Refrigerating and Air-Conditioning Engineers
BMS	Building Management System
CDD	Cooling Degree Days
DA	Daylight Autonomy
DA_{con}	Continuous Daylight Autonomy
DA_{max}	Maximum Daylight Autonomy
DF	Daylight Factors
DGP	Daylight Glare Probability
DOE	Department of Energy
EPBD	Energy Performance of Building Directives
EU	European Union
EUI	Energy Use Intensity
epw	Energy Plus Weather

LIST OF ABBREVIATIONS AND SYMBOLS (continued)

Abbreviations	Descriptions
FC	Footcandles
GHG	Green House Gas
HDD	Heating Degree Days
HVAC	Heating, ventilation and air conditioning
IBD	Intelligent Building Design
IECC	International Energy Conservation Code
IESNA	Illuminating Engineering Society of North America
IR	Infrared
ITC	Information Technology Control
LEED	Leadership in Energy and Environmental Design
LPD	Lighting Power Density
sDA	Spatial Daylight Autonomy
SHGC	Solar Heat Gain Coefficient
UDI	Useful Daylight Illuminance
UFV	User Field of Vision
UK	United Kingdom
UNDP	United Nations Development Program
USA	United States of America
UV	Ultraviolet
VL	Visible Light
VLT	Visible light transmittance
WWR	Window to Wall Ratio

1. INTRODUCTION AND PURPOSE

It is well-acknowledged that the energy used in buildings for space conditioning and other facilities accounts for approximately one-third of global greenhouse gas (GHG) emissions and 40% of the global energy consumption (Nejat et al., 2015). According to Birangal, Admane, and Shinde (2015) buildings are increasingly anticipated to meet higher and more complex performance requirements. Such trend also led to sustainable approaches such as energy efficiency in buildings, which mark a large research domain in recent years.

A significant factor in the energy efficiency of buildings is the building envelope. Existing building façades are commonly composed of static layers and have predictable performance figures based on the exterior environmental conditions, occupant behavior/demands, and the capacity of building services. Once the demand in the indoor environment cannot be met by the static parts of an envelope, occupants tend to compensate for discomfort through the use of building services in order to eliminate the inability of a building envelope to dynamically respond the fluctuating exterior environmental conditions and to address occupant demands leads to further energy consumption (Knaack et al., 2015).

A well-known example of the static features of the building envelope is the fixed exterior shading systems that were designed as louvers and overhangs to regulate the solar radiation and daylight penetration to the indoor environment (Sargent, Niemasz and Reinhart, 2011). It is evident that the architectural means to control daylight and radiation that penetrate from the transparent parts of the building envelope does not always perform optimally throughout the year. Despite their certain qualities based on conventional passive solar architecture, the flexibility required from high-performance buildings cannot be met (Kosir, 2016).

The continuous cycle between occupant controls on the indoor environmental conditions and the everchanging climatic conditions of the exterior environment requires certain balance between these two mediums. Space conditioning, indoor environmental controls, occupant behavior, and the particular micro-environment of a building affect

energy performance and indoor environmental conditions. In order to achieve energy savings in the operation phase of a building, building services that include both adaptive/responsive façade systems and active conditioning and controls provide dynamic optimization throughout the service life of a building, given that the façade is the most significant part of the building envelope in regulating the performance of a building (Knaack et al., 2015).

In the past, most kinetic aspects were incorporated in buildings as interactive devices for aesthetics, social purposes, and media with little regard for environmental mediation (Hansanuwat, 2010). Moloney (2011) argued that the increased interest in environmentally responsive building envelopes, particularly shading systems, was concentrated highly on the kinetic possibilities of the movable parts and the research trajectory leaned more towards sophisticated technical solutions rather than the architectural aesthetics of these façade systems. In other words, it is not only considered as an aesthetic building component but also a functional component that regulates indoor environmental conditions. Hence, the impact of solar shading systems on indoor environment performance, such as daylight availability, glare probability, received increased attention from researchers (Mahmoud and Elghazi, 2016).

According to Ochoa and Capeluto (2008) the concept of *"intelligence in buildings"* created certain excitement among architects and developers, being perceived as the ultimate design solution. Ochoa and Capeluto (2008) further argued that a building that adapts to changing environmental conditions freed designers from carrying out studies to find passive solutions to design problems, in other words, conflict resolution was delegated from the designer to the end product itself. Sala, Gallo, and Sayigh (1999) discussed that the pressing need to improve the performance and the quality of buildings led to improvements in energy conservation in theoretical and applied domains through testing the reliable performance of components. However, intelligent buildings do not only involve advanced solutions for facility management, communication networks, security, and safety in a building but also involve specific measures of building energy performance. It is also claimed that the concept of intelligent buildings allows building elements to respond to occupant needs and environmental changes while being cost-effective and energy-efficient by incorporating various complex adaptive and responsive intelligent technologies (Buğra, 2014). Also, Sala et al. (1999) stated that the contemporary designer should take energy-conscious design as

an essential responsibility and acknowledge that the building envelope is an interface with variable features and its active role is determined by the climatic conditions.

The improvement and realization of adaptive façades are still in their initial stages, even though numerous projects and strategies have been realized. Furthermore, new technologies that enable adaptive behavior in façades, suitable testing methods, and simulation tools must be developed while adapting to existing norms and regulations with the development of holistic concepts that integrate adaptive façades in the overall building system (Knaack et al., 2015). Thus, there is a paramount need for further studies focusing on the strategies to improve the adaptive façade systems (AFSs). It is noteworthy that AFs contribute positively to improving energy performance and user comfort. Although, previous studies addressed the technical and design aspects of AFSs (Martin and Eydgahi, 2019a), very limited studies have been conducted based on the performance of geometrical forms of the AFSs. The premise of this study is based on the need for improved AFSs, thus various AFS designs were investigated for a hypothetical cell-type office unit to determine their effects on daylighting, energy performance, and glare control.

Due to the rapid social and technological developments and the related excessive energy demand, especially in the building sector, intelligent interventions in the building became inevitable due to decreased fossil fuel consumption and use of alternative energy sources (Sala et al., 1999). United States Department of Energy (DOE) and United Nations Development Program (UNDP) encouraged the implementation of Intelligent Building Design (IBD), which is a non-traditional collaborative approach. The key of IBD is a whole-building approach that considers a facility as an interdependent system rather than as a separate component (D.O.E, 2011, as cited in Buğra, 2014).

In addition, the ethos of Arup, a diverse, technical, and highly creative community of professionals, is ‘total architecture’. The approach of ‘total architecture’ was coined by Sir Ove Arup in his key speech. *“Total architecture implies that all relevant design decisions have been considered together and have been integrated into a whole by a well-organized team empowered to fix priorities.”* This approach ensures that each design is improved by a collective of professionals to ensure more resilient, sustainable, intelligent, and robust outcomes (Arup, 2021).

Today, the building industry is trying to minimize the carbon and environmental footprint of commercial and residential buildings. Once again, the need to optimize and conserve resources such as clean air, water, and energy as well as land drives for change, which focus on transformative technologies that meet such the challenges (U.S., 2008). Given the scope above, the present study is expected to serve as a framework for researchers interested in the field of daylight optimization, visual comfort, and the energy efficiency of AFSs.

In parallel with the aim of the study stated above, two main research questions were delineated:

- Does the geometry and form of an AFS affect the overall performance of a façade system?
- How can an AFS optimize the daylight levels, visual comfort, and reduce the solar gain of a building?

The design and testing of various façade components on the cell-type office unit constituted the basis of the present research. The hypothesis of the present study demonstrates that AFSs improve the energy performance, visual comfort, and illuminance level of office space. Also, that three-dimensional (3D) AFS provides better daylighting levels and energy performance in comparison to two-dimensional (2D) AFSs.

Therefore, the present study aims to investigate the impact of adaptive façade systems (AFSs) on the daylight levels and solar gain of a cell-type office unit. Hence,

- the design of Base case model, and script development for the 2D and 3D adaptive façade components was completed
- simulation parameters, boundary conditions, and model setup for simulation were described.
- the base case model, 2D, and 3D adaptive façade systems were simulated to determine the daylight levels and solar gains.
- the results were compared and evaluated for the optimization of daylight levels, visual comfort, and solar gains.

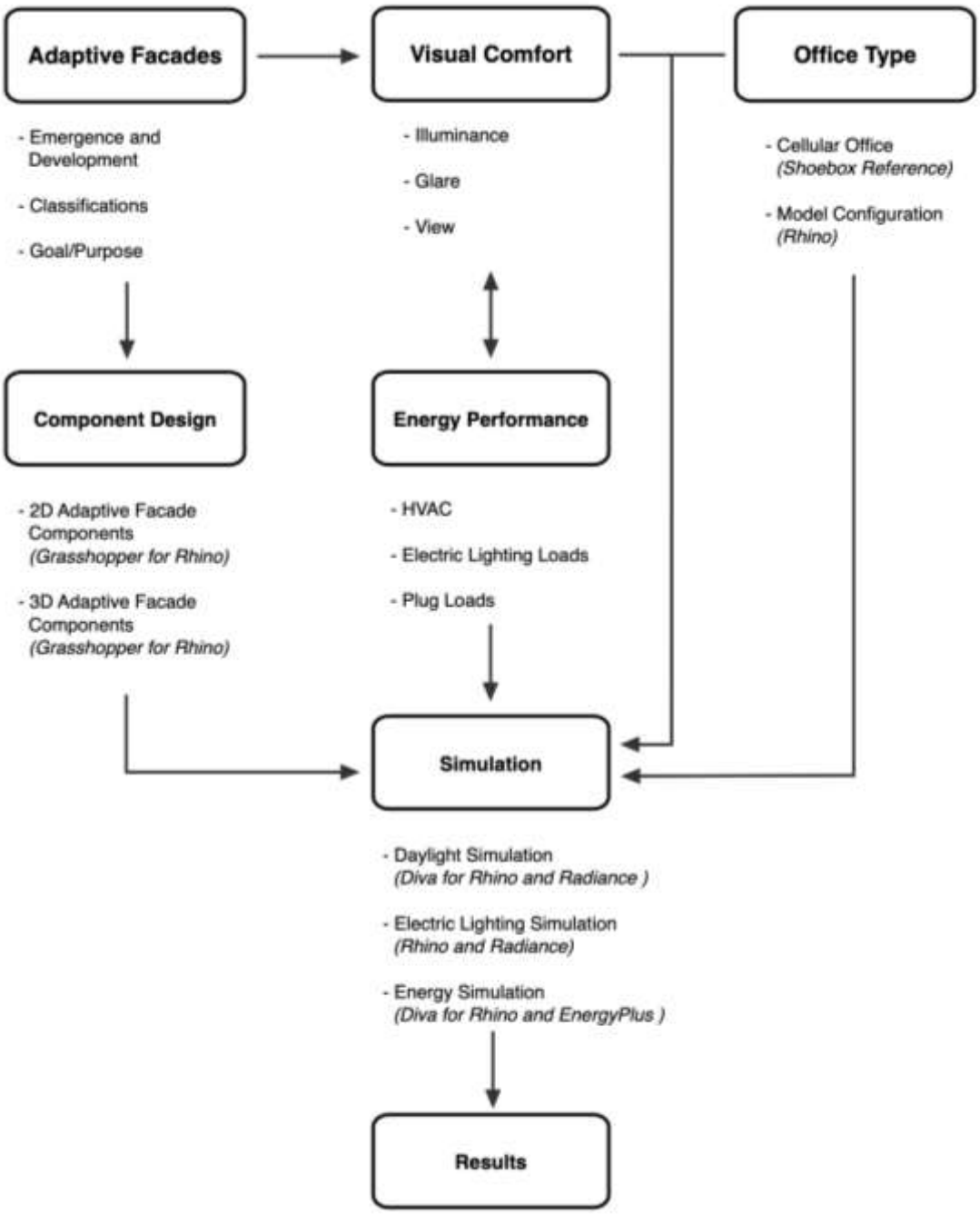


Figure 1.1. Thesis structure

Figure 1.1 delineates the integrations between studied fields, the process employed, research tools, and conducted simulations. Based on the abovementioned hypothesis and aims, the present study focuses on the investigation of dynamic façade systems and the impact they have on the daylight levels, visual and solar gain of a cell-type office unit. The present study adopts a simulation approach and certain boundary conditions to test the developed adaptive façade configurations. Initially, a hypothetical cell-type office unit (MIT

reference office) without AFSs were simulated and accepted as the base case model (Reinhart, Jakubiec, and Ibarra, 2013). Simulations were completed to test the developed adaptive façade configurations on the base case model to investigate the daylight level and solar gain of the cell-type office unit. The design of the base case model (MIT reference office) was conducted using Rhino, Grasshopper for various façade component geometry and motion scripting, Energy Plus for thermal simulation, and daylight simulations RADIANCE in DIVA for Rhino was used (Solemma, 2020). DIVA is an acronym for Design Iterate Validate Adapt, it is a great environmental analysis plugin for the NURBS modeling program Rhinoceros 3D (McNeel, 2010). The parametric nature of these software allows for complex simulations through seamless workflow. The results retrieved from the simulations were compared and analyzed in the context of investigating daylight levels, visual comfort, and energy performance.

2. LITERATURE REVIEW

This chapter was intended to deliver the knowledge on the research domain, hence a literature review was carried out to define adaptive façade systems, their emergence and development, classifications, effects on the building performance and indoor environmental conditions, and implementation principles. Furthermore, the highlighted knowledge on daylighting studies, solar gains, energy efficiency, and the role of adaptive façade in building performance optimization were included in the review.

2.1 Adaptive Façades

Building envelope, especially the façade, is a mediator between the indoor and outdoor environment. It controls heat and mass transfer both through the transparent and opaque parts and regulates daylight and solar gains. Boeke, Knaack, and Hemmerling (2019) stated that current strategies that focus on decreased energy use for space conditioning and increased occupant wellbeing require more effective façade systems, hence argued that the main potential of a façade is energy efficiency.

Current technological advances enable building envelope designs that alter their properties and operate dynamically. Adaptive façade systems are also known as dynamic, kinetic, active, adjustable, responsive, advanced, intelligent, smart, switchable, interactive systems, etc. Such abundance in terminology does not necessarily originate from synonyms yet it is often challenging to differentiate between the terminologies. However, the common emphasis in the terminology is certain aspects of a façade that are adaptive, material or system-wise (Hraska, 2018).

The complex approaches towards the adaptive façade systems lead to the question, whether there exists a particular definition for the adaptive, responsive, dynamic, intelligent, and/or smart façade systems. A plethora of professionals and academics work on adaptive façade systems focusing on dynamic and intelligent features, their potential use and

applications, and improvements on the overall performance (Knaack et al., 2015). Despite such efforts, there is no consensus on an exact terminology (Hraska, 2018). The present study addresses the dynamic and intelligent features of a façade as “adaptive façade systems”.

Façade is a mediator between the indoor and outdoor environment. Among its numerous functions, it defines the aesthetical narrative of a building, allows for interior and exterior visibility, bears its self-weight, wind forces, and weight of other buildings components. The façade protects the interior space from the sun while allowing daylight when required, serves as insulation against heat, cold, and noise (Knaack et al., 2014). The façade handles humidity and protects the interiors from rainwater penetrations. Figure 2.1 illustrates the complex responsibilities of a façade (Knaack et al., 2014).

Currently, increased integration of building services in scales up the functional scope of the building envelope (Klein, 2013). The energy consumption and interior comfort of a building are highly influenced by the façade. The increased demands by users on both aspects affect the building envelope performance (Böke, Knaack, and Hemmerling, 2019).

For a long time, engineers and designers considered building envelopes as barriers that protect the interior space from the effects of the external environment. Building services were developed to achieve indoor environmental conditions independent of the exterior climatic conditions (Addington, 2009). The performance of a building envelope is determined by how well a building envelope protects the indoor environment from the effect of the exterior environment. This approach is currently extended to the idea adaptivity in building envelopes (Favoino, Jin and Overend, 2014). Adaptive building envelopes react dynamically to changing requirements and conditions. They reduce energy consumption for the maintenance and comfort of the interior climate by utilizing the fluctuations in the exterior climatic conditions (Böke et al., 2019). The evolution and application of adaptive façade concepts are in their preliminary stages (Knaack et al., 2015). Recently, adaptive façade systems became quite a research interest since their significance was apparent to designers. Adaptive façades are comprised of highly multifunctional adaptive systems that allow the alteration of shape, position, function, behavior, and/or material characteristics in response to transient performance requirements and boundary conditions, to improve occupant comfort and overall building performance (Loonen et al., 2015). Further

advantages derived from these envelope systems were their ability to adapt to prevailing weather conditions and immediately respond to occupant needs and controls, thereby simultaneously meeting the required comfort levels and energy savings (Loonen et al., 2013; as cited in Aelenei et al., 2018).

Furthermore, Knaack et al. (2015) stated that the next big milestone in façade technology was the adoption of dynamic, multifunctional, and adaptive façade systems. These systems are capable of interacting with the environment by reacting to the dynamic nature of the climate outdoor while interacting with the user and adapting to their behavior and functionality accordingly.

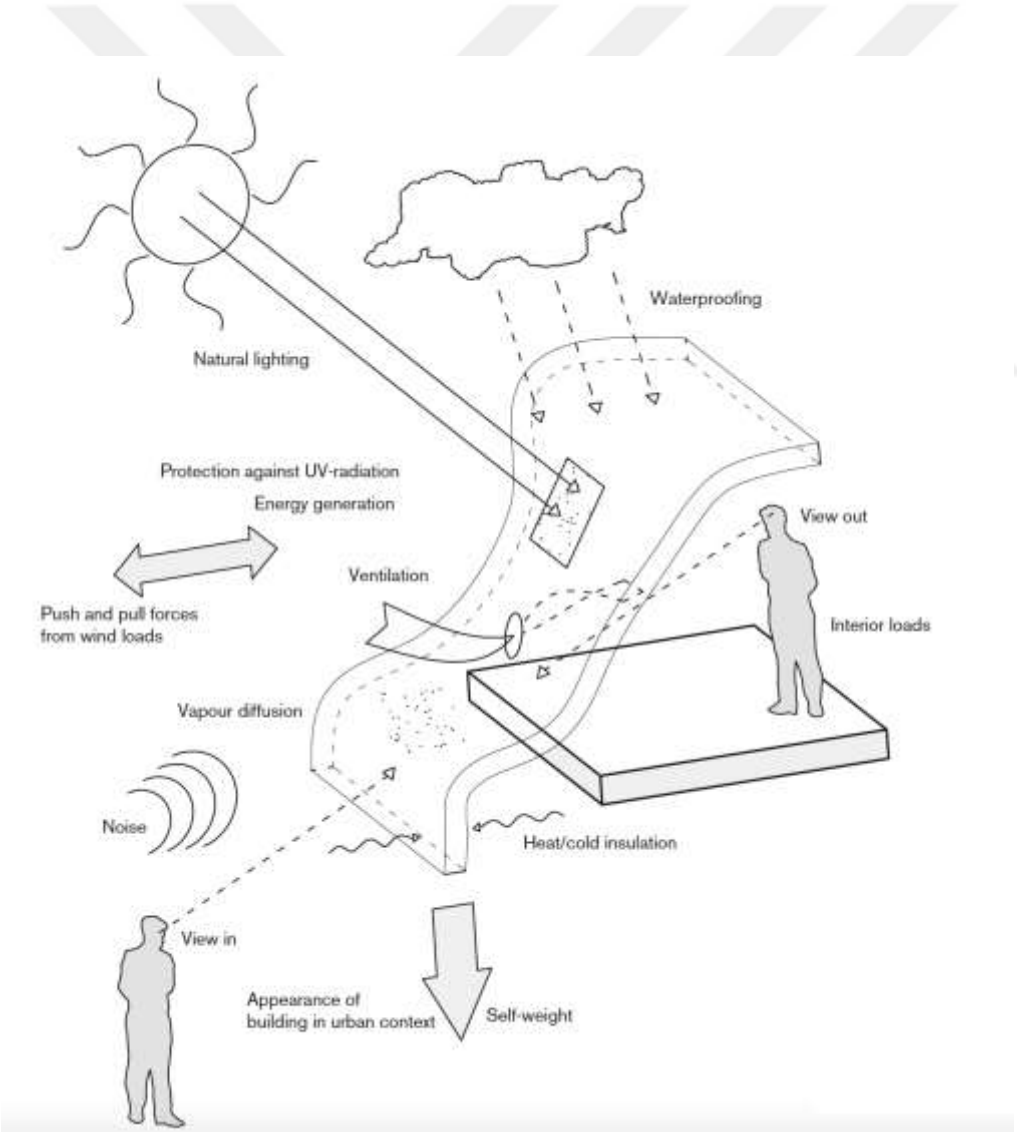


Figure 2.1. Façade functions (Source: Knaack et al., 2014)

2.1.1 Definitions of Adaptive Façades

Adaptability is the ability of a system to respond to changing environmental parameters. The adaptability of a structure allows for the adjustment of its geometric topology as well (Carl, Schein and Stepper, 2017). According to Ferguson et al. (2007), adaptability is the ability of a system to carry out intended functionality based on various criteria for varying conditions. Furthermore, the adaptability of a system lies between the idea of flexibility and polyvalency. A system flexible enough to make changes, when necessary, but polyvalent enough to allow for differing interpretations is considered an adaptable system (Hansanuwat, 2010). The series of definitions for adaptability above might raise questions as to, "what is the difference between adaptability, flexibility, and polyvalency?"

Flexibility in architecture is a modernist term that offers the temporal and unknown as design parameters. Flexibility was developed as a movement against the presumption that all building parts must be designed for a specific use and recognized that all functions within a building cannot be foreseen (Forty and Forty, 2000). In contrast to the concept of flexibility, Hertzberger (2005) argued that *"Flexibility signifies - since there is no single solution that is preferable to all others - the absolute denial of a fixed, clear-cut standpoint. The flexible plan starts from the certainty that the correct solution does not exist because the problem requiring solution is in a permanent state of flux, i.e., it is always temporary."* Moreover, Hertzberger (2005) mentioned that flexibility makes architecture vague and left spaces unfinished. He rather prefers the concept of polyvalent spaces that were clearly defined, and can also open for different uses (Ćetković, 2012). The Schroder House by Gerrit Rietveld and Truus Schroder (Figure 2.2) is an example of flexible space. The walls are movable, and they allow for the spaces to be shared by day and divided into bedrooms, living rooms, and bathrooms at night with the aid of movable panels (Architecture Design, 2012).

The Polyvalency of an object necessitates the capacity to be reinterpreted for various functions over time (Ring, 2017). Another definition of polyvalency indicates that a system that executes numerous functions over time by allowing for multiple interpretations of available options (Hansanuwat, 2010). Theoretically, the idea of polyvalence is strong but can be perceived as an answer to the idea of a utopian design, yet essentially lacks the

consideration of the diversity and irrationality of humanity (Hertzberger (1991); as cited in Ring, 2017). MVRDV, Ypenburg ‘VINEX’ development (Figure 2.3) are dwellings designed with the polyvalence approach, spaces are organized in a star shape, and access is designed as an open stair plan to preserve space. The kitchen is between the living room and a room, the open plan concept allows for a possibility to change the function of the spaces when desired (Leupen, 2013).



Figure 2.2. The interior of Rietveld Schröder House by Gerrit Thomas Rietveld (Source: Archilovers, 2018)



Figure 2.3. MVRDV, Ypenburg ‘VINEX’ development (Source: MVRDV, 2005)

In architectural design, the concept of adaptability is mostly addressed through a spatial organization, however, in building physics adaptability refers commonly to building elements that are capable of environmental control, especially for specific building envelope elements. Aelenei et al. (2018) mentioned that adaptive façades were considered as the last frontier of contemporary architectural and technological research, which is closely related to the desire for novel dynamic envelope solutions that utilize sensors, system components for the production of energy and smart materials, to contribute towards the reduction of building's energy demand. Aelenei et al. (2018) further expanded such definition through a classification of adaptive façade systems based on the proposed technological solutions to manage energy flows in the building envelope through altering the properties of fixed devices via smart materials or by manually or automatically controlling moving parts of components such as sunshades, ventilation outlets, and windows, due to the building type and complexity.

2.1.2 Emergence and Development

Over the years, the possibility that building envelopes have certain levels of adaptability and responsiveness to changes in environmental conditions was anticipated by professionals and academics. In the 1960s, Herman Hertzberger a Dutch architect presented the idea of polyvalency as a concept in architecture, to criticize the flexibility concept by laissez-faire (Ring, 2017). Also, he stressed that flexibility is not capable of solving a certain problem, whereas, a flexible object tries to adapt itself to each change as it presents itself (Hertzberger, 2016). In 1962, one of the first examples of a responsive building skin is the Los Angeles County Hall of Records designed by Richard Neutra and Robert Alexander. The T-shaped building is installed with a solar-powered aluminum louver (Figure 2.4) on the south façade (Khoo and Salim, 2013). The mechanically controlled mechanism for the Los Angeles County Hall of Records was inspired by Kaufmann's hand-operated facade also by Richard Neutra (Neutra, 1998). Another early example of automated climate-adaptive envelopes was Buckminster Fuller's façade, presented in Figure 2.5. The geodesic dome was constructed for the United States Pavilion 1967 Montreal Expo. The skin of the dome was controlled by a computer program to adjust the interior canvas sunshade's position in relation to the movement of the sun (Trubiano, 2013).



Figure 2.4. Aluminum louvers on south façade of Los Angeles County Hall of Records (Source: Kevin, 2012)



Figure 2.5. Buckminster Fuller's façade (Source: Trubiano, 2013)

In 1975, N. Negroponte conceptualized the idea of a responsive environment with the ability to activate through the functions of complex or simple computations expected to initiate a greater or lesser degree of change (Negroponte, 1975; as cited in Aelenei et al., 2018). In 1981, The polyvalent wall (Figure 2.6) was proposed by Mike Davies as an idea of an envelope system where several functions can be combined in a layer-integrated wall (Davies, 1981; as cited in Aelenei et al., 2018). The idea was not immediately realized through the concepts of intelligent walls, integrated façades, etc., yet served as a driving

force that inspired researchers over the last two decades to create new façade technologies (Solla, 2010, August 20). Motivated by Mike Davies concept for polyvalent wall, Knaack et al. (2014) presented the concept of integrated façade based on the advances in façade technologies and downsized and decentralized heating and cooling systems, where it was reasonable to integrate air-conditioning and ventilation unit, heating elements, light-directing, artificial lighting, movable shading, energy generation with solar panels and other appliances into the module of a façade. This method can be implemented in a modular design approach and will significantly reduce the time needed for building services assembly and construction time.

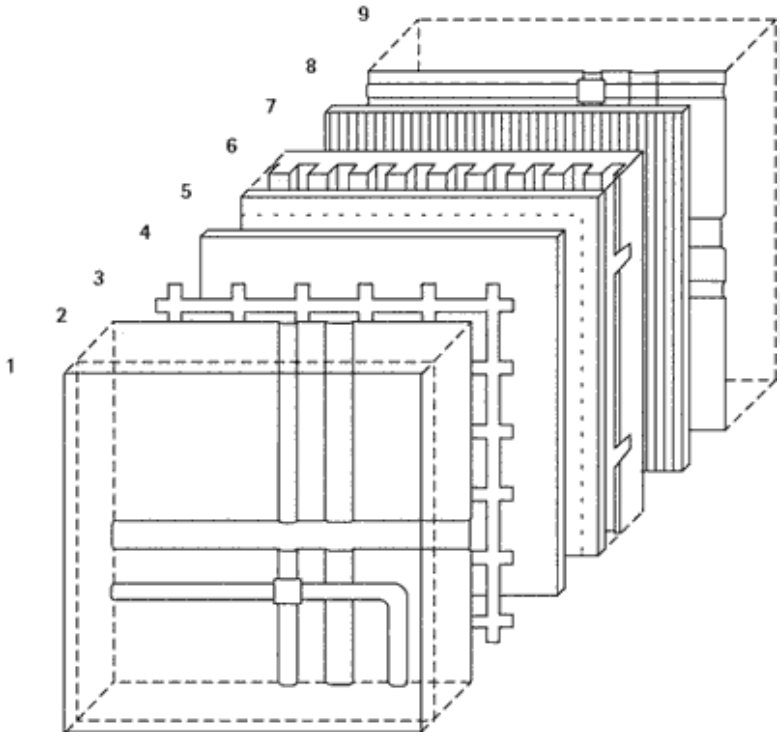


Figure 2.6. The Polyvalent Wall by Mike Davies (Source: www.hl-technik.de, as cited in Hövels, 2007)

The integrated façade principle was also implemented in the Capricorn House in the Medienhafen Düsseldorf by Gatermann + Schossig in Figure 2.7. Decentralized air-conditioning units, heat recovery systems, and daylight-directing louvers were integrated within the enclosed façade elements (Knaack et al., 2014).

The BIX façade, at the Kunsthaus Graz (Figure 2.8) is another example of a polyvalent system, it is a communicative display skin developed by Peter Cook and Colin Fournier. The building is enclosed in pixelated compact fluorescent lights to form a

curvilinear glazed exterior. The lights on the façade function as kinetic media façade and are controlled individually by a computer. The 930 pixels of a façade were designed as translucent with the idea to emphasize the connectivity between indoor spaces and the surrounding neighborhood, nevertheless, was discarded during the design process (Isenstadt, Petty and Neumann, 2014).



Figure 2.7. Capricorn House, Düsseldorf. Gatermann + Schlossig, 2006 (Source: Solla, 2010)



Figure 2.8. BIX Communicative Display Skin for the Kunsthaus Graz (Source: Archdaily, 2010)

Furthermore, recent research, technological advances, and state-of-the-art experimentation placed an emphasis on the capability and dynamic quality of a process of exchange that concerns energy and mass flows through the building envelope (Altomonte, 2008). For instance, the current research domain partly focuses on mimicking the movement

and geometric alterations in biological organisms in a way to manage the energy behavior of building envelope components, thus explore the possibility to equip vertical enclosures with dynamic features (Aelenei et al., 2018). Early examples of the dynamic façade systems were observed in the Arab World Institute by Jean Nouvel (Figure 2.9) and Al Bahar Towers by Aedas Architects (Figure 2.10). These new frontiers of innovation in the architecture were intended for novelty in which building elements, similar to organisms, become autonomously capable of ensuring occupant comfort. Given the above, the evolution and propagation of Information Technology Control (ITC) systems (from home automation to Building Management System - BMS) create an enabling environment to transfer artificial intelligently equipped systems into building components and systems scale, which regulates spatial conditions even in the absence of the occupants through a whole series of requirements to optimize the indoor environmental conditions (Aelenei et al., 2018).

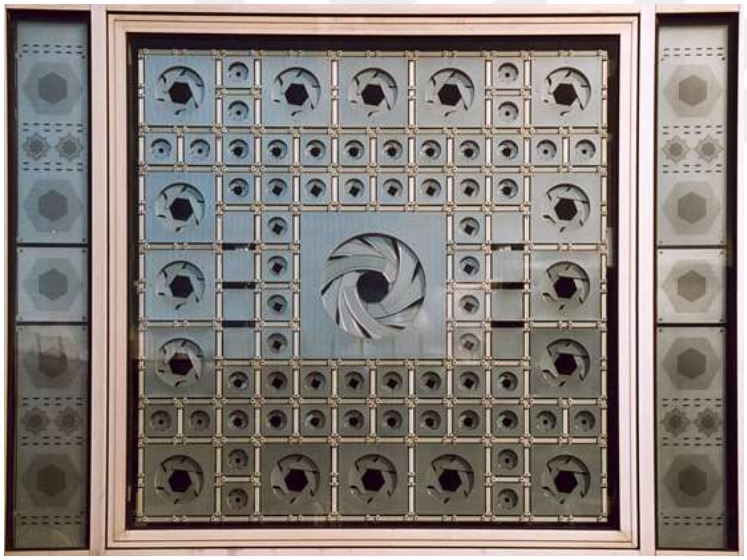


Figure 2.9. Kinetic façade that regulates sunlight and illumination in Arab World Institute, Jean Nouvel (Source: Visuallexicon, 2017)



Figure 2.10. The responsive facade that reduces solar gain and glare, Aedas Architects (Source: Archdaily, 2012)

2.1.3 Adaptive Façade Classifications

Given the numerous possible approaches to adaptive façade systems, a classification becomes necessary to further recognize the multiple variables affecting the system's performance, capabilities, and the available technologies to achieve the objectives of adaptive façades. Although several studies attempted to address the topic (Aelenei et al., 2018; Matin and Eydgahi, 2019b; Khoo and Salim, 2013; Loonen et al., 2013), there are no exact classifications for adaptive facades. An example of the efforts in literature to categorize this considerably new research domain is a comparative study by Matin and Eydgahi (2019b), in which the authors classified adaptive facades based on various control technologies and the extensive data on sensors, actuators utilized in the systems. Matin and Eydgahi (2019b) classified adaptive façades based on control technologies such as passive technology, information technology, material-based technology, mechanical technology, electro-mechanical technology, and Integrated technology (Figure 2.11).



Figure 2.11. Adaptive facades classification based on various control technologies (Source: adopted from Matin and Eydgahi, 2019b)

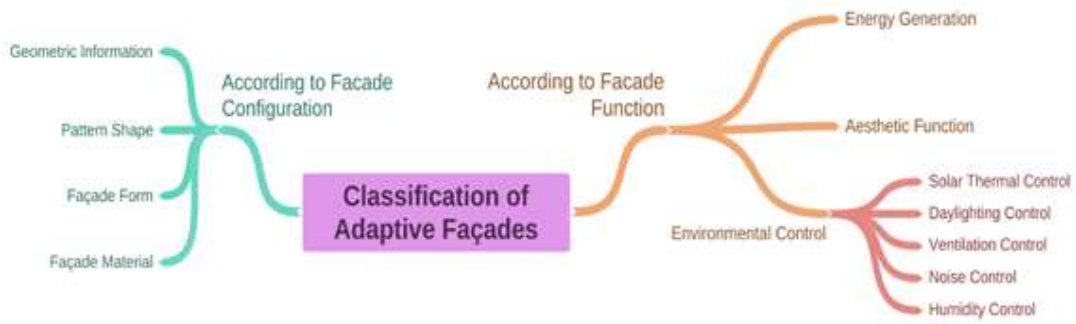


Figure 2.12. Kinetic Facades main and sub-Categories (Source: adopted from Waseef and El-Mowafy, 2017)

According to Waseef and El-Mowafy (2017), classifications of adaptive facades in the past were mostly based on their geometric aspects and the motion of the façade component. However, the classifications could be broader and comprise further

transformation capacities, whereas the existing classification approaches fail to include the evolved forms of adaptive facades. Accordingly, Waseef and El-Mowafy (2017) proposed a new classification for adaptive façades based on the used transformation type, the purpose of use, and the motion mechanism. Figure 2.12 presents the two main adaptive façade classification factors proposed by the authors:

1. Façade configuration
2. Façade function

These main factors were then classified into sub and secondary categories to further categorize the systems (Waseef and El-mowafy, 2017).

The study conducted by Hraska (2018), which focused on adaptive solar shading systems also proposed an adaptive façade classification for further research. Hraska (2018) emphasized the proposed adaptive façade classification was fundamental and could be used for selecting appropriate adaptive façade configurations during the design process. Hraska's classification for adaptive façade systems is comprised of four groups: kinetic shading, multifunction systems, switchable glazing, and specific systems (Figure 2.13). Hraska also discussed the advantages and disadvantages of various adaptive facades in different contexts (Hraska, 2018).

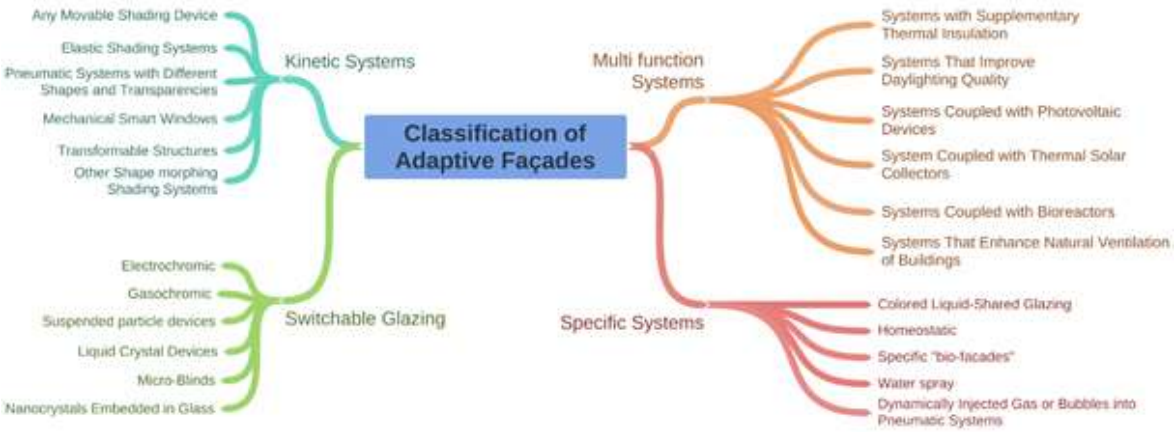


Figure 2.13. Typology of adaptive Façade systems (Source: adopted from Hraska, 2018)

Furthermore, a collaborative study by COST Action TU 1403 research team categorized adaptive façades based on technologies and their utilization purpose. Figure 2.14

presents the classification of adaptive facades based on their utilization purpose, responsive functions, operation capacities, response time, materials and systems, visibility, and spatial scale. Utilization purpose was based on criteria such as thermal comfort, indoor air quality, visual comfort, etc. (Aelenei et al., 2018).

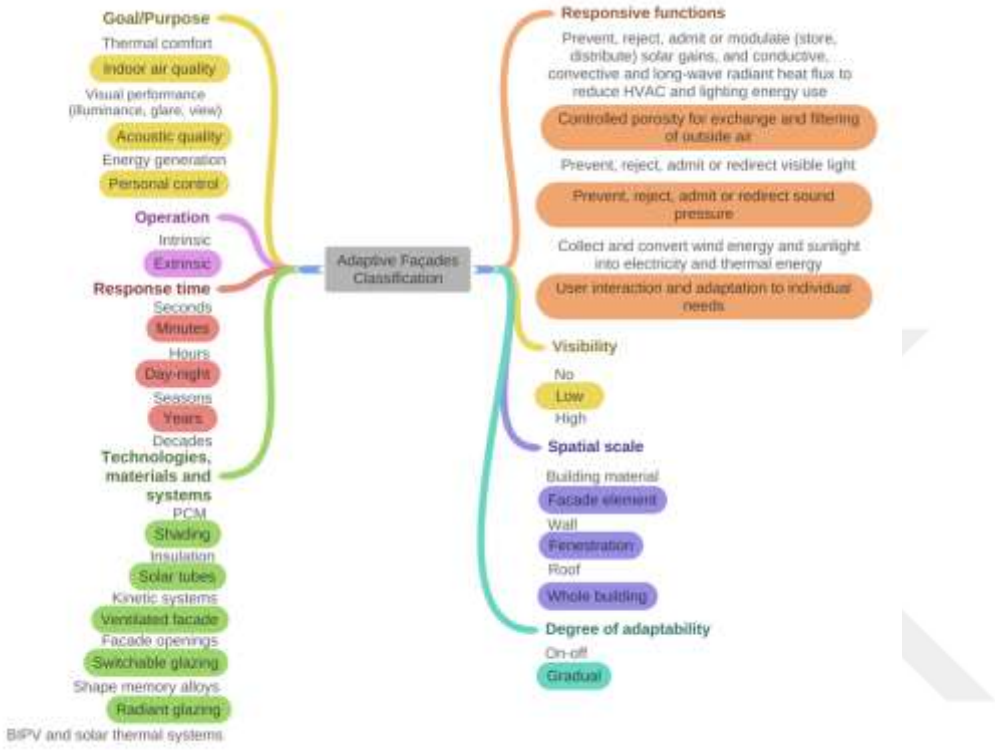


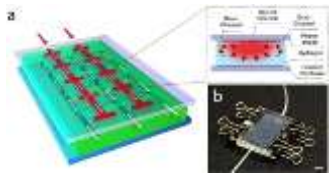
Figure 2.14. Overview of characterization concepts for envelope adaptivity (Source: adopted from Loonen et al, 2015)

WG1 (2018) research team proposed a systematic approach and identified various façade systems. The researchers evaluated the adaptive façade systems based on components (high-rank elements) and materials (low-rank elements). Thus, it was possible to extensively and independently study the sub-structures that make up the façade systems (Aelenei et al., 2018). Hence, the researchers organized a database on case studies and three main groups were distinctive in providing a clear understanding of sub-elements in relation to the overall system (Aelenei et al., 2018; Ahmed et al., 2016; Loonen et al., 2015):

(1) Material: In the classification of (Aelenei et al., 2018) materials were taken into consideration based on their unique qualities and characteristics, such as raw, coated, or extruded. Furthermore, the composites such as bi-metals, polymers, phase change materials

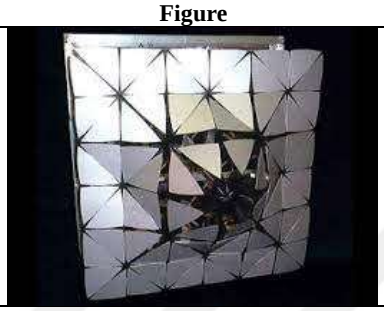
were also identified to understand the characteristics and varieties of adaptive materials. Instances of materials and their applications were described in Table 2.1.

Table 2.1. Examples for adaptive façade materials

Material / Project	Year	Figure	Goal/Purpose
Shape Memory Alloy Nitinol Alloy (Source: Aelenei et al., 2018)	2005		Nickel-titanium (NiTi) alloys can deform in two different phases based on applied temperature and change in the crystalline state. The alloy changes to Austenite state when high temperature is applied, and changes to Martensite state when the temperature is low. The material bends back and forth without strain, useful as actuators for façade (Addington and Schodek, 2005)
Homeostatic Façade Open and closed state of Homeostatic facade by Decker Yeadon (Source: Architecture, 2018)	2011		The electrochromic engineered ribbon made of dielectric elastomers responds to environmental changes such as sunlight and temperature. The material as an AF element helps in regulating indoor temperatures (Architecture, 2018).
Thermalbimetal, Bloom in courtyard application (Source: Furuto, 2012)	2011		The thermochromic smart thermobimetal material responds to heat and opens to allow air flow and shading when cooled the cut pieces close. Approximately 14,000 laser cut pieces curls when heated with peak performance on spring equinox March 20, 2012 (Furuto, 2012).
Regenerable photovoltaic devices with a hydrogel-embedded microvascular network Biomimetic photovoltaic device and a photograph of the prototype μ-FGPVs device (Source: Koo andVelev, 2013)	2013		The proposed material is to replace the solar cells with dye-embedded hydrogel or naturally derived photoactive molecules. They are regarded as a simple and economic way to generate energy. The smart glazing electrochromic material infuses the organic dye u-FGPV to generate energy (Koo and Velev, 2013)
Hydro-membrane textile for passive cooling The Hydromorph at the inactive state (Source: Roth, 2015)	2015		Hydro-membrane is a humidity-sensitive component developed by Luisa Roth, a student at the institute of advanced architecture of Catalunya. When dry (inactive) the membrane is closed, when humidity rises, the membrane opens to ventilate the space and cool the interior through evaporative cooling (Roth, 2015).

(2) Component: Aelenei et al. (2018) defined components as a set of elements combined to create a functional unit that is placed on a façade or is part of the façade to serve a certain purpose. For instance, an insulated glass unit, sun-shading device, and a window frame with glazing were treated as components. The instances and applications of components on building façades are represented in Table 2.2.

Table 2.2. Examples for adaptive façade components

Component/Project	Year	Figure	Goal/Purpose
Council House 2 Adaptive facade component for Aegis hyposurface (Source: Goulthorpe, 2001)	2006		The adaptive façade component comprises of triangles that respond to light. Each component has independent light/sonic sensors which are connected to form a responsive surface (Goulthorpe, 2001).
Kiefer Technic Showroom Adaptive façade components of Keifer Technic (Source: Vinnitskaya, 2010)	2007		The AFC of Kiefer Technic showroom are made of perforated aluminum panels, and control electro mechanically to optimize indoor climate (Matin and Eydgahi, 2019b).
KAFD Spas Façade (Tesselate™ technology) CNC cut metal perforated adaptive elements (Parametrichouse, 2021)	2008		The tesselate technology was proposed for KAFD spa façade. the AFC is proposed to regulate light and solar gain (www.Parametric house.com, 2021).
Q1, Thyssenkrupp quarter Essen Stainless steel adaptive elements of Q1 facade (Source: Archdaily, 2013b)	2010		400,000 stainless steel lamellas were proposed for the façade of the Q1 building. The adaptive elements are responsive to the sun's location and tilt to redirect light into the office space without compromising the view (Archdaily,2013b).
Sun Break by NBBJ Stainless steel adaptive elements of Q1 facade (Source: Rawn, 2014)	2017		The proposed sun break is an AFC that regulates daylight and solar gains both manually and automatically giving users more autonomy and control of the façade component (Matin and Eydgahi, 2019b).

(3) Façade-system as defined by (Aelenei et al., 2018) comprises of technical components or various transparent or opaque structures. A façade system composed of several material or components is expected to fulfill basic technical façade functions such as rain protection, wind tightness, and insulation. Instances of façade systems are double-skin façade, ventilated façade, curtain wall, and prefabricated modules. Table 2.3 describes buildings that utilize façade systems.

Table 2.3. Examples for adaptive façade systems

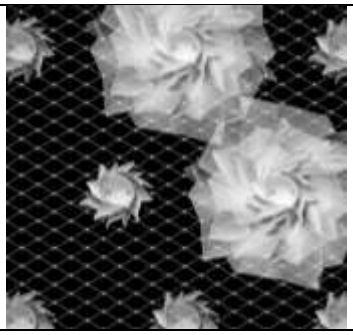
Façade System	**Year**	**Figure**	**Goal/Purpose**
Cycle bowl, Hannover Expo Pavilion for Hannover Expo (Source: www.manfred-roeben.com, 2021)	2000		A pavilion built by Duales system for world exposition 2000 utilized an AFS as façade system of the pavilion. Texlon foil was used to construct a 3 layered system with positive and negative leaf patterns printed in the chambers of the outermost and middle layers. Controlled pneumatically to manage daylight level and glare (Aelenei et al., 2018).
Articulated Cloud, Pittsburgh Translucent white plastic squares (Source: Smith, 2011)	2004		The façade of the children's museum was developed by Ned Kahn, Hank Koning, and Julie Eisenberg. Thousands of translucent white plastic squares wrap the façade and move with the wind to create the notion of clouds. This AFS is intended to serve as a beacon in the Northside neighborhood (Smith, 2011; Aelenei et al., 2018).
Yale Sculpture Building, New Haven Connecticut (USA) Yale Sculpture Building Façade with solar shading (Source: Architizer, 2007)	2007		The studio building's envelope is covered with solar glazing, a triple glazed Low-E vision panel, operable windows, and a double cavity spandrel panel that is translucent. The cavities between Low-E IGU panels are filled with Nanogel insulation. The façade of the building actively admits light and regulates temperature (Aelenei et al., 2018).
Oval Cologne Offices AFS skin of Oval office cologne (Source: Dienst, 2010)	2010		The folding shutters wrapped the envelopes of the two Oval office buildings. The AFSs are mechanically controlled and can be overridden by the users of the space. They are made of colored glass and regulates the amount of daylight and insolation getting into the office space (Detail, 2011).
Allianz Headquarters, Wallisellen The Aluminum Coated Silver Curtain AFS (Source: Wiel Arets Architects, 2014)	2014		The Allianz Headquarters consists of a 17 story Tower, and a 5-story block perimeter building with facades made of highly insulated multiple glazing (2 glass elements, foil framed to depict an abstract image of an onyx marble) with aluminum-coated silver curtains installed at its cavity which is computer controlled to protect the indoor space from solar gain. The façade elements are hermetically sealed and ventilated mechanically to prevent moisture (Wiel Arets Architects, 2014).

2.1.4 Adaptive Facades for Energy Efficiency

Adaptive Façades have the potential to increase the quality of indoor comfort and to increase the energy efficiency of a building compared to traditional shading systems. There is a growing trend to switch from static to dynamic designs of building envelope in contemporary architecture to improve energy performance and user comfort indoors (Hraska, 2018). This idea inspires the Energy Performance of Building Directives (EPBD), an EU energy policy. Both legislative aims to improve the energy performance of existing buildings and new designs and reduce environmental degradation (Climate Action Network, 2021). Advances in material sciences and technologies are essential to achieve energy-efficient buildings. It is argued that a responsive and dynamic design of building envelope parts is promising in achieving the objective of energy efficiency (Ahmed et al., 2016; Mahmoud and Elghazi, 2016). Adaptive facades are designed to respond to environmental changes and occupant demands. Designers are open to new aesthetic possibilities with the elements and systems of the concept (Hraska, 2018).

As stated in the Introduction, the building envelope is responsible to control the heat and mass transfer through the opaque and transparent parts and light and radiation penetration through the transparent parts, thus control energy performance and indoor environmental conditions. Commonly, a building envelope is considered a thermal barrier that protects the indoor environment from undesired solar gains and prevents heat loss (Al-Obaidi, Ismail and Abdul Rahman, 2015, 2016; Oral and Yilmaz, 2003). Most building envelopes are constructed to offer static design solutions (López et al., 2017). Also, traditional solutions for building envelopes cannot adapt to environmental issues and user needs (Ali, Bashir and Ali, 2015). Recently, envelope designs exhibited certain evolution towards dynamic and responsive systems, achieved mostly through the integration of an adaptive system layer that is designed to execute a specific task (Fiorito et al., 2016). Several types of adaptive facades aim to increase energy efficiency for buildings and provide flexibility of control to occupants of static buildings (Al-Obaidi et al., 2017). Table 2.4 below illustrates instances where adaptive façades were proposed as means of achieving energy efficiency in buildings.

Table 2.4. Adaptive façades for energy efficiency in buildings

Project Title	Year	Figure	Goal/Purpose
Council House 2 Adaptive facade louvers on the façade of Council House 2 (Source: Archdaily, 2013)	2006		The adaptive façade consists of timber louvers on an aluminum frame. The louvers reduce the energy consumption of the building and shade the building from the sun (Knol, Kneepkens, and Zvironaite, 2014).
POLA Ginza Pola Ginza adaptive façade (Source: Mamoru, 2009)	2009		The adaptive façade, designed to reflect the tenet of the cosmetic company, protects the indoor climate from the sun and reduces the HVAC annual energy consumption by 30% (Knol et al., 2014).
RMIT Design Hub Adaptive glass disc façade (Source: PTA, 2013)	2013		The skin of the building is wrapped with white glass discs adaptive façade. The building façade system can be upgraded with solar panels to power to entire building (PTA, 2013).
SDU Kolding Campus Triangular adaptive façades (Source: Alan, 2015)	2014		The isosceles triangular adaptive façades utilize sensors to respond to heat and light levels, the building is recorded to meet the energy target of Denmark's 2015 building code (Alan, 2015).
Pneumatically Actuated Origami Sun Shading Actuated origami shading system (Source: Eisenbarth et al., 2021)	2021		The use of a pneumatically actuated Origami sun shading system to prevent glare, solar exposure, and attain energy efficiency (Eisenbarth et al., 2021).

Additionally, studies employ the use of AFSs on buildings to achieve not just energy efficiency but thermal comfort, indoor air quality, visual comfort, and energy generation potentials (Loonen et al, 2015). Instances of studies that utilize AFSs to achieve various outcomes are subsequently stated. Lim et al. (2012) conducted an empirical study in an existing office building in a hot-humid climate in Malaysia and determined that simple modifications such as omitting the existing overhang in the office, changing glazing type and shading elements to the light shelf and 45° tilted blinds affected the overall daylight performance of the building. For instance, the addition of a light shelf led to more evenly distributed daylight levels in the indoor environment, however failed to reduce glare on vertical panels. Hybrid use of the light shelf with partial blinds tilted at 45° showed improved performance. Visual comfort improvements in both daylight quality and quantity were recorded.

Also, several studies addressed development factors by identifying the points of reference that should be taken into consideration for AFs. For instance, Nagy et al. (2016), indicated that adaptive façades were smart facade elements that provided visual comfort, daylight, and energy efficiency. As a strategy for a novel adaptive solar facade development, the researchers proposed a 7-step process to guide the design process of the adaptive solar façade. Steps 1 and 2 were based on the positioning of the proposed façade system on the case building, step 3 focused on the stability of the structure, and an appropriate support system was proposed. Steps 4 to 6 focus on the aesthetics of the adaptive solar façade by selecting panel shapes, patterns, material color, and relative position. The final step 7 focused on the control of the adaptive solar façade, where the decision-making on granularity, motion, and module movement (together, in band, individual, etc.) was finalized.

Mahmoud and Elghazi (2016) conducted a study to determine the effects of rotational and translational motion of a hexagonal façade pattern in daylight optimization. The authors highlighted six main factors to be taken into consideration in designing a dynamic façade system: (1) size and form of kinetic pattern, (2) direction and type of motion, (3) double skin spacing, (4) capacity to block direct sun light, (5) improve daylight quality and (6) maintain a minimum level of contact with outside.

Hosseini, Mohammadi, and Guerra-Santin (2019) conducted a similar study on the optimization of daylight levels and visual comfort through 2D and 3D interactive kinetic façade implementation based on the position of the occupants. The authors evaluated a four-step interactive logic for the design of an interactive façade system to improve daylight performance and visual comfort. The four-step interactive logic was based on occupant position in the office space and solar position to create a user field of vision (UFV) line, attraction point, the intersection between the UFV line and the façade surface, assigned as the actuator of the parametrically decentralized façade apertures logic utilized to reconfigure the façade module element and utilizing real-time shape-change and self-shading façade form to improve occupant visual comfort.

The above studies showed great use of strategies and key factors that influence the successful development of adaptive façade systems to optimize daylight level, visual comfort, and regulate solar gain in office spaces. These factors guided the development of the façade systems proposed for this study.

2.2. Daylighting

Daylight is essential for interior spaces. For centuries, daylight was the primary source of light in building interiors and an implicit part of architecture and buildings. Daylight is defined as the union of all direct and indirect lights coming from the sun during the day. 40% of the total solar energy received on the surface of the earth is visible light (VL). The rest are ultraviolet (UV) and infrared (IR) wavelengths (Figure 2.15). The glazing prevents the UV from entering the building. Various strategies are implemented in controlling visible light and infrared. Especially, the visible light represents the portion that human eyes can perceive which is between 380 and 780 nm in the electromagnetic spectrum. This is the portion that is regulated to control the amount of daylight required in a space. The infrared is responsible for the solar heat gain in a building (Lechner, 2014). Daylight availability varies for various locations. The sun position and sky conditions through the course of the day, season, or year is a factor. Also, daylight levels vary drastically on horizontal and vertical surfaces by the time of the day or season, directly connected to the sun path and condition of the sky. Daylight is an important parameter in an energy-efficient

design. Implementing daylight in a design not only reduces the energy consumption for lighting in the daytime but also influences the heating and cooling loads. Also, recent studies proved that the implementation of daylight in design provides a comfortable and healthy environment that is essential for building occupants (Velux, 2021). Energy reduction and occupant comfort in a building are achievable through proper utilization of daylight and proper shading device control. electric light with dimming control can complement daylight and save energy consumption in a building (Park and Athienitis, 2003).

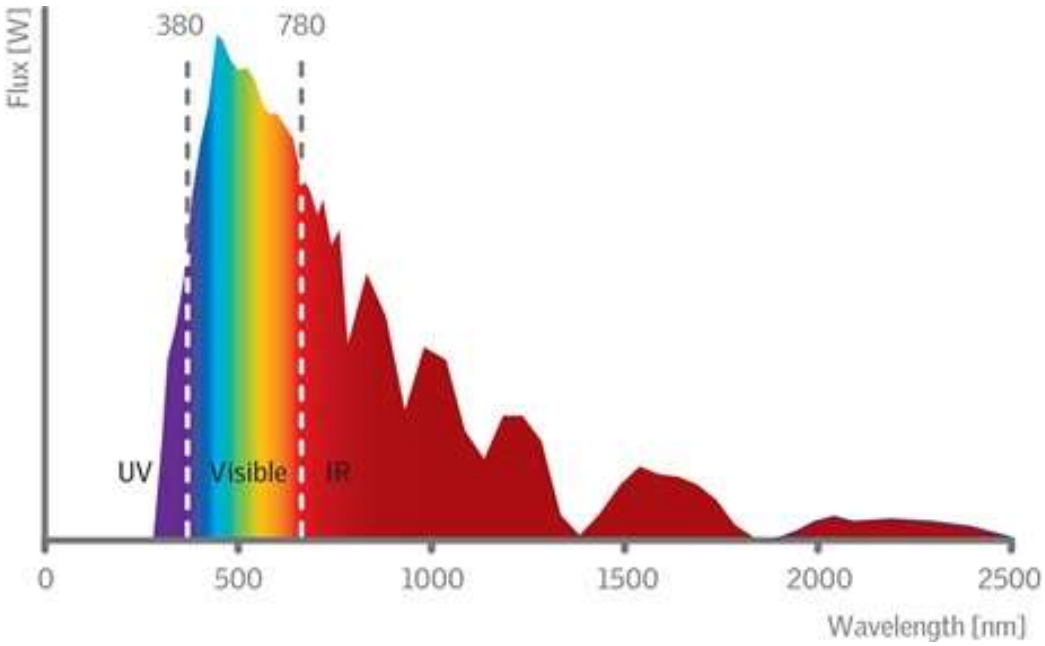


Figure 2.15. The visible part of the electromagnetic spectrum (Source: Velux, 2021)

2.2.1. Basic Daylight Characteristics

Daylight in buildings comprises direct sunlight, diffuse skylight, and reflected light from the surrounding elements and the ground (Figure 2.16) (Velux, 2021). Daylighting design needs to implement passive design strategies from the conceptual stage of the design such as; consideration of building site features, building orientation, façade and roof characteristics, size and window placement, shading systems and glazing options, geometry, and indoor surface reflectance. A good daylighting design ensures adequate light in the daytime (Velux, 2021). Direct sunlight is of very high intensity and movement. The illuminance of more than 100 000 lux is produced on the surface of the earth by the sun with the brightness varying depending on the season, time of the day, sky condition, and location

of the sun. an intelligent design is required to control the daylight, diffuse, reflect, and shading of buildings in a sunny climate. Skylight is considered as scattered sunlight by the atmosphere and clouds, providing diffuse light (Ayoub, 2019; Velux, 2021). The illuminance of an overcast sky can be up to 10 000 lux in the winter and 30 000 lux in a bright overcast day in the summer. Diffuse light is the main light source in cloudy climates. Reflected light is the light from either direct sunlight or skylight that is reflected from the ground: vegetations, trees, neighboring buildings, and terrains. The total amount of reflected light reaching a building façade is greatly determined by the surface reflectance of the surroundings (Velux, 2021).

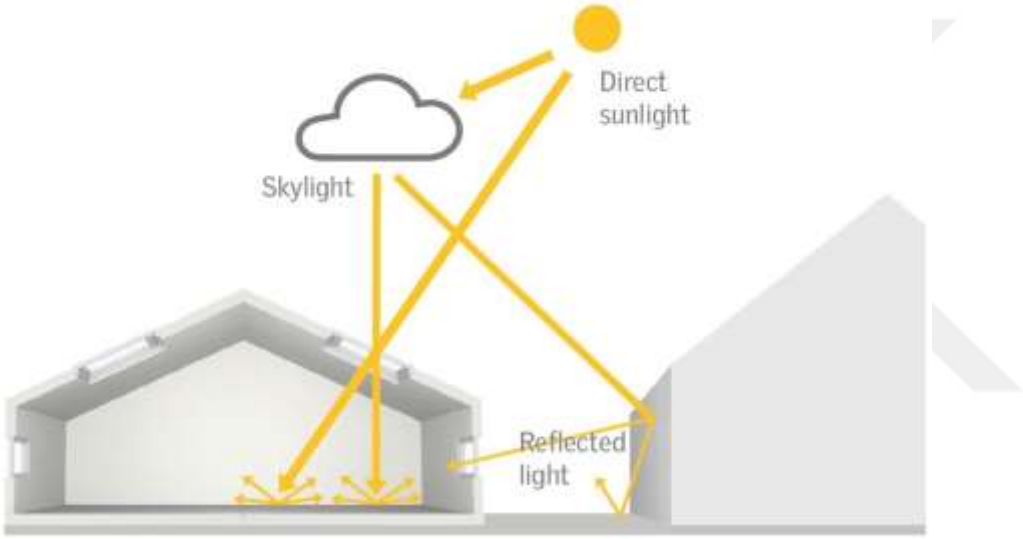


Figure 2.16. The components of daylight (Source: Velux, 2021)

According to Reinhart (2014), daylighting represents the controlled use of natural light within and around a building. It is the act of allocating windows and other transparent media and reflective surfaces to illuminate the indoor space with natural light during the day. Considerations from the initial design stages to the final design amount for successful daylighting (Velux, 2021). The use of daylighting in a building is one of the most essential energy-saving strategies that conserve energy and reduces heat gain in a building (Sala et al., 1999).

Visual comfort: The European standard EN 12665 defined visual comfort as a subjective condition of visual satisfaction caused by the visual environment (EN12665, 2011). The façade design is a great determinant of the level of visual comfort that can be achieved in a building. The two main parameters of visual comfort are light and view. Light

is studied more since it includes daylight and artificial lighting. The view, despite its relevance in the health and user productivity of space, is a rarely studied subject (Masoudi, 2018). Windows play a vital role on the occupant comfort in indoor space based on the access to daylight and view. Commonly, building occupants prefer sitting close to the window as daylight levels are considered more comfortable compared to artificial lighting (Hasselaar, 2013). Hellinga (2010) mentioned the importance of implementing daylighting in a design and that office employees are satisfied with a daylit space and having a view of the environment. Research indicated that stress and illness can be reduced by utilizing daylight in designs and providing views. Our sleep-wake rhythm is influenced by the dynamic nature of daylight which our body is accustomed with (Hellinga, 2010).

The design for daylighting is considered complex due to the dynamic nature of daylight. Daylight parameter changes in respect of the season, weather condition, and particular point in time. An understanding of the daylight parameter is necessary for devising design strategies to control daylight entering a space and prevent heat gain.

Daylighting requirements: Daylighting is a difficult-to-investigate building performance strategy. Initially, calculations for daylight performance were based on scale models (Aizlewood and Littlefair, 1994), analytical formulas (Athienitis and Tzempelikos, 2002), and static daylight modeling which concentrates on a single sky condition generally overcast sky. A common instance of a static daylight model is the daylight factor (DF). The method is limited to certain parameters and is not suitable in providing a detailed daylight performance measure. Currently, computational simulation (Ward, 1994) and machine learning (Kazanasmaz, Günaydin, and Binol, 2009) are in use for daylight studies. Commonly, they are categorized as dynamic daylight performance metrics and climate-based daylight modeling which provide detailed varieties for daylighting studies (Ayoub, 2019; Reinhart, Mardaljevic, and Rogers, 2006). Important parameters and terminologies necessary to conduct a successful daylight performance metric will be discussed as daylighting requirements in this section.

Illuminance: Illuminance is the amount of lumen that falls on each square meter (foot) of a surface. Illumination is measured in lux (lx) in the SI system and footcandles (FC) in the inch-pound system. According to indoor environmental activity, the required

illuminance changes to attain a certain standard of comfort (Lechner, 2014). According to IECC (2021), the minimum accepted illuminance level for office space is between 300-500 lux. The European standard dictates that the work plane of an office at the height of 0.85 m is required to have a minimum value of 300-500 lux, for half of the year (EN, 2011). Moreover, a uniform spread of light is necessary at the work plane level to avoid visual stress and strains due to over or under-lit areas (Group, 1994).

Luminance: According to Lechner (2014), the words "brightness" and "luminance" are closely related. Humans perceive the brightness of an object. An object's luminance is the objective measurement of a light meter. Luminance is the amount of reflected light by a surface that reaches an observer's eye. Luminance is measured in candle per square meter (cd/m^2) and it is dependent on the geometry, color, material of the observed object, and observers position in relation to the object. For a comfortable visual environment, the luminance should not exceed 3000 cd/ m^2. The perceived brightness is very crucial in lighting design. Light appears brighter at night than at day time but a light meter registers the same luminance regardless of the time of the day. Since we design for space users, it is necessary to consider brightness rather than luminance.

Daylight Factor (DF): Daylight factor is the ratio of the illumination indoors to outdoors under a CIE overcast sky which signifies how effective a design lets daylight into an indoor environment (Lechner, 2014; Moon and Spencer, 1942). Daylight factor as reviewed historically was never meant to be used as a measure for good lighting design but rather, as a minimum legal lighting requirement (Reinhart et al., 2006). Daylight factor is influenced by the dimension of the openings, window typology, geometry of the indoor space, window position, presence of a shading device, and the condition of the sky (Lechner, 2014). Also, DF is a static method of daylight calculation and does not require extensive computation, it is still in use by researchers to quickly calculate estimates of daylighting provision.

Daylight Autonomy (DA): Daylight autonomy is defined as the percentage of the year where a minimum illuminance threshold is met by daylit alone as mentioned in a Swiss norm (Association Suisse des Electriciens, 1989). As mention in the norm, DA is a function of DF and the minimum required illuminance of a space. Work plane is used in DA calculations to

determine whether daylight is sufficient for the occupant of space and the need to use artificial lighting would not be necessary. The percentage of annual daylight time where a certain space reaches an illuminance level higher than a specified illuminance value. When DA is space-related, it is called Spatial Daylight Autonomy (sDA) also referred to as Daylit area in this study and it is considered as the area of a space that receives sufficient daylight for at least 50% of the annual occupied hours. The value of sDA ranges between 0 to 100% of the floor area in a study. An office space requires an illuminance level of 300-500 lux, the illuminance level is task-dependent. The DA is therefore a vital parameter to measure the energy consumption for electrical lighting of a space (Ayoub, 2019; Kevin and Alen, 2016; Reinhart et al., 2006) and tthe higher the DA of a space, the less energy use for electric lighting.

Useful Daylight Illuminance (UDI): The UDI is a dynamic daylight performance measure based on work plane illuminances. This method was proposed by Nabil and Mardaljevic in 2005 (Nabil and Mardaljevic, 2005). The calculation is aimed at determining when daylight level is deemed useful to the occupant of space, that is, neither too bright (>2000 lx) nor too dark (<100 lx). Based on the upper and lower threshold of 2000 lx and 100 lx, the result is in three metrics. That is, when the percentage is achieved, fell short, or exceeds the threshold (Nabil and Mardaljevic, 2005; Reinhart et al., 2006). UDI can be useful when determining either electric lighting should be utilized, or when visual and thermal comfort is compromised due to excessive daylight that may cause glare or solar gain.

Continuous Daylight Autonomy (DA_{con}): DA_{con} was proposed by Rogers to consider illuminance levels that were not up to the required threshold at a time step. He justified this method by claiming that instead of a hard threshold, the transition from compliance to noncompliance illuminance value should be softened. Studies further justify that preferences for office illumination are subjective and vary between individuals (Rogers and Goldman, 2006). Essentially, the metric acknowledges that there is benefit in partial daylight as it also contributes to illuminate a space. Also, maximum Daylight Autonomy (DA_{max}) is proposed to work in synchrony with DA_{con}. DA_{max} determines the percentage of the occupied hours when a space experience direct sunlight or exceeding the desired illuminance level required. The DA_{max} is assigned as 10 times the illuminance level required (Reinhart et al., 2006; Rogers and Goldman, 2006).

Glare: Glare is caused by natural or artificial light. It is the measure of the physical discomfort caused by excessive lighting or contrast in the field of view of an occupant in a space. It is dependent on the illuminance distribution perceived by the occupant, when glare is perceived by an occupant, it negatively affects the work plane illuminance metrics such as the daylight autonomy and daylight factor. Most especially spaces that are top-lit. Glare is generally classified as either disability glare, discomfort glare, or veiling glare. Disability glare impairs vision by the presence of a very bright light source in the field of view of the observer. Discomfort glare is considered hard to detect at first. Unlike disability glare and veiling glare, it causes irritation and strain. Though the light sources in this case are small and can gradually grow to become disability glare. Veiling glare has to do with the brightness from a reflected surface other than a light source (Jakubiec and Reinhart, 2012). Glare can occur when the light reaching the observer's eye is of a wide range of illuminance values (Lechner, 2014). Various strategies are implemented on building facades to mitigate glare which in turn affects the amount of daylight getting into the space and the view to the outdoor environment. The utilization of adaptive façades that can prevent glare indoors and also grant view outdoor would improve the visual comfort of the occupants.

2.2.2. Daylighting for Commercial Office Buildings

A century ago, new urban zones were proposed to allow pedestrians avoid the shadow cast by high-rise buildings due to the discovery of the health benefits of daylight. The strategy was highly appreciated and accepted by urban inhabitants and daylight became a public right and was translated into a policy that ensures daylight for all (Turan et al., 2020; Willis, 1995). Cities around the world manifested policies to provide access to daylight as urban zoning policies. The ancient light doctrine, dating back to 1663 and still in practice in the United Kingdom (UK) protects access to light through an existing window (Kerr, 1865). Several states in the United States of America (USA) protect building occupant's right to light through regulations and litigations (Howard, 1989; Pfeiffer, 1982). In the 20th century, zoning policies were enacted to protect both public and private rights to light. These policies shape the urban cities we see today (Howard, 1989). The most apparent example is New York City. Due to the issue of shaded streets, the 1916 to 1961 zoning regulation stipulated

that building forms and exterior should be designed to minimize shading and ensure that daylight reaches pedestrians on the street (Willis, 1995).

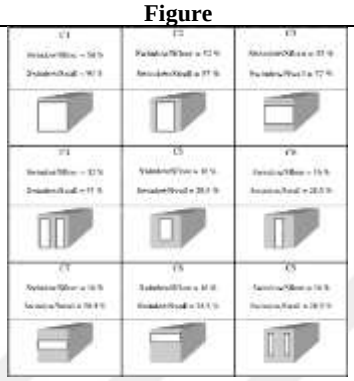
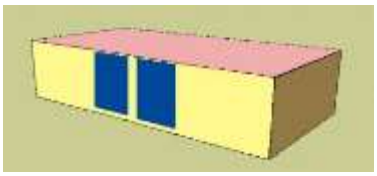
Daylight has a positive impact on human well-being. Access to daylight is beneficial to people, both physiological and psychological. Although environmental conditions affect human health, a large body of literature points out particularly in workplaces, daylight leads to greater productivity, increase employee satisfaction, and decreased stress in the workplace (Al Horr et al., 2016; Aries, Veitch, and Newsham, 2010; Böke, Knaack, and Hemmerling, 2020; Elghazi, Wagdy, and Abdalwahab, 2015; Frontczak and Wargocki, 2011; Galasiu and Veitch, 2006). Given that majority of working adults across cultures spend their working hours indoors (Khajehzadeh and Vale, 2017; Leech et al., 2002; Odeh and Hussein, 2016), the indoor workplace should be rendered beneficial. Optimizing and improving indoor factors such as acoustics, air quality, and daylight for space inhabitants (Turan et al., 2020).

Daylight is considered an essential component of building sustainability (EIA, 2017). Acknowledging the human health benefit of daylight, as well as the energy-saving potentials by reducing electric energy load, most green building rating systems reward buildings for implementing daylight in the design. Systems like Leadership in Energy and Environmental Design (LEED) certification and WELL building standard are widely used and provide certification that is used to rate a project (Council, 2013; Turan et al., 2020; WELL Certification, 2017).

The value of daylight in office buildings is widely acknowledged. A study conducted by Turan et al. (2020) on 905 office buildings was intended to determine the effect of daylight on the rental prices of office space in Manhattan. They discovered that tenants pay 5-6% more for spaces with high access to daylight than those with low daylight access. According to (Li and Lam, 2001), in offices and educational buildings, it was recorded that electric lighting significantly contributed to the total energy use. In an office building in Hong Kong, 20-30% of the total electricity loads were due to electric lighting. Recently, there is a flux of interest in utilizing daylight and artificial lighting to reduce energy consumption. This strategy will not only minimize the use of electric lighting but will also reduce the cooling load and consequently small air conditioning systems will be installed (Al-Ashwal and Hassan, 2017; Hassan and Al-Ashwal, 2015). The value and importance of

daylight in architectural design are apparent. The design of office space that would incorporate daylight and shade the building from solar gains would significantly reduce the energy consumption and improve occupant comfort. Table 2.5 shows instances where daylighting was implemented to reduce energy consumption.

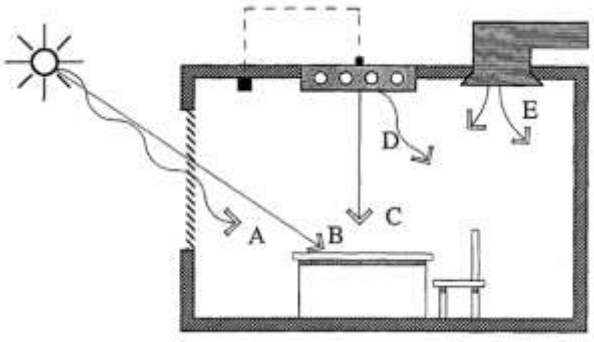
Table 2.5. Daylighting studies for office buildings as an energy-saving strategy

Project Title	Year	Figure	Goal/Purpose
Global energy savings in offices buildings by the use of daylighting. Right: Proposed window configurations (Source: Bodart and De Herde, 2002)	2002		The study conducted simulations (using TRNSYS and ADELINE) of various modeled façade configurations of a new office building in Belgium to evaluate the impact of electric lighting on its total energy consumption. the study recorded lighting energy savings from 50-80% and a total energy savings of 50% (Bodart and De Herde, 2002).
An investigation of daylighting performance and energy saving in a daylit corridor Right: Interior view of the daylit corridor (Source: Li and Lam, 2003)	2003		The study was an experimental study conducted on an air-conditioned daylit corridor. The study aimed at measuring the impact of daylight on energy performance. Results showed a reduction of 70% electric lighting energy as a result of implementing Daylight and using a dimming control strategy (Li and Lam, 2003).
Impact of window blinds on daylight-linked dimming and automatic on/off lighting controls Right: Interior view of the office space (Source: Galasiu, Atif, and MacDonald, 2004)	2004		The research focused on field measurement of blinds and electric lighting with dimming and automatic on/off control systems and their impact on energy consumption. Both control systems linked with daylight reduced the energy consumption by an average of 50-60% under clear sky (Galasiu et al., 2004).
A simplified method to estimate energy savings of artificial lighting use from daylighting Right: Building geometries considered in the analysis (Source: Krarti, Erickson, and Hillman, 2005)	2005		A simulation study utilized DOE-2.1E, a whole building simulation tool to estimate the energy-saving potential of incorporating daylight and electric lighting. 70% of lighting energy was saved as a result of utilizing daylight in office designs (Krarti et al., 2005).
Estimation of lighting energy savings from daylighting Right: Perspective view of the office room used in the testing analysis (Source: Ihm, Nemri, and Krarti, 2009)	2009		Estimating energy-saving potential by using daylight in the office building. several combinations of building geometry, window size, and glazing type were investigated in the USA.60% of lighting energy savings were recorded (Ihm et al., 2009).

2.3. Solar Gains in Buildings

Solar gain is the short-wave radiation from the sun. Solar radiation penetrates the building directly through the windows or indirectly through the fabric of the building (Designing buildings, 2020). Successfully controlling the radiative characteristics of the external surface of a building can prove highly effective in reducing the heating and cooling demand of the internal space (Ascione et al., 2010).

Globally, 30 to 40 percent of all primary energy use, greenhouse gas emissions, and waste generation are generated by buildings (Huovila, 2007). In a typical building, most of the total energy use is by lighting, heating, and cooling load. In a residential building, large energy is consumed for the heating of spaces. In the case of a commercial building, lighting consumes the highest amount of energy (Energy, 2011). Among all the components of a building envelope, windows have a five times greater heat transfer coefficient (U-value). Windows greatly influence the energy consumed for the lighting, heating, and cooling of a building. They also provide light, view, and fresh air to the occupants of a building. It is recorded that about 20-40 percent of energy is lost through windows in a building (Bülow-Hübe, 2001).



A. Solar Heat Gains
B. Daylight Availability
C. Electric Lighting
D. Heat Gains from Lights
E. Mechanical Cooling

Figure 2.17. Schematic diagram showing the interaction between fenestration solar gains and daylighting (Source: Sullivan et al., 1992)

Façade-related properties such as U-value, G-value, daylight factor, shading, and light control, have an impact on a building's energy consumption (Figure 2.17) (Heiselberg et al., 2009; Sullivan, Lee, and Selkowitz, 1992). According to (Etheridge, 2010); Littlefair (2001), houses in cooler climates value solar gains during winter seasons. In warmer climates, solar gains cause overheating and are generally unwanted. Solar gain is likely to be welcomed all year long in a cooler climate. Also, Air has a low thermal capacity, an increase in thermal energy also increases the air temperature in a space and can lead to discomfort. Solar gain contributes largely to the internal heat gain of a space, and it is necessary to factor that in the design process of buildings in a warmer climate (Etheridge, 2010). There are already more established strategies of dealing with solar gain, e.g., external solar shading devices (CIBSE, 2005) and smart glazing technology (Wigginton, 1996). In this study, adaptive façade systems were utilized to shade the base case model (*Reference office*) from solar gains to reduce the cooling load of the office unit.

3. MATERIALS AND METHODS

The methodology of the thesis covers five distinct phases. Figure 3.1. illustrates these phases employed throughout the study.

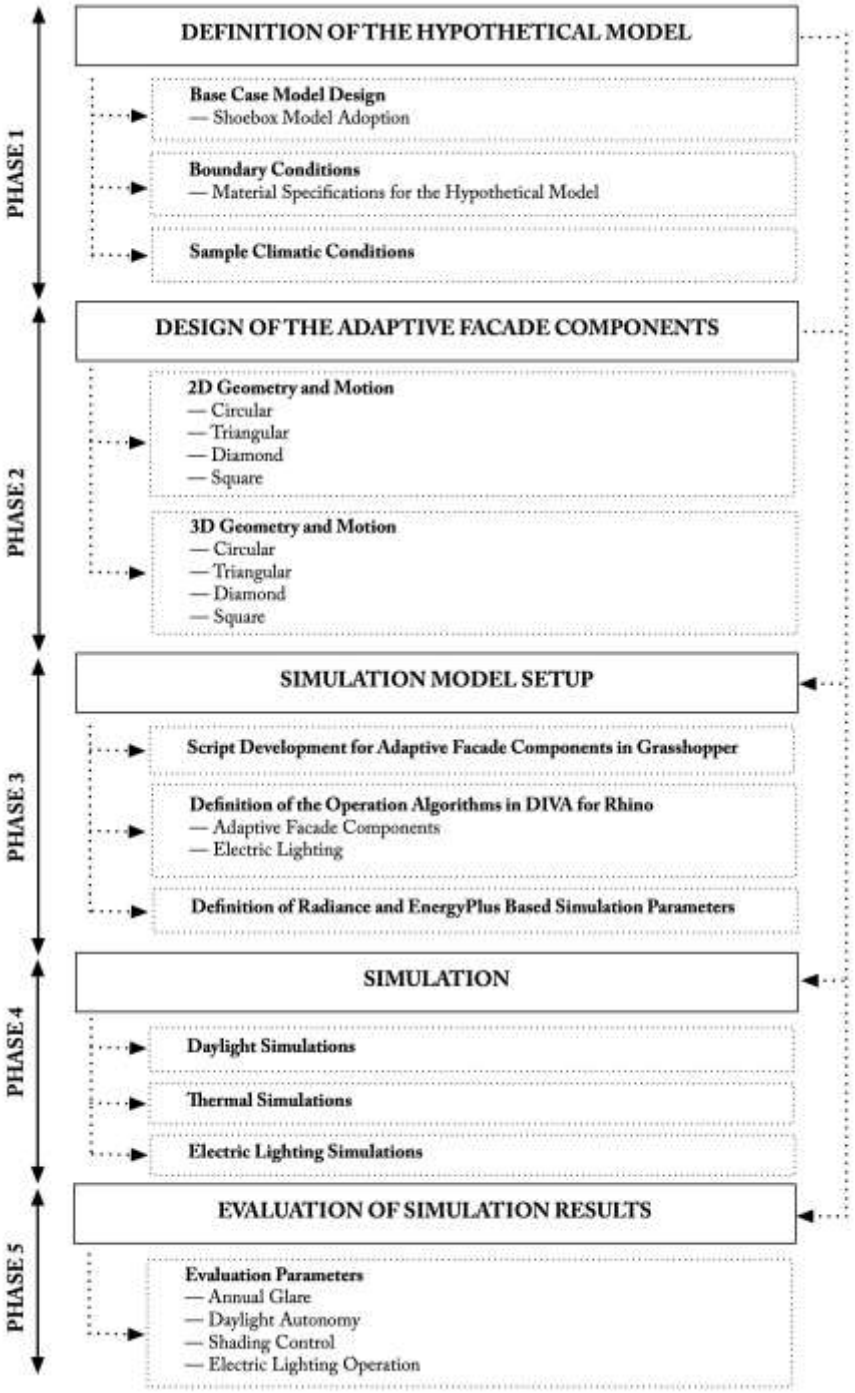


Figure 3.1. Steps of the thesis methodology

The first phase addressed the decisions based on the hypothetical model and climatic conditions used in the simulation study. The second phase focused on generating 2D and 3D adaptive façade components, their geometry specifications, and motion principles. In the third phase the simulation models were setup. The scripts for the adaptive façade components were written in *Grasshopper* and integrated in *Rhino* to ascribe operation algorithms and control parameters of the adaptive façade components and electric lighting in *DIVA for Rhino*. Consequently, parameters were defined for the Radiance and EnergyPlus based simulation. In the fourth phase the simulations were conducted. The base case model (*Reference office*) was first simulated for daylight, electric lighting, and thermal simulation. After simulating the base case model, 2D and 3D adaptive façade components were simulated. In the fifth phase, the simulation results obtained in phase four were evaluated. The results were compared and evaluated for glare, daylight autonomy, shading control, electric lighting operations, and energy use intensity as clearly illustrated in Figure 3.1.

3.1. Definition of the Hypothetical Model

The present study focuses on evaluating daylight autonomy, annual glare reduction, shading control, electric lighting operation, and related energy end-use for proposed 2D and 3D adaptive shading component designs. In order to model different geometries and motion principles Phase 1 of the methodology was intended to define the hypothetical cell type office space to be used in daylight and thermal simulations.

3.1.1. Base Case Model Design

The base case model is an adaptation of the reference office by Reinhart, Jakubiec and Ibarra (2013). It is an open-source model provided in the MIT Sustainable Design Lab (SDL, 2020). The reference office was a hypothetical office unit designed based on the Shoebox Model. This model was widely used for building performance simulations due to its simplicity and ability to analyze certain design parameters quickly (Dogan and Reinhart, 2013; Koene et al., 2014; Reinhart and Davila, 2016; Dogan and Reinhart, 2017). The shoebox model (Figure 3.2).

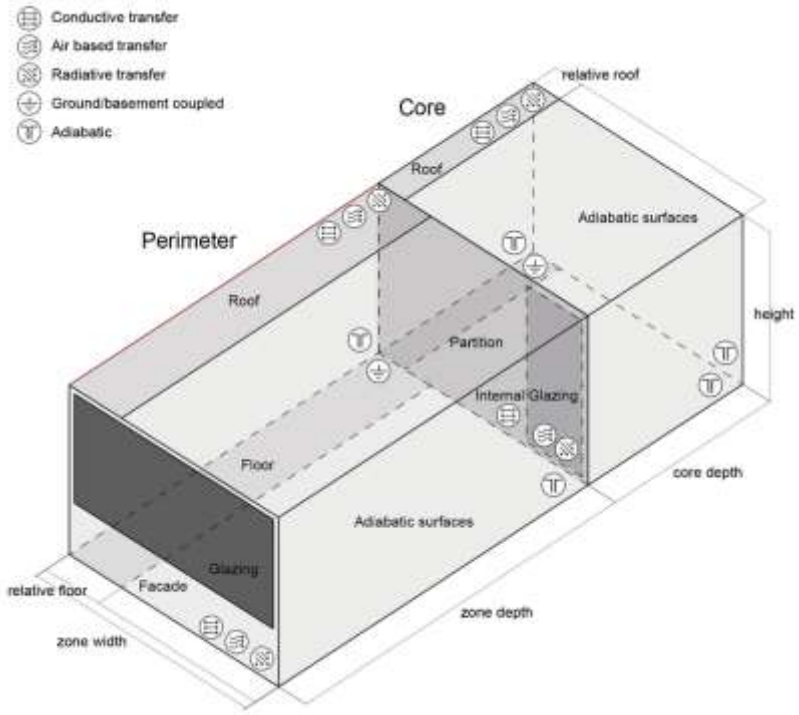


Figure 3.2. Shoebox geometry and heat transfer setup per surface (Dogan and Reinhart, 2017)

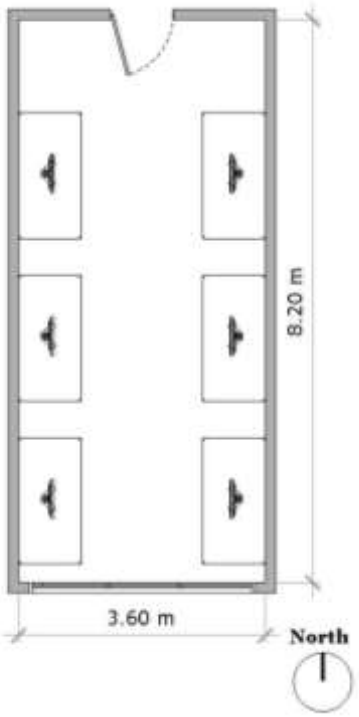


Figure 3.3. The floor plan showing the furniture layout of the reference office

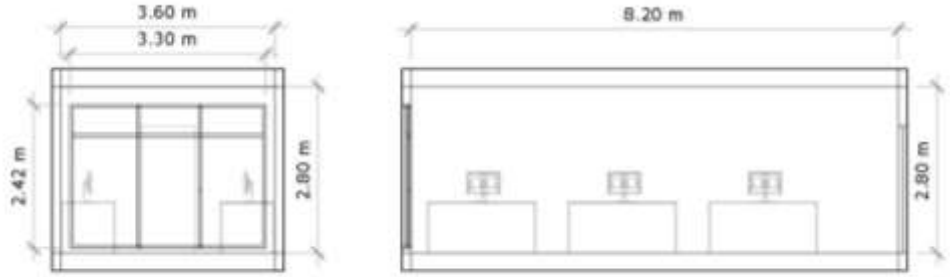


Figure 3.4. South façade of reference office and sectional view of Reference office

The reference office selected for the present study had a deep plan, with a depth of relatively three times the window head height. The interior width, length, and height of the reference office were 3.6 m, 8.2 m, and 2.8m respectively with a floor area of 29.52 m^2. The ceiling height from the floor was 2.8 m. The window of the base case model was located on the south façade with a window to wall ratio WWR of 73%. The outer frame and mullion width are 0.05 m. The walls were 0.15 m thick, and a floor-to-floor height of 3.1 m as illustrated in Figures 3.3 and 3.4 (SDL,2020).

The reference office was assumed to be part of a medium-sized multistory office building of (2300 m^2) floor area. Reinhart et al. (2013) stated that 40% WWR is the optimum size for the reference office and mentioned that utilizing larger WWR on a façade triggers discomfort glare which causes the occupants lower the blinds. Despite the stated condition, this study increased the WWR of the reference office to 73% to test how the various adaptive facades would perform in the case of a larger opening.

3.1.2. Boundary Conditions of the Base Case Model

Materials with different reflectance, R-value, and U-values were assigned to the base case model (*Reference office*) and were identical for all simulations. Table 3.1 indicates the daylight model material assignment, material reflectance, and visible light transmittance for the glazing. Initially, the components of the model were grouped into layers as shown in the component-based on layers column of the table. This was necessary since materials would be assigned in DIVA for Rhino based on these layers. Such approach enables DIVA to successfully send the model to Radiance/Daysim for the daylight simulation. Surfaces with

different reflectance values were assigned to the daylight model and were rendered in greyscale. A correlation study by Lim et al. (2012), between colored and greyscale models for daylighting simulation, confirmed that the performance results were the same and advised the simplification of the model through the use of greyscale model rather than imitating the actual color so long as the surface reflectance values are correctly assigned in the model.

Table 3.1. Shoebox cell-type office model materials and their properties

S/N	Component-based on layers	Assigned material	Material reflectance	Visible light transmittance (VLT)
1	Ceiling	Generic Ceiling_80	80%	
2	Door	Generic Furniture_50	50%	
3	Floor	Generic Floor_20	20%	
4	Furniture	Generic Furniture_50	50%	
5	Glazing	Glazing Double Pane_LowE_65		65%
6	Ground plane	OutsideGround_20	20%	
7	Mullions	Sheetmetal	50%	
8	Roof	OutsideGround_10	10%	
9	Interior Walls	Generic interior walls_50	50%	
10	Exterior Walls	Generic Exterior walls_50/35	50%/35% (inside/outside)	

Table 3.2. Thermal simulation materials

Base Case Model	Materials	U-value	SHGC
Energyplus_Adiabatic: interior walls ceiling floor	Wall_ASHRAE_90.1_2010_Climate_Zone_1-2_Ext_Wall_SteelFramed_IP. R-13+R-3.8ci	Adiabatic surfaces	
Energyplus_Wall: Exterior wall	Wall_ASHRAE_90.1_2010_Climate_Zone_1-2_Ext_Wall_Steel Framed_IP. R-13+R-3.8ci	0.365 W/m^2K	
Energyplus_Glass: window_glazing	Glazing_DoublePane_LowE	1.6 W/m^2K	28%

Table 3.2 presents the materials assigned to the energy model for thermal simulation. The energy model was based on a simplified shoebox model of single planes to serve as walls, ceiling floors, and glazing. The energy model in this study was utilized to simulate heating/cooling load, electric lighting load, and equipment load on an hourly basis for the span of a year. The acquired results were used to generate the energy use intensity (EUI) for the base case model (*Reference office*) and the models that employed 8 different AFSs. As described in Section 3.1.1, the reference office was assumed as a unit in a mid-sized multi-story office building. Such decision makes the internal walls, floor, and the ceiling adiabatic. But the wall facing the south façade was exposed to solar radiation and assigned different layers and materials as shown in Table 3.2. The third row of the table indicates the glazing

material, U-value and the solar heat gain coefficient (SHGC). Separating layers and assigning materials based on the layers is crucial for DIVA to successfully send the energy model to EnergyPlus for thermal simulation.

3.1.3. Sample Climatic Conditions

The sample climatic condition selected for the present study was the Houston climate (Texas, USA). According to the International Energy Conservation Code (IECC) zone map developed by the Department of Energy (DOE, 2020), Houston falls in the Hot-Humid climatic region (Figure 3.5). The climatic regions are classified based on heating degree days (HDD), cooling degree days (CDD), average temperatures, and precipitation. Houston receives more than 20 inches (50 cm) of annual precipitation, 67°F (19.5°C) or higher wet bulb temperature for more than 3,000 hours, 73°F (23°C) or higher wet bulb temperature for more than 1,500 hours during the warmest six consecutive months (April-September) of the year (Michael et al., 2015; NWS, 2011).

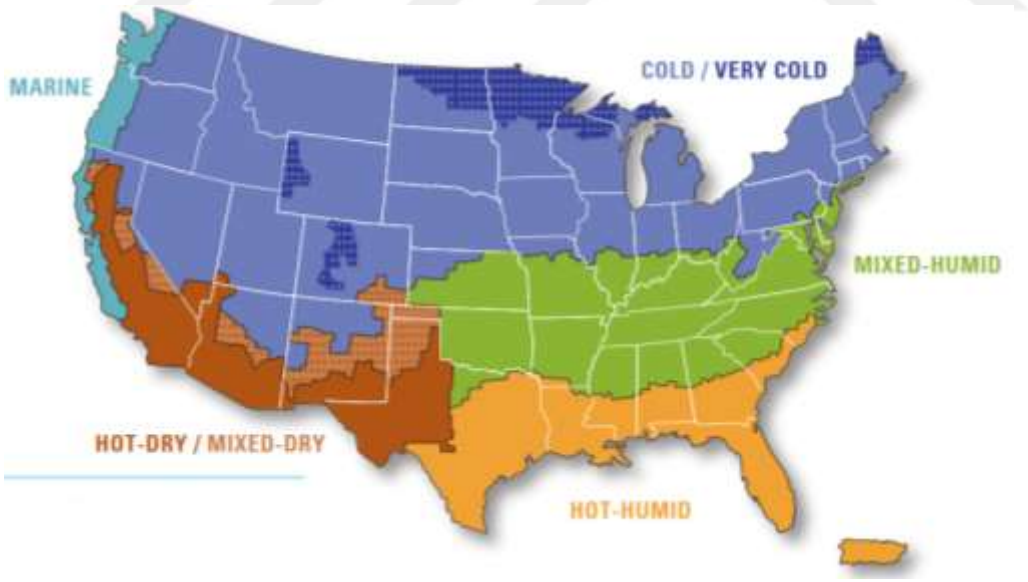


Figure 3.5. Seven climate zones recognized by Building America in the continental US (Source: Michael et al., 2015)

A climate analysis study of the impact of shading strategies for Hot-Humid climate zones and Three (3) other climate zones reported a substantial increase of 13.3% to 26.9%

of indoor comfort in cooling and heating seasons respectively for building envelopes with appropriate shading systems. Studies also indicated that hot-dry, hot-humid, as well as colder mid-western regions with proper implementation of shading strategies, can have a great impact during the summer months with substantial cooling summer loads (Elzeyadi, 2017). Thus, Houston was selected as the main context to evaluate the effects of proposed 2D and 3D adaptive shading component designs in a cell-type hypothetical office on daylight autonomy, annual glare reduction, shading control, electric lighting operation, and related energy end-use. The energy plus weather (epw) file for Houston was retrieved from the EnergyPlus database (EnergyPlus, 2020) and used in DIVA and Rhino 6.

3.2. Design of the Adaptive Façade Components

Eight adaptive façade components were proposed for the south façade of the base case model (*Reference office*), where four were two-dimensional AFCs and four were three-dimensional AFCs. Each AFC is different from others based on geometry, and motion principles. Façade component forms were derived based on four basic geometric shapes: circle, diamond, triangle, and square. The main reason for selecting these AFCs is their ability to respond to the needs of the occupants, change in climate, and improve visual comfort in a building and their capacity to alter their geometry based on daylight levels, daylight intensity, and risk of glare. The system can improve visual comfort, control daylight levels, and the energy performance of a building. Such potentials of AFSs inspired the design of the modules.

2D AFCs were designed as flat surfaces without a depth but with kinetic abilities to respond to changing environments. In comparison to the 2D AFCs, the 3D AFCs have a sectional depth in their typology. These AFCs were classified into 2D and 3D components to investigate their potential of improving visual comfort, daylight levels, and energy performance. Their motion principles and geometric features were further explained in the latter subsections. All AFCs were designed to respond to illuminance levels and Daylight Glare Probability (DGP) levels. Further explanations were discussed in (section 3.3.2.) of this study concerning the operation algorithm of the AFCs.

3.2.1. 2D Geometry and Motion Characteristics for Adaptive Façade Components

The present subsection describes the general design and development process for the 2D adaptive facade systems, the motion, and geometric attributes. Four total 2D AFCs were proposed to create the AFSs:

- 2D Circle
- 2D Triangle
- 2D Diamond
- 2D Square

The 2D Circle component was designed as a circle in a 600 x 600 mm square frame. The framing system of the façade was considered static, but the circle was the kinetic element of the component. The circle rotates at its horizontal axis as illustrated in Table 3.3. The circular element rotates through four stages at an increment of 45 degrees from Stage 1 to Stage 4. This rotation allows the component to open and allow for outdoor view or close to shade the building from direct sunlight and glare. 30 circular 2D AFC were proposed to shade the south façade of the base case model (*Reference office*).

Table 3.3. 2D Circle geometry and motion features

2D Circle (rotational motion)				
	Stage 1	Stage 2	Stage 3	Stage 4
Front	Angle of rotation 180	Angle of rotation 135	Angle of rotation 90	Angle of rotation 45
Side				
Isometric				

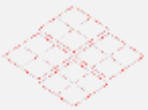
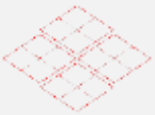
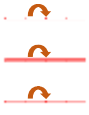
2D Triangle is also an AFC proposed for the south façade of the office space. An equilateral triangle of 700 mm was designed to open and close from its midpoint. The motion

assigned to the geometry is a scaling motion. This allows the triangle to expand and contract from its center to the triangular frame creating the open and close motion. 60 triangular 2D AFCs were placed on the south façade of the office. The 2D triangular AFS moves through 4 stages, Stage 1 is the open stage, and the system continues to close through Stage 2, Stage 3, and Stage 4 as illustrated in Table 3.4.

Table 3.4. 2D Triangle geometry and motion features

2D Triangular (scaling motion)				
	Stage 1	Stage 2	Stage 3	Stage 4
Front	Scaling factor 0.9	Scaling factor 0.6	Scaling factor 0.3	Scaling factor 0.1
				
Side				
Isometric				

Table 3.5. 2D Diamond geometry and motion features

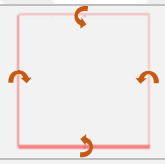
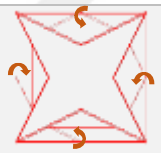
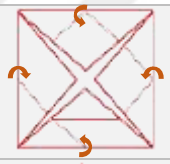
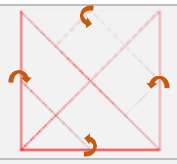
2D Diamond (rotational motion)						
	Stage 1	Stage 2	Stage 3	Stage 4	Stage 5	Stage 6
Front	Degree of rotation 150	Degree of rotation 120	Degree of rotation 90	Degree of rotation 60	Degree of rotation 30	Degree of rotation 0
						
Side						
Isometric						

2D diamond AFC is a 2-dimensional quadrilateral-shaped element that rotates on its horizontal axis as illustrated in Table 3.5. The sides of each diamond element were 340 mm. In this system, the entire elements were adaptive and installed on the south façade were 112

on a diamond grid. The components form the AFS rotates in 6 states with an increment factor of 30 degrees at each stage.

2D Square was designed as a 600 mm AFC dissected diagonally into 4 triangles. The triangles served as the kinetic elements. The elements moved via the flap motion. The diagonal split allowed triangular elements to open and close as indicated in Table 3.6. A total of 30 square 2D components were used on the south façade of the hypothetical model as AFSs.

Table 3.6. 2D Square geometry and motion features

2D Square (flap motion)				
	Stage 1	Stage 2	Stage 3	Stage 4
Front	Degree of flap 90	Degree of flap 60	Degree of flap 30	Degree of flap 0
				
Side				
Isometric				

3.2.2. 3D Geometry and Motion Characteristics for Adaptive Façade Components

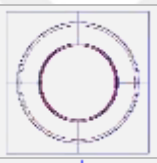
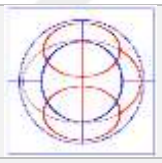
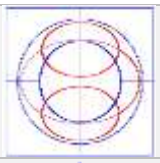
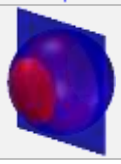
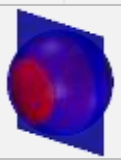
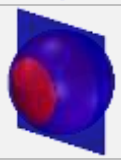
The 3D geometries were designed with a considerable sectional depth compared to 2D geometries. The 3D geometries shared the same motion principled as the 2D geometries based on shape, except the 2D triangular and 3D triangular geometries. The motion of the 2D triangular geometry was a scaling motion while the 3D triangular geometry is a flapping motion as indicated in Table 3.4 and 3.6, respectively. The proposed 3D modules were:

- 3D Circle
- 3D Triangle
- 3D Diamond

- 3D Square

3D Circle module was designed similar to the 2D Circular component in terms of motion principle. The 3D circle AFCs were inscribed in a square frame of 650 mm with a depth and were transformed into a sphere. The sphere was split in both ends to create openings. This sphere was static (in blue). The second sphere (in red) was designed as the kinetic part. It rotates from the horizontal axis within the initial sphere through 4 stages as delineated in Table 3.7. the motion from close to open state is at an increment of 45 degrees.

Table 3.7. 3D Circle geometry and motion features

3D Circle (rotational motion)				
	Stage 1	Stage 2	Stage 3	Stage 4
	Angle of rotation 180	Angle of rotation 135	Angle of rotation 90	Angle of rotation 45
Front				
Side				
Isometric				

The motion principle of the 3D Triangle was different from the 2D Triangular module. The geometry of the 3D Triangle was designed to have certain depth when closed. It was an equilateral triangle divided at its center of gravity, which had a depth used to create 3 triangular flapping elements. The element, shown in Table 3.8, flaps from a closed state 0 degrees to fully open at 45 degrees with an increment of 15 degrees.

The 3D Diamond façade component was designed with a depth of 200 mm from the center of gravity. Depth difference is significant when compared to the 2D Diamond Façade component. The element entirely rotates at the horizontal axis, as represented in Table 3.9. The motion principle was similar to that of the 2D Diamond AFC.

The motion principle of 3D Square AFC was a flap motion. Similar to 2D Square adaptive façade component. The major difference between the 2D and 3D square façade geometry was the attributed depth to the 3D façade geometry. The module at closed state had a depth of 220 mm from its center of gravity. The square module is fully kinetic, in other words has no fixed parts. Table 3.10. illustrates the motion state from 1 to 4.

Table 3.8. 3D Triangle geometry and motion features

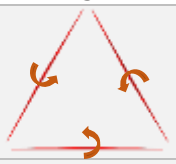
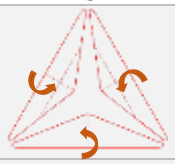
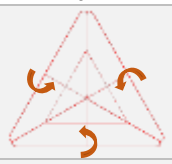
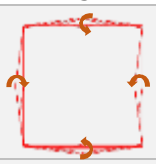
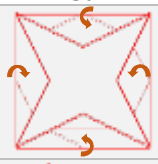
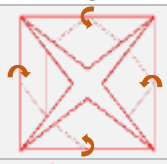
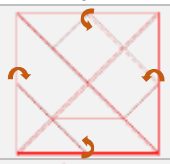
3D Triangular (flap motion)				
	Stage 1	Stage 2	Stage 3	Stage 4
Front	Degree of flap 45	Degree of flap 30	Degree of flap 15	Degree of flap 0
				
Side				
Isometric				

Table 3.9. 3D Diamond geometry and motion features

3D Diamond (rotational motion)						
	Stage 1	Stage 2	Stage 3	Stage 4	Stage 5	Stage 6
Front	Degree of rotation 150	Degree of rotation 120	Degree of rotation 90	Degree of rotation 60	Degree of rotation 30	Degree of rotation 0
						
Side						
Isometric						

Table 3.10. 3D Square geometry and motion features

3D Square (flap motion)				
	Stage 1	Stage 2	Stage 3	Stage 4
Front	Degree of flap 45	Degree of flap 30	Degree of flap 15	Degree of flap 0
				
Side				
Isometric				

3.3. Simulation Model Setup

Prior to the simulation of the base case model *(Reference office)* and 8 AFSs, key parameters and boundary conditions were defined. These parameters were carefully selected and assigned to the model for simulation. The same parameters used to simulate the base case model were utilized in the simulation of the 8 AFSs. This is crucial to warrant a comparative study. The subsequent sections explain the processes carried out to set up the models for daylight, electric lighting, and thermal simulation study.

3.3.1. Script Development for Adaptive Façade Components in Grasshopper

Scripts for the generation of AFCs were developed in Grasshopper. Grasshopper is a visual programming language plugin in Rhino (Scribd, 2021). It was used to generate the geometries and motion principles of the 8 AFSs through mathematical functions and juxtaposition of geometries. Due to its flexibility and algorithm generative ability. It was used to generate the proposed AFSs for the South façade of the base case model *(Reference office).*

The scripting process for the AFSs were initiated from left to right. The scripts begined by defining the location (origin) of the systems and the plane specification which in this case was the XZ plane (South façade). The panel for the placement of each component was defined next based on the geometry of the AFCs. The width and length were specified for each component and the before the formation of geometries. The process of assigning origin, plane, and grid patterns was fairly similar throughout the present study and were delineated in purple in Figures 3.6 - 3.13. Further details for the script development of the AFSs were explained below.

3.3.1.1. 2D Circular Adaptive Façade System

The script for the 2D circular AFS was created using mathematical functions illustrated in Figure 3.6. After assigning the origin and panel orientation, square cells of 600mm were exploded and midpoints were assigned. The midpoints of the exploded frames were used as the tangents of the circular geometry. Tangent circle was attached to the square frame to create a boundary surface. The created surface was extruded to have a depth of 10mm and assigned blue color. This frame element is not kinetic but static. The kinetic element of this module was created by inscribing a circle within the frame. The circle was scaled to a factor of 0.97 and assigned a horizontal rotating axis. The circle was assigned a surface and extrusion of 10mm to have a depth. This element was assigned a red color for visualization and was designed as the kinetic part. The element rotates from 0 to 135 degrees to perform an opening and closing motion illustrated in Figure 3.6. The component was tessellated to form an AFS on the south façade of the base case model *(Reference office)*.

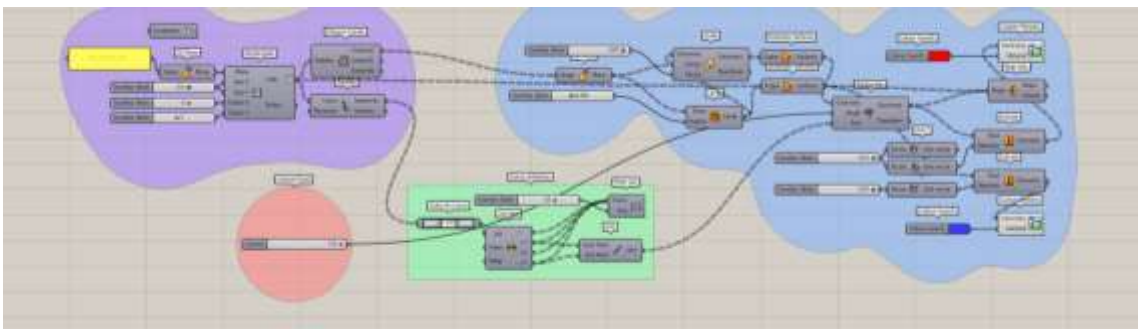


Figure 3.6. 2D circular adaptive façade system script developed in Grasshopper

3.3.1.2. 3D Circular Adaptive Façade System

The scripting of the 3D Circular AFS was similar to the 2D Circular system. After assigning the origin, plane, grid, and size, the square frame was exploded to assign the midpoints as illustrated in pink (Figure 3.7). The points were merged into a circle to create the static frame of the system. A sphere was installed in the static frame and split at both ends to create openings. The sphere was static and attached to the square frame and colored in blue as described in Section 3.2.2. A second sphere was inscribed in the static sphere with a scaling factor of 0.95. The second sphere was assigned a horizontal rotational motion and delineated in green in Figure 3.7.

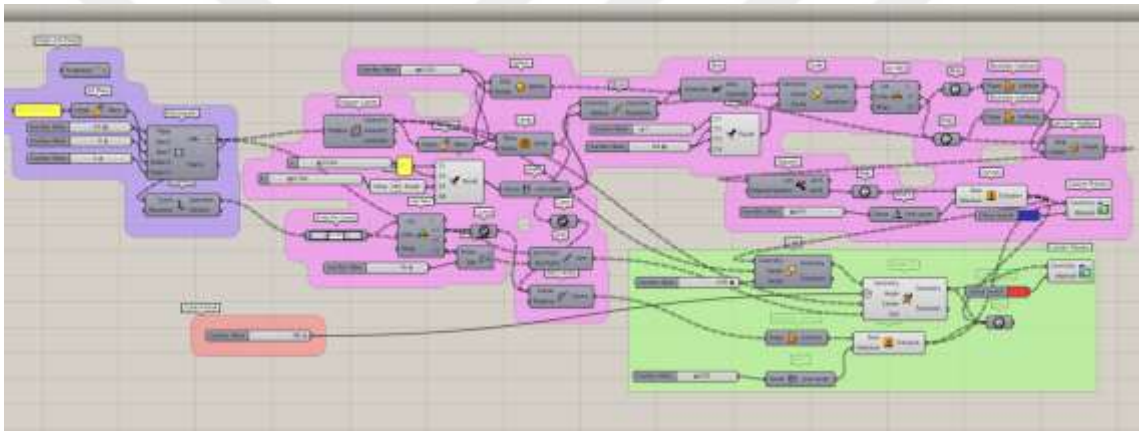


Figure 3.7. 3D circular adaptive façade system script developed in Grasshopper

3.3.1.3. 2D Triangular Adaptive Façade System

The 2D Triangular AFC was assigned a scaling motion. After the origin and plane were defined in the script, a triangular grid tessellation was introduced. The tessellation defined the number of elements installed on the south façade of the hypothetical office unit. The grid of each component was scaled based on the center of gravity with a factor of 0.9. the module was exploded to generate the points needed to extrude the component for a depth of 40mm as seen in Figure 3.8.

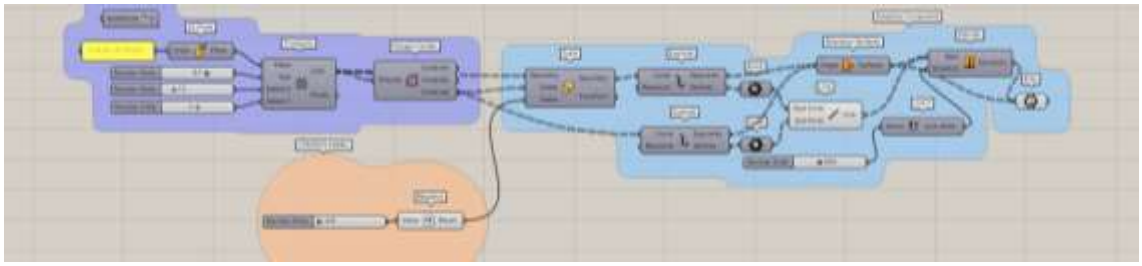


Figure 3.8. 2D Triangular adaptive façade system script developed in Grasshopper

3.3.1.4. 3D Triangular Adaptive Façade System

The 3D triangular AFC was designed with a flap motion at an angle of 45 degrees. The script for this component included the definitions of the origin and triangular grid tessellation. Unlike the 2D triangular AFC, the 3D triangular AFC was exploded and assigned a depth based on its center of gravity. The assigned depth guided the development of the flapping elements of the module. The 3 flapping elements were assigned a fillet function of 2mm at the edges and rotate function at the triangular frame. Surface characteristics were attributed to the elements. The control button for the system was represented in pink (Figure 3.9).

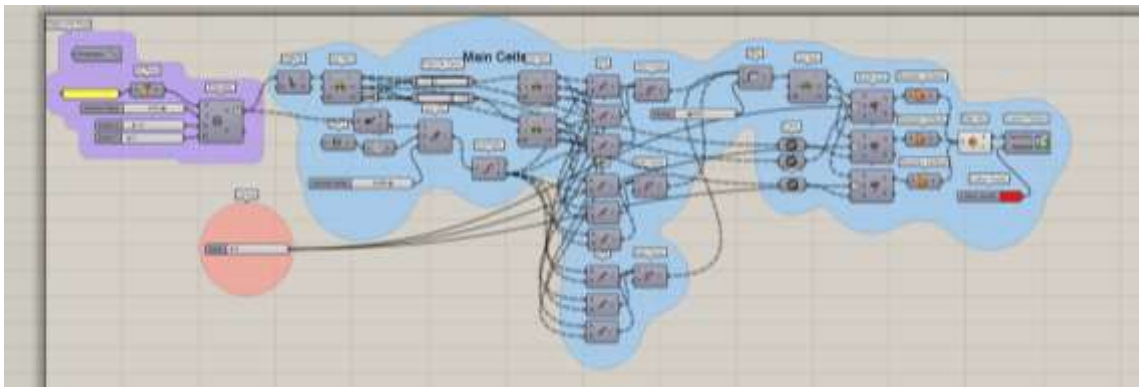


Figure 3.9. 3D Triangular adaptive façade system script developed in Grasshopper

3.3.1.5. 2D Diamond Adaptive Façade System

The scripting for the 2D AFCs were always initiated by defining the origin, plane, and panels. In the 2D Diamond shape, the panel was scaled to a factor of 0.98 and assigned via a horizontal rotating axis as illustrated in Figure 3.10. Each AFC rotates from 0 to 150

degrees for opening and closing. The elements were assigned a depth using the extrude function. The control button marked in blue executed the motion of the system.

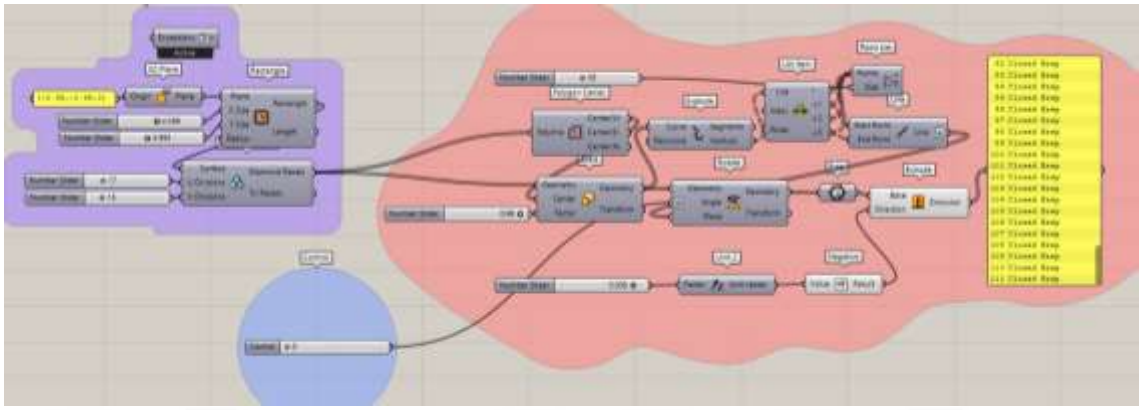


Figure 3.10. 2D Diamond adaptive façade system script developed in Grasshopper

3.3.1.6. 3D Diamond Adaptive Façade System

The script for the 3D Diamond AFC was similar to that of the 2D Diamond AFC. The major difference was indicated in blue in Figure 3.11. After assigning the scale factor, depth was introduced based on the center of gravity of the geometry. The depth was used to assign 4 triangular shapes from the center point to the edges of the scaled diamond geometry. The 4 triangles were assigned boundary surfaces, an extrusion of 8mm, and a horizontal axis that defined the rotation of the AFC.

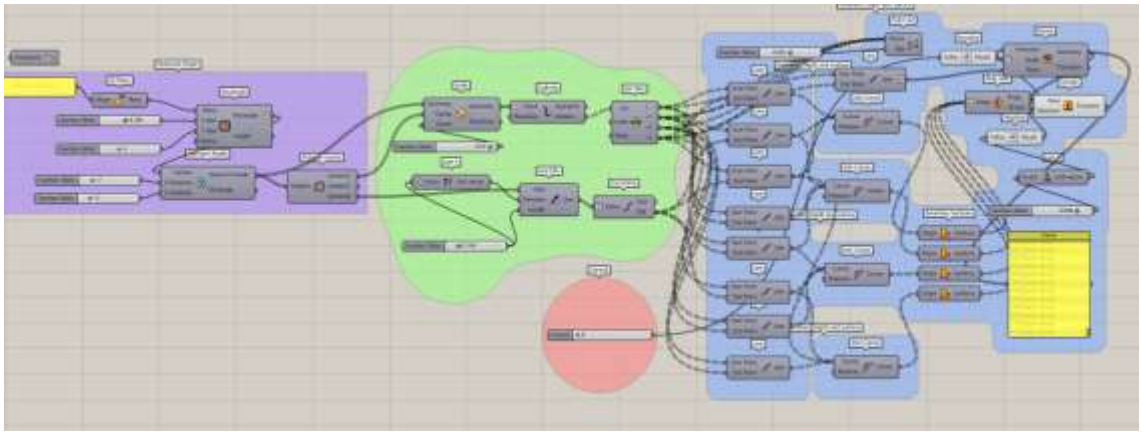


Figure 3.11. 3D Diamond adaptive façade system script developed in Grasshopper

3.3.1.7. 2D Square Adaptive Façade System

The script for 2D Square AFC was initiated via the definition of the origin, plane, and the square grid. The grid was exploded to utilize the edge of each square. The center point of the grid was used to diagonally dissect the square into 4 triangles. The four triangles were assigned surfaces and a rotational motion at the edges. The elements rotate from stage 1 to 4 with an increment of 30 degrees from 0. A thickness of 10mm was assigned to the elements of the module as delineated in Figure 3.12.

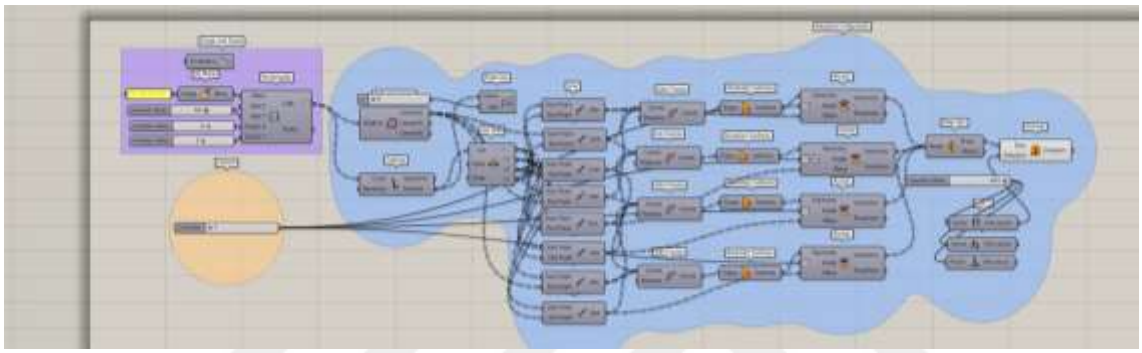


Figure 3.12. 2D Square adaptive façade system script developed in Grasshopper

3.3.1.8. 3D Square Adaptive Façade System

3D Square AFC is similar to 2D Square AFC based on the motion principle; however, their geometries were different. First, the origin and square grid were defined in the script, then the grid was dissected into 4 triangles from the center of gravity. The depth of the component from the center of gravity was 200mm. The endpoint of the 200mm depth was utilized to create the 4 sloped triangles that defined the shading elements. These elements flapped in the frame in 4 stages, between 0 and 45 degrees. The control slider was represented by orange in Figure 3.13.

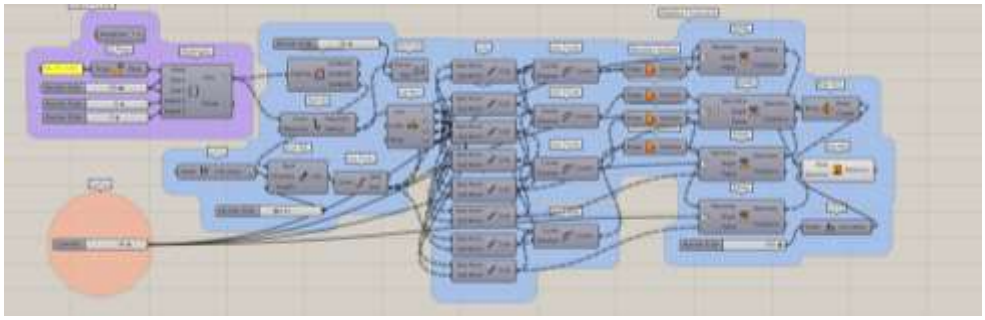


Figure 3.13. 3D Square adaptive façade system script developed in Grasshopper

3.3.2. Definition of the Operation Algorithms in DIVA for Rhino

This section explains the operation algorithm assigned to each AFC described in Section 3.1.1 and its subsections. Figure 3.14 illustrates the algorithm of the AFSs. After writing the script for each AFS, the shading states (see Table 3.11.) were prepared in Grasshopper and exported to DIVA for Rhino. Assigned layers were differentiated to represent the states between open and close.

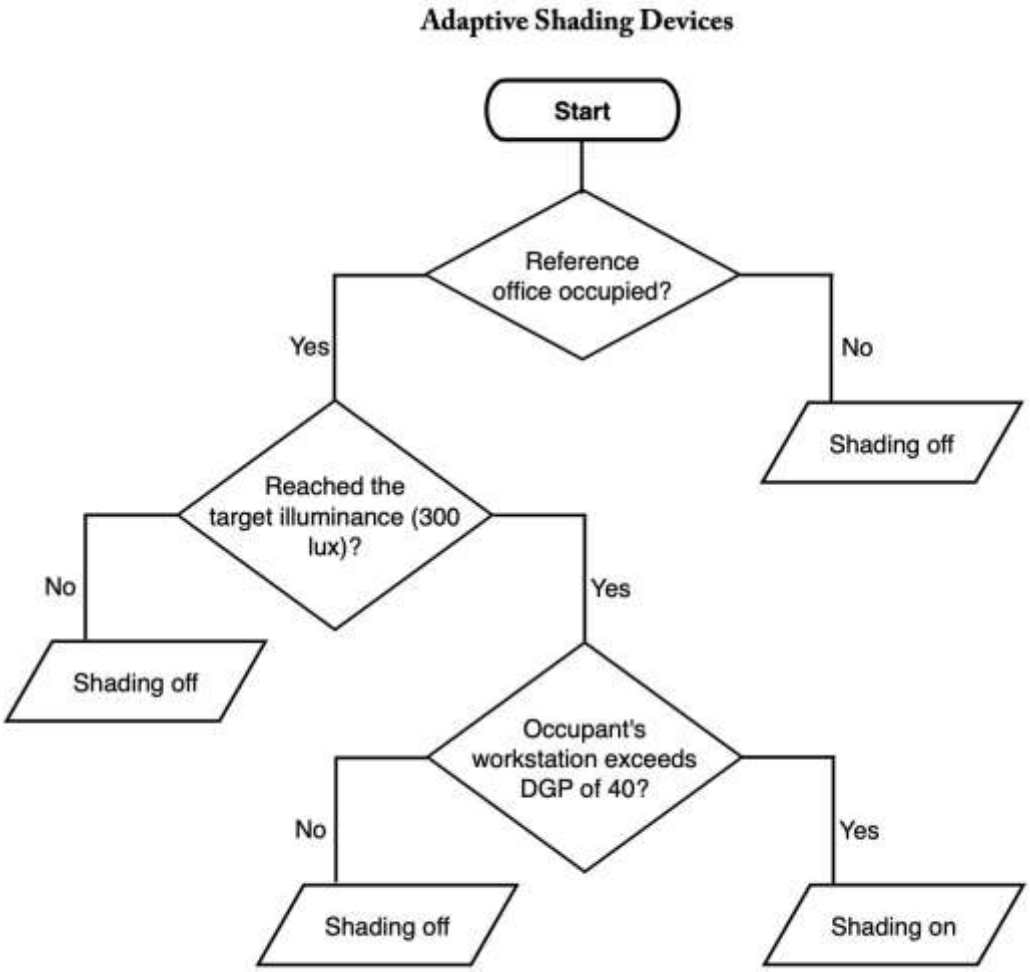


Figure 3.14. Operation algorithm for the Adaptive Façade Systems

The shading type was defined in DIVA for rhino as a mechanical system. Hence, the motion stages of each AFS was defined in DIVA as fully open, half-open, half-closed, or fully closed. The operation state was set to utilize the acquired DGP file from the glare studies conducted in Section 4.1. The light switch algorithm, a user behavior model (Reinhart 2004; 2006), was utilized in the operation of each AFS. As shown in Figure 3.14. and Table

3.11 the AFSs become active when the office space was occupied. The sensors in the office detected the presence of the occupants and the AFSs opened to allow daylight into the space. The sensors also detected if the target illuminance of 300 lux was reached. If not, the shading opens to allow daylight andd if yes, sensors utilize the DGP file to detect point in time experiences for disturbing glare greater than or equal to 40%. Such environmental interaction triggered the AFSs to close by selecting the suitable shading state.

Figure 3.15 illustrates the operation algorithm for the electric lighting of the reference office. The electric lighting control was grouped into two groups (see Figure 4.6). This was a result of the DA simulation which indicated that 47% of the base case office floor area was daylit and one-third of the floor area was underlit (Figure 4.3). The two groups were designated as the Lighting Group 1 (occupancy_always_on) and Lighting Group 2 (occ_dimming). Lighting Group 1 was assigned to the underlit area of the office space. This lighting setup was manually controlled for the 2 occupants of the underlit area of the office space. They utilize the manual (on/off_switch) combined with a switch-off occupancy sensor with 5 minutes delay time. The occupancy sensor switches off the light when the space is not occupied and the light is left on. The lighting fixture has 42.0 W electric power with 0.40 W standby power as stated in Table 3.13. Lighting Group 2 was allocated to the areas benefitting from daylight. The lighting system has 2 lighting fixtures of 84.0 W. the system is manually controlled by an (on/off switch). With a switch-off occupancy sensor similar to lighting group 1. The major difference is the dimming system with photocell control with a ballast loss factor of 0.00 percent. Figure 3.15. shows the operation algorithm of the proposed light control systems. When occupied the lights are switched on, if the target illuminance reaches 300 lux from daylight, the electric lighting goes off. If the target illuminance is not reached. The lighting system operates and illuminates the office space when occupied.

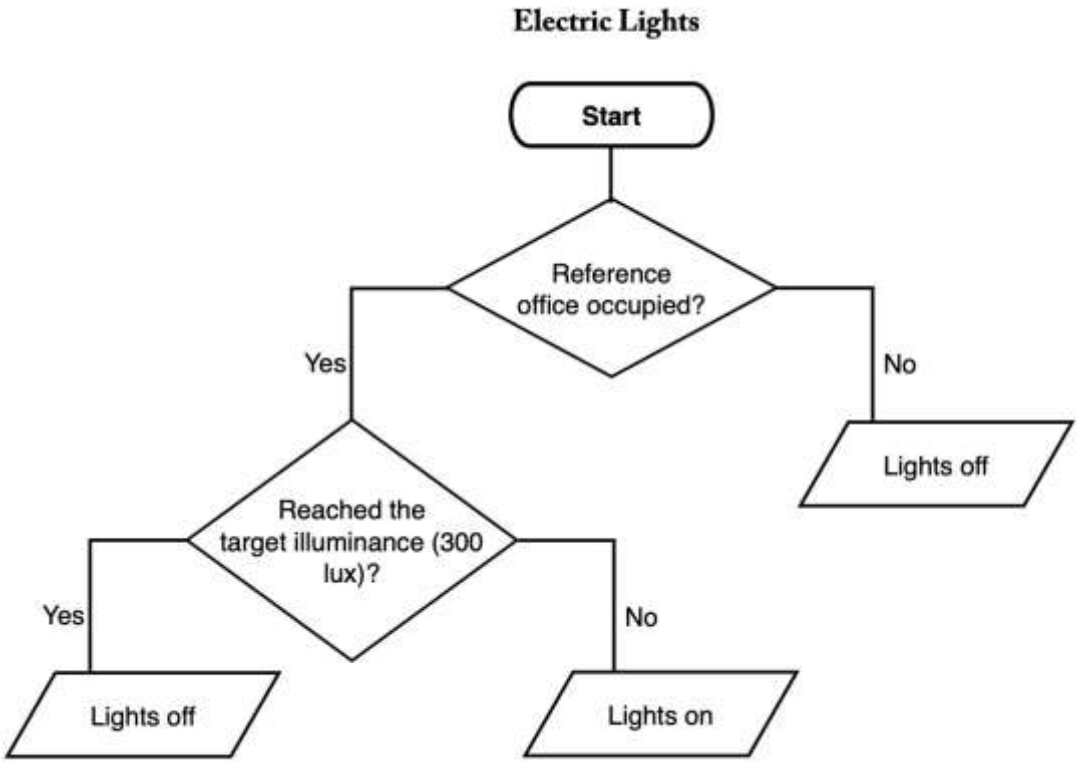


Figure 3.15. Operation algorithm for Electrical Lighting

Table 3.11. illustrates the shading states and shading control of the AFSs. Each AFS moves from an open to close state. The movement principle of each AFS defines the degree or function of motion. Shading groups 1 and 2 are colored in red and blue to distinguish the frames from the kinetic element. All elements in red are kinetic and exhibit motion while elements in blue are static. The AFSs were classified into 2D and 3D systems. Showing each shading state as a component and when applied on the south façade of the base case model *(Reference office)* as a system.

Table 3.11. Shading control and shading states of 2D and 3D AFSs

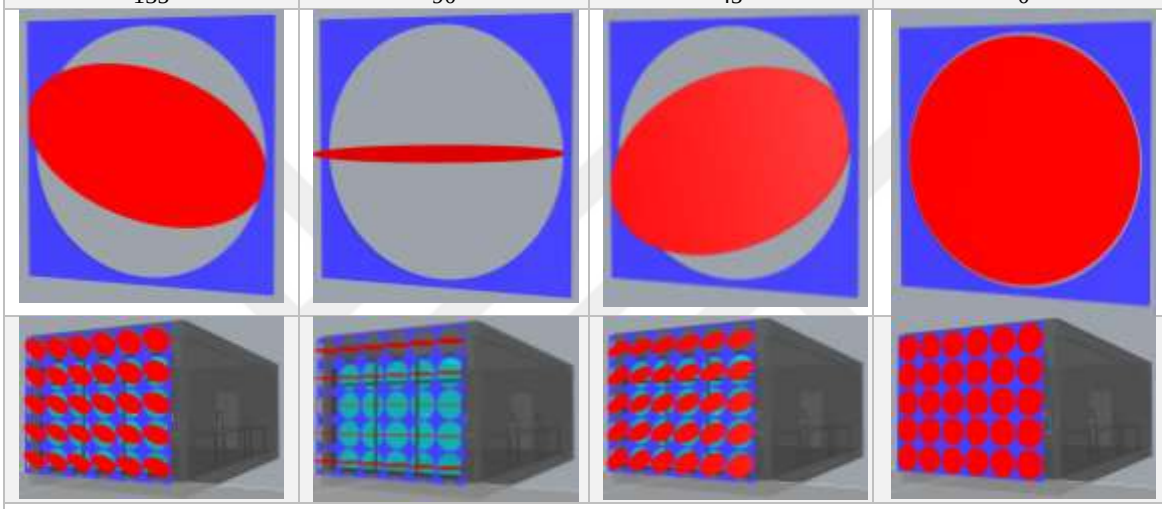
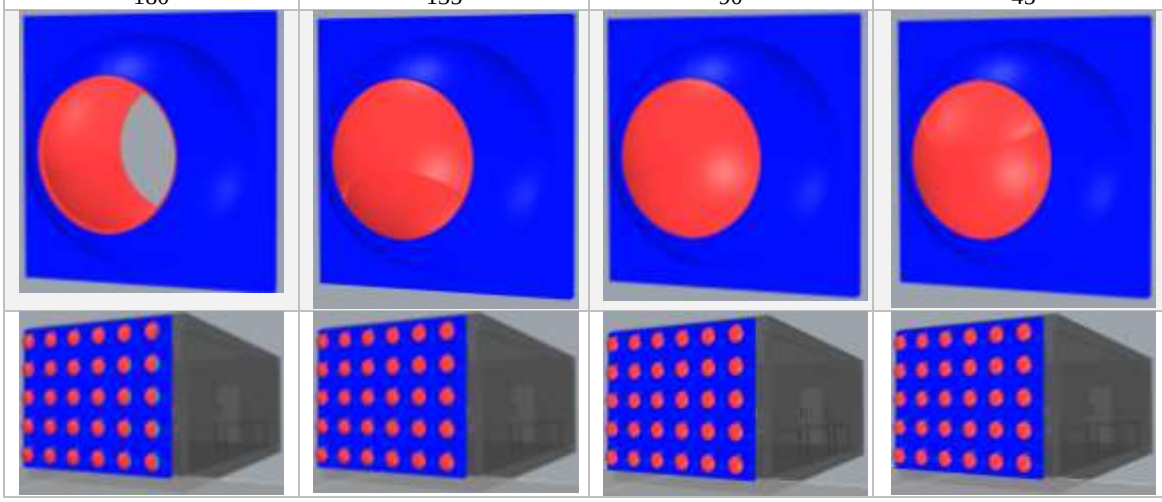
Shading Control			
Shading type	Mechanical		
Operation	DGP controlled_Light switch		
Shading material	SheetMetal		
Base Geometry Layer	Window_Glazing		
Shading Group 1- 2D Circular			
State 1	State 2	State 3	State 4
Angle of rotation 135	Angle of rotation 90	Angle of rotation 45	Angle of rotation 0
			
Shading Group 2- 3D Circular			
State 1	State 2	State 3	State 4
Angle of rotation 180	Angle of rotation 135	Angle of rotation 90	Angle of rotation 45
			

Table 3.11. *continued*

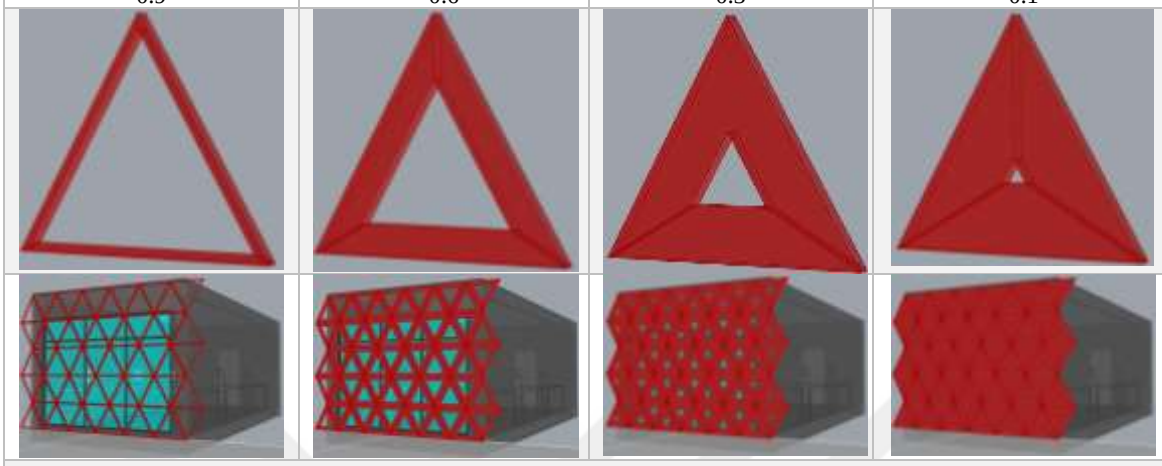
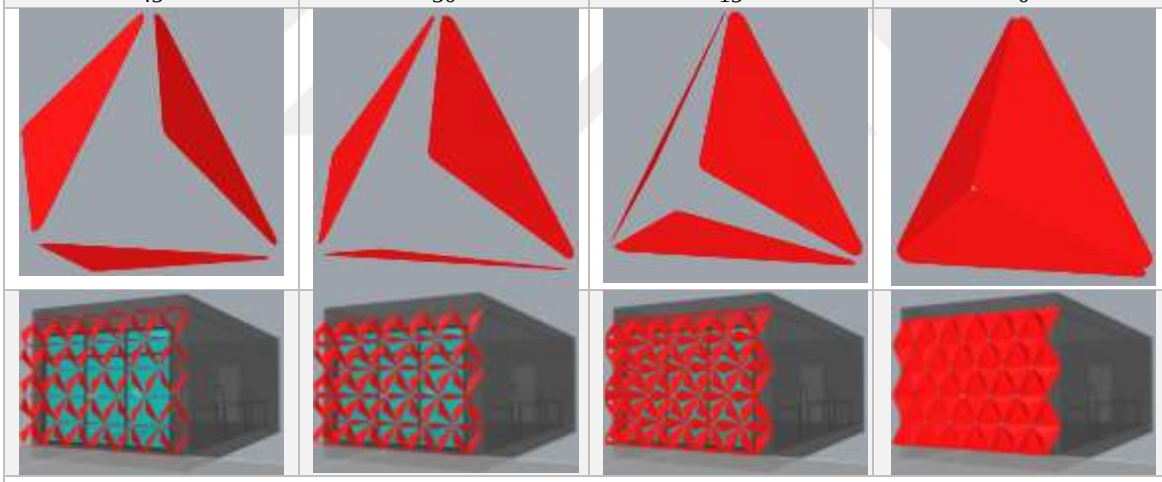
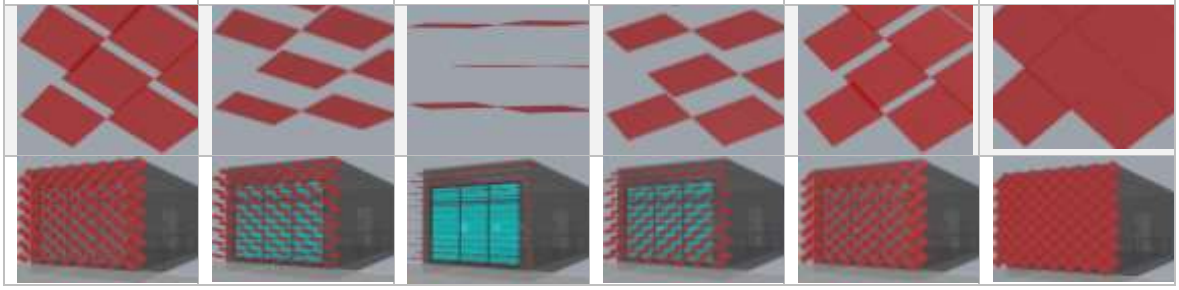
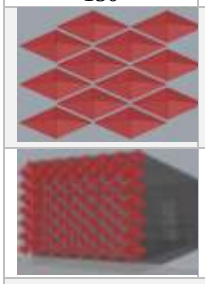
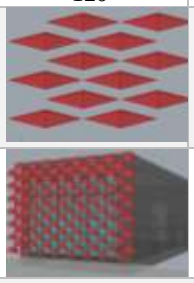
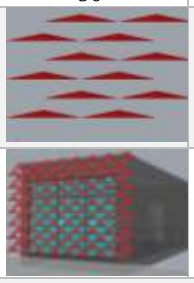
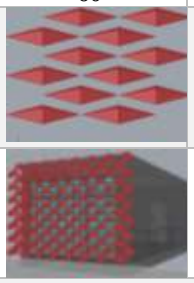
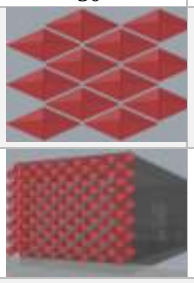
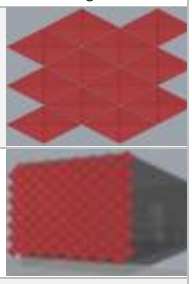
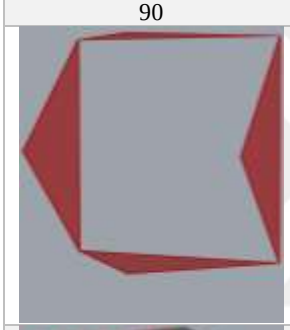
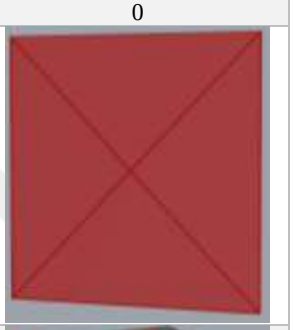
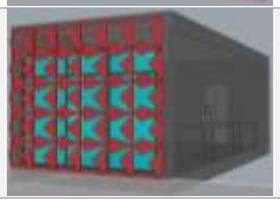
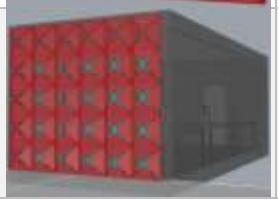
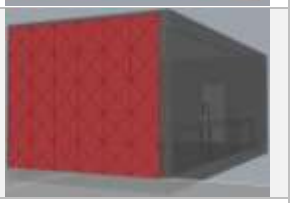
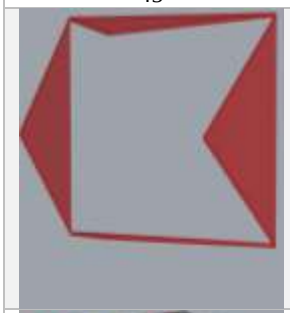
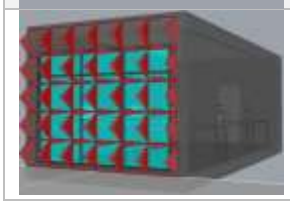
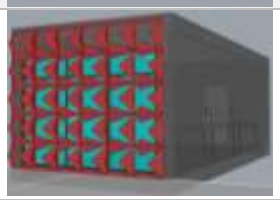
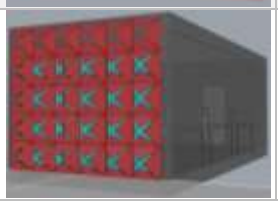
Shading Group 3- 2D Triangular			
State 1	State 2	State 3	State 4
Scaling factor 0.9	Scaling factor 0.6	Scaling factor 0.3	Scaling factor 0.1
			
Shading Group 4- 3D Triangular			
State 1	State 2	State 3	State 4
Degree of flap 45	Degree of flap 30	Degree of flap 15	Degree of flap 0
			
Shading Group 5- 2D Diamond			
State 1	State 2	State 3	State 4	State 5	State 6
Degree of rotation 150	Degree of rotation 120	Degree of rotation 90	Degree of rotation 60	Degree of rotation 30	Degree of rotation 0
					

Table 3.11. *continued*

Shading Group 6- 3D Diamond					
State 1	State 2	State 3	State 4	State 5	State 6
Degree of rotation 150	Degree of rotation 120	Degree of rotation 90	Degree of rotation 60	Degree of rotation 30	Degree of rotation 0
					
Shading Group 7- 2D Square					
State 1	State 2	State 3	State 4		
Degree of flap 90	Degree of flap 60	Degree of flap 30	Degree of flap 0		
					
					
Shading Group 8- 3D Square					
State 1	State 2	State 3	State 4		
Degree of flap 45	Degree of flap 30	Degree of flap 15	Degree of flap 0		
					
					

3.3.3. Definition of Radiance Based Simulation Parameters

The parameters described in this subsection were assigned to the Radiance tool through DIVA for Rhino. Table 3.12 describes the parameters that concern ambient light and intensities of light coming into the space. These parameters were used by Radiance to back trace the light path from the spectator's eyes to the light source. The values of the parameters were allocated to each simulation process. It is crucial that the parameters remain the same during each conducted simulation.

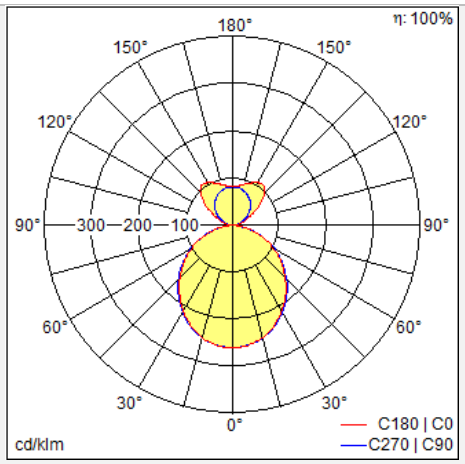
Table 3.12. Radiance simulation parameters

S/N	Name	Value
1	ambient bounce	2
2	ambient division	1000
3	ambient sampling	20
4	ambient resolution	300
5	ambient accuracy	0.1

Three electric lighting fixtures, each with a 42 W luminance power, were proposed for the present study. Semi-direct lighting fixtures were placed on the ceiling above each row of the occupant's desk. Table 3.13 shows details of the lighting fixtures used for the electric lighting study. These details were essential to inform Radiance for running annual electric lighting simulations and to assess the energy consumption due to electric lighting in the office space. Further details were discussed in Section 4.3.

Table 3.13. Electric lighting fixture details

SLOIN DI K SL 830 L005 LDE WH



Semi-direct Light distribution

Light Source	LED Luminaire
Luminous flux	4315 lm
Luminaire efficacy	103 lm/W
Color temperature	3000Kelvin
Luminaire input power	42 W Power factor = 0.88
Standby Power	0.4 W
Dimming: LDE dimmable to 1%; over DALI, DSI and switchDIM; DC level is adjustable	

Occupancy schedules: These schedules involve the duration by which the office space is in use by the occupants daily, through 8 am to 6 pm taking the daylight savings differences of 60 minutes into consideration. The total annual occupied hours of the office space are 3650. This defines the duration of each annual simulation.

Recommended light levels by space: The US General Services Administration provides lighting levels and LPDs as a guide for government buildings and other buildings (U.S. General Services Administration, 2021). Table 3.14 presents recommended light levels from IESNA Lighting Handbook and LPD levels from the IECC 2021 (IECC, 2021; Wotton, 2000). The required light levels appear to be within a range since different tasks require certain amount of illumination. Commonly, detailed tasks require more amount of light while high contrast and less detailed task require less lighting (Archtoolbox, 2021).

Target illuminance: A target illuminance of 300 Lux was assigned for the office space. Table 3.14. inspired the selection of the 300 lux as the target illuminance. This served as a vital parameter for Radiance based simulations.

Table 3.14. Recommended light levels and lighting power density by space

Room Type	Light Level (Foot Candles)	Light Level (Lux)	Iecc 2021 Lighting Power Density (Watts Per Sf)
Cafeteria - Eating	20-30 FC	200-300 lux	0.40
Classroom - General	30-50 FC	300-500 lux	0.71
Conference Room	30-50 FC	300-500 lux	0.97
Corridor - General	5-10 FC	50-100 lux	0.41
Corridor - Hospital	5-10 FC	50-100 lux	0.71
Exhibit Space (Museum)	30-50 FC	300-500 lux	0.31
Gymnasium - Exercise / Workout	20-30 FC	200-300 lux	0.90
Gymnasium - Sports / Games	30-50 FC	300-500 lux	0.85
Kitchen / Food Prep	30-75 FC	300-750 lux	1.09
Laboratory (Classroom)	50-75 FC	500-750 lux	1.11
Laboratory (Professional)	75-120 FC	750-1200 lux	1.33
Library - Stacks	20-50 FC	200-500 lux	1.18
Library - Reading / Studying	30-50 FC	300-500 lux	0.96
Loading Dock	10-30 FC	100-300 lux	0.88
Lobby - Office/General	20-30 FC	200-300 lux	0.84
Locker Room	10-30 FC	100-300 lux	0.52
Lounge / Breakroom	10-30 FC	100-300 lux	0.59
Mechanical / Electrical Room	20-50 FC	200-500 lux	0.43
Office - Open	30-50 FC	300-500 lux	0.61
Office - Private / Closed	30-50 FC	300-500 lux	0.74
Parking - Interior	5-10 FC	50-100 lux	0.15
Restroom / Toilet	10-30 FC	100-300 lux	0.63
Retail Sales	20-50 FC	200-500 lux	1.05
Stairway	5-10 FC	50-100 lux	0.49
Storage Room - General	5-20 FC	50-200 lux	0.38
Workshop	30-75 FC	300-750 lux	1.26

3.3.4. Definition of EnergyPlus Based Simulation Parameters

The parameters required for a successful thermal simulation were defined in this section. These parameters were assigned to the energy model through DIVA for Rhino. The office setpoint and setback for heating and cooling were defined in this section. Table 3.15 outlines the heating, ventilation, and air conditioning (HVAC) configurations, occupant density, equipment power density, and air exchange rate. These parameters were assigned to the energy model in Figure 3.18, before running the thermal simulations.

Setback controls: ASHRAE 90.1 2010, section 6.4.3.3.2 states that, heating systems located in climate zones 2–8 should be equipped with setback controls that can automatically restart and temporarily operate the system as required to maintain zone temperatures above a heating setpoint adjustable down to 55°F (13°C) or lower. Cooling systems located in climate zones 1b, 2b, and 3b should be equipped with controls that have the capability to automatically restart and temporarily operate the system as required to maintain zone temperatures below a cooling setpoint adjustable up to 90°F (32°C) or higher or to prevent high space humidity levels" (ASHRAE, 2010). Specifically, the investigated Office unit is located in the second climate zone which is a hot-humid climate zone, therefore, the setback control in ASHRAE 90.1 2010 was adopted, the heating setpoint and cooling setpoint was set to 22 °C and 26 °C respectively. The heating setback and cooling setback were set to 15 °C and 32 °C respectively.

Equipment power density and process load and plug loads: According to ASHRAE 211 (2018), the appropriate installed power density (W/ft^2 or W/m^2) of plug loads in the building, can be estimated based on observed densities of office equipment, including number and type of computer equipment. The resulting peak occupant load is $7.38W/m^2$/occupant. Also, ASHRAE 90.1-2007 (Table G3.1.1), as cited in Reinhart et al. (2013) asserted that the baseline HVAC system for such a building is a packaged rooftop VAV unit with reheat (ASHRAE, 2007). Cooling and heating energy consumption calculations are simplified by multiplying loads by an annual mean COP of 3.02 for the cooling system and 0.8 for a natural gas boiler as per ASHRAE/USGBC/ANSI 189.1 (2010) for >70kW and <223kW cooling capacity. No plenum was considered. Ventilation rates

were assumed based on ASHRAE guidelines. Only energy use for conditioning the fresh air was considered.

Table 3.15. Parameters for EnergyPlus based simulation

THERMAL SINGLE-ZONE PARAMETERS	
Occupant Density (m^2/occ)	4.92
Equipment Power Density (W/m^2)	11.00
Air Change per Hour (ACH)	0.3
CONDITIONING SYSTEMS	
Heating Efficiency	0.9
Cooling Efficiency	3.0
Cooling Setpoint (°C)	26
Cooling Setback (°C)	32
Heating Setpoint (°C)	22
Heating Setback (°C)	15

3.4. Simulation of the Hypothetical Cell-Type Office Unit

3.4.1. Daylight Simulations

Climate-based daylight metrics for the proposed adaptive façade systems were simulated annually via DIVA for Rhino. Prior to the daylight simulations, 6 occupants in the office were investigated for Daylight Glare Probability (DGP). According to Hosseini et al. (2020), HarperCollins defined glare as the human sensation towards light within the field of vision of the eye that exceeds the brightness the eye is adapted to.

Reinhart (2012), in daylight performance predictions asserted that Glare was classified into disability glare and discomfort glare. Disability glare is the inability of a person to clearly see objects in a scene due to the presence of glare and discomfort glare is the tiring of the eyes prematurely. Although disability glare is easy to identify in a daylit interior space, discomfort glare is hard to figure out due to being closely linked to the overall indoor environmental satisfaction of the occupant. Discomfort glare is a highly subjective phenomenon and was studied for years. It was widely accepted that the horizontal plane was

a poor predictor of discomfort glare as a person's visual experience of a space was partly affected by the amount of light falling on the work plane. Instead, glare analysis should be based on an observer's luminance distribution in their field of view. Therefore, daylight glare probability (DGP) was derived by Wienold and Christoffersen as a discomfort glare index in laboratory studies. A glare index is a result derived from human studies through numerical evaluation of high dynamic range images using a mathematical formula. DGP has been categorized in four groups: imperceptible (30–35), perceptible (35–40), disturbing (40–45), and intolerable (45–100) (Hensen and Lamberts, 2012).

DGP is mathematically defined via the following equation;

$$DGP = 5.87 \times 10^{-5} E_v + 9.18 \times 10^{-5} \log\left(1 + \sum_i \frac{L_{s,i}^2 \omega_{s,i}}{E_v^{1.87} P_i^2}\right) \qquad \text{Equation 3.1.}$$

Where E_v is the vertical eye illuminance; $L_{s,\,i}$ is the luminance of source 'i'; ω_s, i is the solid angle of source l and P is the Guth position index, a weighing function that varies with the distance of a glare source form the field of vision (Hensen and Lamberts, 2012).

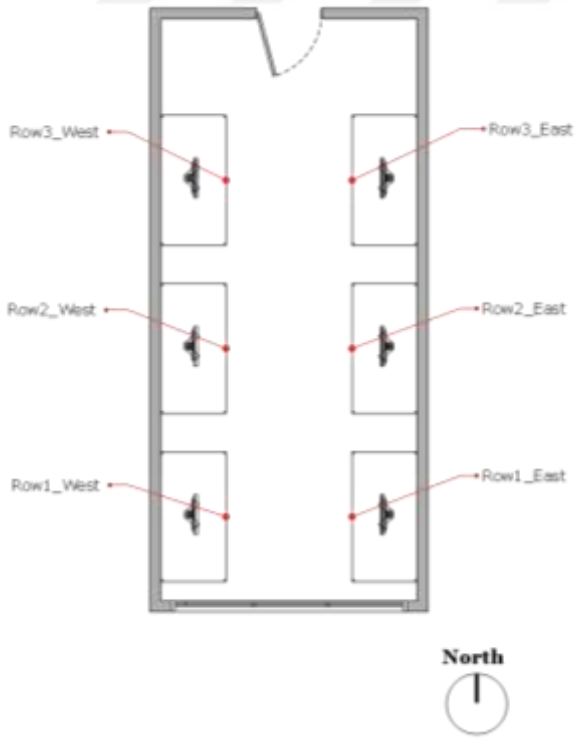


Figure 3.16 Plan showing occupant work plane

Given the scope above, each work plane was studied for glare simulation to determine the occupant with the most glare disturbance. This helped in selecting the appropriate workstation to generate the daylight glare probability (DGP) index. Figure 3.16 illustrates the work plane of occupants in the office. Six workstations were simulated (see figure 4.1) and row1_west was the workstation experiencing the most percentage of DGP. A DGP of 100 was recorded. This acquired DGP was used in the control of the AFSs for the DA and Thermal simulations.

3.4.2. Thermal Simulations

The thermal simulation requires a simplified geometry of the office space. The model is a single zone model that replicates the volume of the actual model of the office space. Walls, floor, ceiling, and fenestrations were replaced with single plane geometry. These planes as illustrated in figure 3.18. were defined as single planes with their normal facing outward not inward. Materials with different R-values and U-values were assigned to these planes as explained in Table 3.2. The south façade wall was assigned a different layer where heat transfer occured and the internal walls, ceiling, and floors were defined as adiabatic.

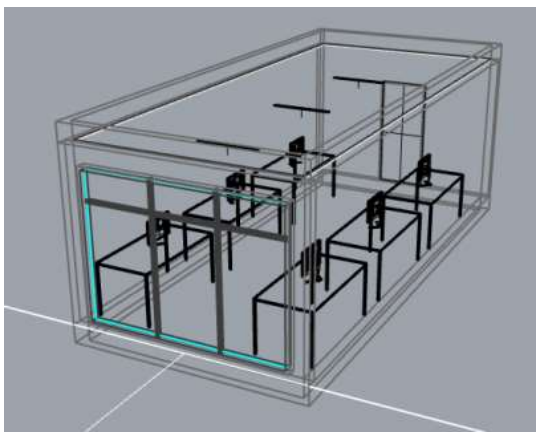
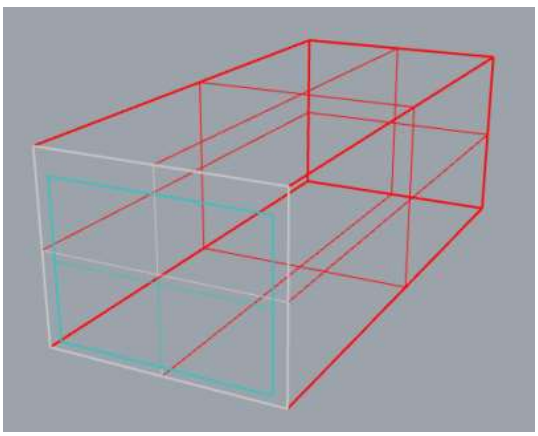

(a)

(b)

Figure 3.17. The geometry of reference office (a) Base case model (b) Energy model

4. RESULTS AND DISCUSSION

The present section discusses the outcomes of the conducted simulations. The results from the dynamic performance metric simulations such as Daylight Autonomy, Electric lighting, Shading Control, Annual Glare, and Thermal simulations were discussed in subsections. The performance of the 2D and 3D AFSs and their impact on building EUI, daylight distributions, and glare management were analyzed in detail in comparison to the base case model. The logic behind this simulation study to investigate daylight levels and solar gains of the base case model *(Reference office)* and the 2D and 3D AFSs were based on;

- Conducting a ***glare study*** for all occupants in the office space to identify occupants experiencing high DGP levels and generate the DGP file for the subsequent simulations.
- Identifying the ***daylit*** and ***underlit*** areas of the office space through DA simulation.
- Assigning electric lighting fixture with occupancy sensors to the underlit parts of the space and assign electric lighting fixture with occupancy sensors combined with photo sensors to the daylit area to compensate for situations with insufficient illuminance from daylight.
- Utilizing the acquired DGP file from the glare studies in the operation algorithm of the 2D and 3D AFSs.
- Conducting an annual climate-based daylight metrics simulation of Daylight Autonomy, Electric lighting study, and Thermal simulations for the 2D and 3D AFSs. Also, generated shading control for the AFSs and EUI.

The steps mentioned above were observed meticulously and the obtained results were presented in the subsections below.

4.1. Annual Glare Simulation Results

The annual glare simulation was essential to identify the office space occupants that experience visual discomfort due to glare. Table 4.1 shows the annual glare simulation and

point-in-time simulation studies conducted for the 6 occupants of the base case model *(Reference office).* The point-in-time glare simulations for the 6 work planes were run for 9 am on 21st of September. The results indicated that the occupant at Row1_West experienced 100% DGP which makes it intolerable glare. Row1_East experienced 72% DGP, which was also classified as intolerable glare. Row2_West and Row2_East experienced a 34% and 33% DGP, respectively, both of which were imperceptible glare. Row3_West and Row3_East experienced 24% and 23% of DGP, respectively, both of which were also imperceptible glare. This indicated that Row1_West experienced the most percentage of discomfort by glare. In other to corroborate the findings. An annual glare simulation was conducted to show the DGP level for each hour the office was occupied. Row1_West and Row1_East exhibit intolerable glare towards mid-October to February. This is as a result of the altitude of the Sun. from the Equinox to the Winter Solstice the altitude of the sun gets low. The annual glare simulation result of Row1_West was selected as the work plane position for the simulation of the 2D and 3D AFSs.

After studying the work planes for glare and selecting for Row1_West position, the AFSs were simulated for DGP by conducting an annual glare simulation. The tables below explain the processes of each AFS.

Table 4.2 illustrates the 2D Circular façade system, including the shading state, shading geometry, and annual glare simulation for each state. DIVA conducts annual glare simulation for each shading state of the 2D Circular façade system. After the results for each stage were generated, DIVA analyzed the results and generated a single optimized shading for the annual glare simulation as illustrated in Table 4.10. The generated annual DGP with shading for the 2D circular façade system was used in the DA, Electric lighting, and thermal simulation of the 2D circular AFS.

Table 4.1 Glare study for all work planes

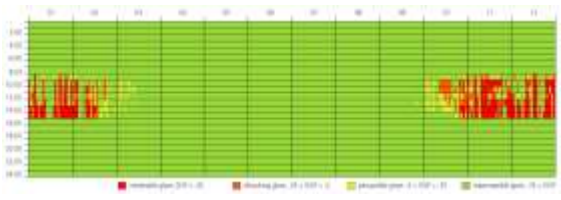
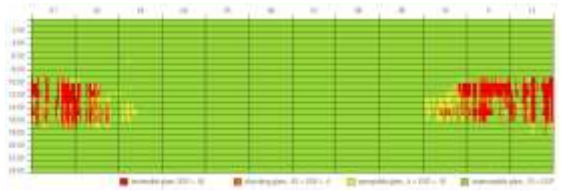
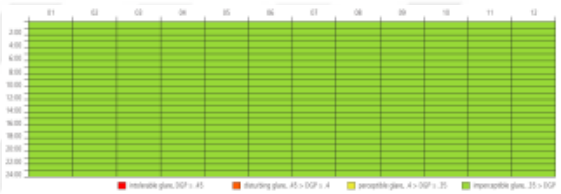
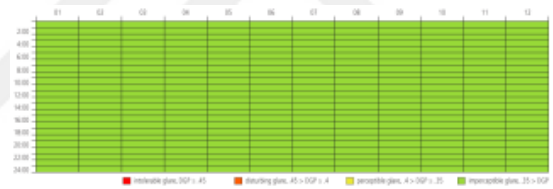
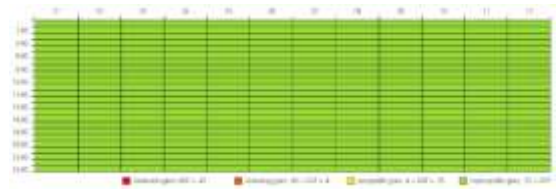
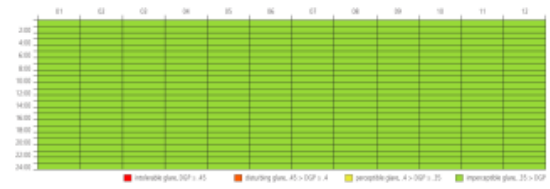
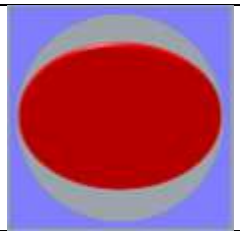
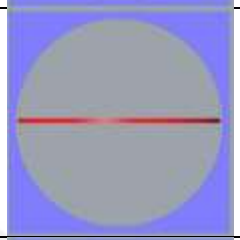
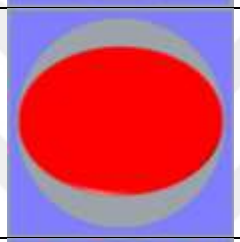
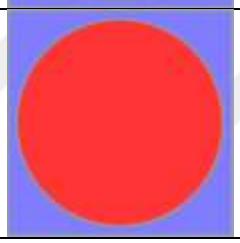
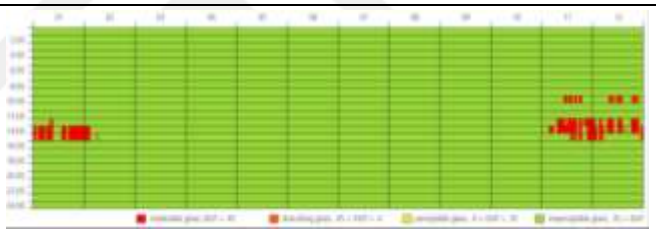
S/N	Work plane	Point in time glare simulation	Annual glare simulation	(DGP)
1	Row1_West			100
2	Row1_East			72
3	Row2_West			34
4	Row2_East			33
5	Row3_West			24
6	Row3_East			23

Table 4.2 Annual glare simulation (2D Circular façade system)

S/N	Shading State	Shading geometry	Annual Glare Simulation
1	2D Circular @ 135 open		
2	2D Circular @ 90 open		
3	2D Circular @ 45 open		
4	2D Circular @ 0 closed		

The annual glare simulation for the shading states of the 3D Circular façade system were presented Table 4.3. Shading state 1 partly reduced the DGP, while shading states 2 and 4 eliminated the DGP. The single shading annual glare simulation result for this AFS was illustrated in Table 4.10. It eliminated the disturbing and intolerable glare for the whole year. The generated DGP from the annual glare simulation was used to simulate the 3D circular façade system for DA, Electric Lighting, and Thermal simulation.

Table 4.3 Annual glare simulation (3D Circular Facade system)

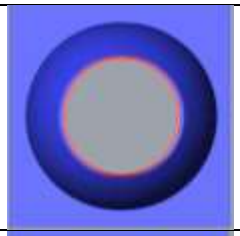
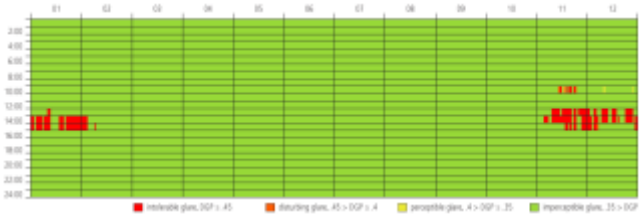
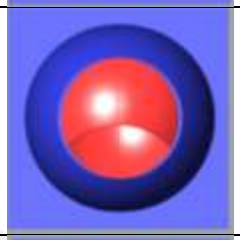
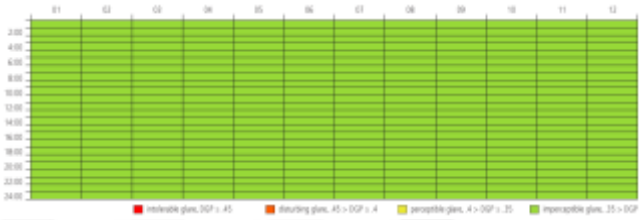
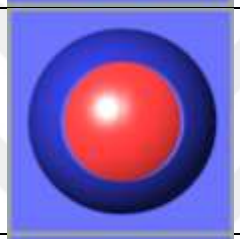
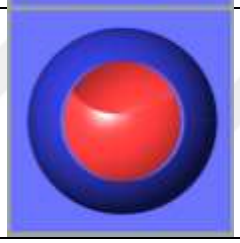
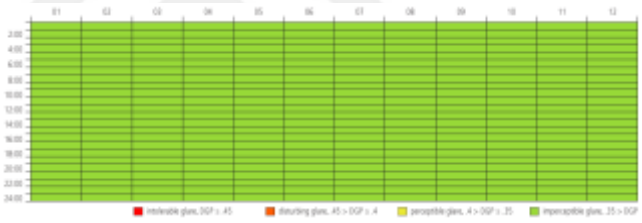
S/N	Shading State	Shading geometry	Annual Glare Simulation
1	3D Circular @ 180 open		
2	3D Circular @ 135 Half-open		
3	3D Circular @ 90 closed		
4	3D Circular @ 45 Half closed		

Table 4.4 delineates the shading states, shading geometries, and annual glare simulation results of the 2D Triangular AFS. Shading state 1 performed poorly in reducing the intolerable glare experienced during the winter months. Shading state 2 reduced the perceptible glare disturbance but not the intolerable glare. Shading stage 3 slightly reduced the intolerable glare compared to the shading state 2. Shading state 4, the closed shading geometry, performed better compared to the other three shading states. No glare was recorded.

Table 4.5 shows the shading states and results of the annual glare simulation conducted for the 3D Triangular façade system. Shading states 1, 2, and 3 partly reduced glare. Shading state 3 eliminated the glare in the office space.

Table 4.4 Annual glare simulation (2D Triangular Facade system)

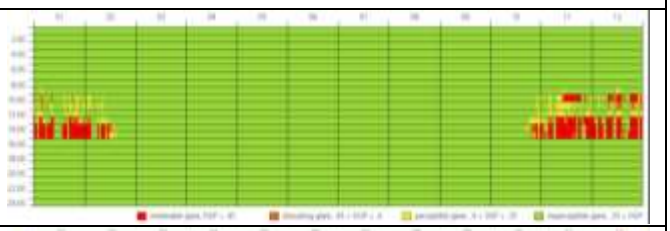
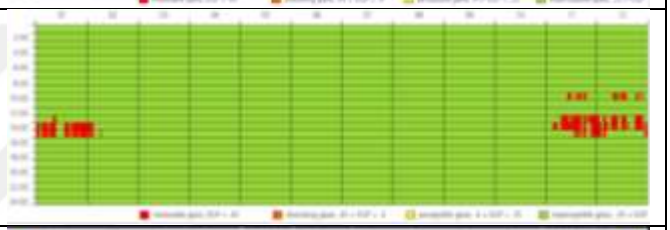
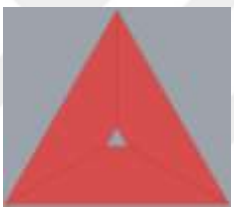
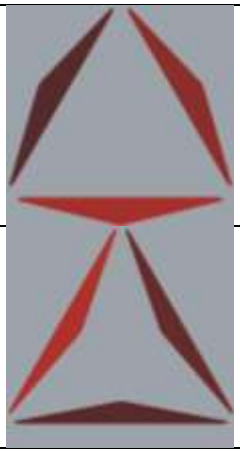
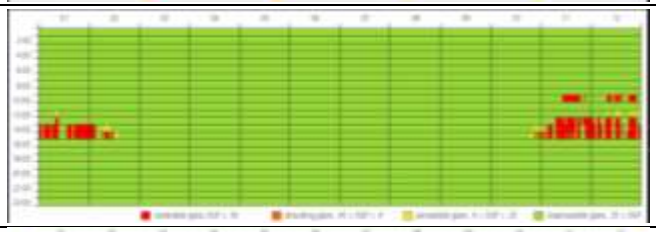
S/N	Shading State	Shading geometry	Annual Glare Simulation
1	2D Triangular @ 0.9 open		
2	2D Triangular @ 0.6 Half open		
3	2D Triangular @ 0.3 Half closed		
4	2D Triangular @ 0.1 closed		

Table 4.5 Annual glare simulation (3D Triangular Facade system)

S/N	Shading State	Shading geometry	Annual Glare Simulation
1	3D Triangular @ 45 open		
2	3D Triangular @ 30 Half-open		
3	3D Triangular @ 15 Half closed		
4	3D Triangular @ 0 closed		

The 2D Diamond façade system was simulated for annual glare simulation. The glare simulation results for the six shading states were presented in Table 4.6. Shading states 1 and 2 reduced the perceptible glare but not the intolerable glare. Shading state 3 partly reduced most of the perceptible glare. Furthermore, intolerable glare was not eliminated in shading state 3. Shading state 4 demonstrated the least performance in reducing both the perceptible and the intolerable glare. Shading states 5 and 6 reduced the majority of the perceptible glare and partly the intolerable glare.

The shading states of the 3D Diamond façade system were also simulated for annual glare. As illustrated in Table 4.7, Shading states 1,2, and 3 eliminated perceptible glare and reduced intolerable glare. Shading state 4 performed poorly in reducing both perceptible and intolerable glare. Shading states 5 and 6 eliminated perceptible glare and reduced intolerable glare.

Table 4.6 Annual glare simulation (2D Diamond facade system)

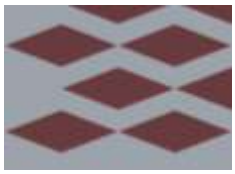
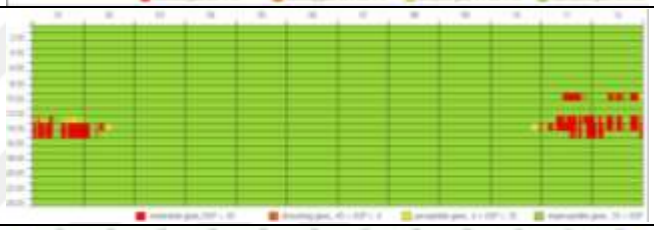
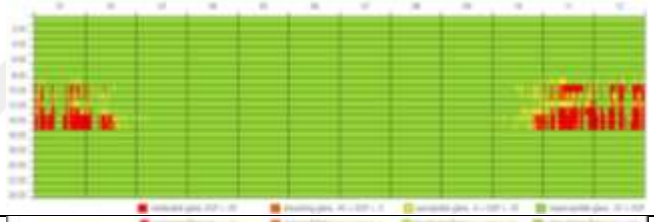
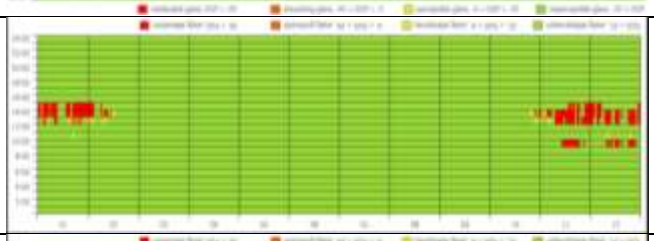
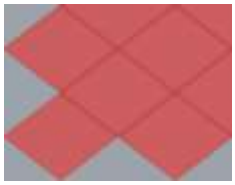
S/N	Shading State	Shading geometry	Annual Glare Simulation
1	2D Diamond @ 150 Half-open		
2	2D Diamond @ 120 open		
3	2D Diamond @ 90 open		
4	2D Diamond @ 60 Half closed		
5	2D Diamond @ 30 closed		
6	2D Diamond @ 0 closed		

Table 4.7 Annual glare simulation (3D Diamond facade system)

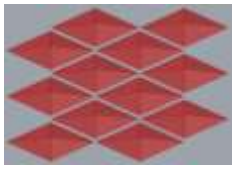
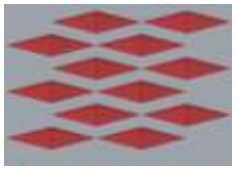
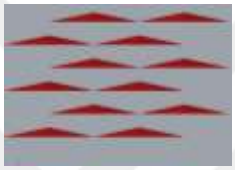
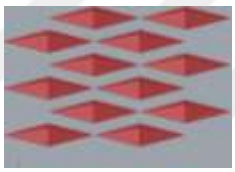
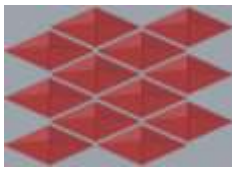
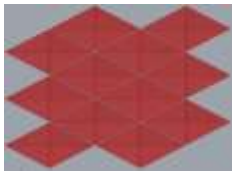
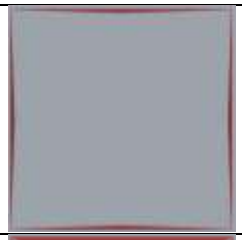
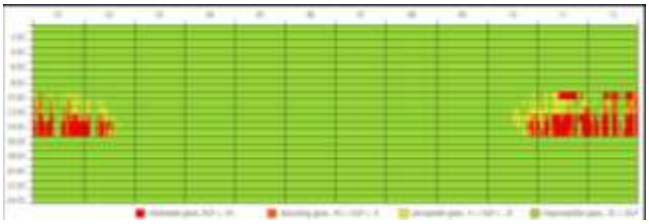
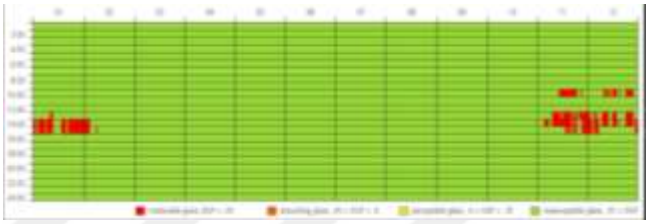
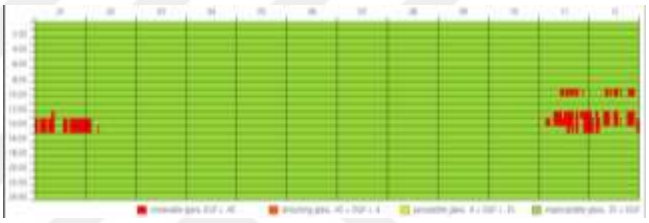
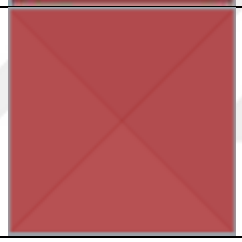
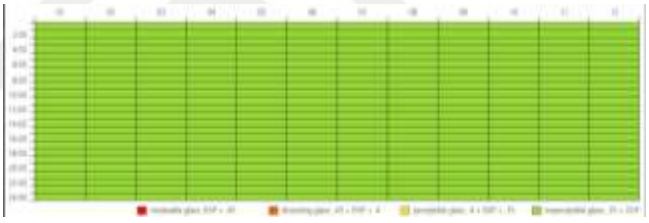
S/N	Shading State	Shading geometry	Annual Glare Simulation
1	3D Diamond @ 150 Half-open		
2	3D Diamond @ 120 open		
3	3D Diamond @ 90 open		
4	3D Diamond @ 60 Half closed		
5	3D Diamond @ 30 closed		
6	3D Diamond @ 0 closed		

Table 4.8. illustrates the shading geometry, the shading states, and the annual glare simulation result for the 2D Square façade system. Shading state 1 had a little effect in reducing both perceptible and intolerable glare as shown in Table 4.8. Shading states 2 and 3 eliminated the perceptible glare but not the intolerable glare. Shading state 4 completely protected the occupants of the office space from experiencing glare.

Table 4.8 Annual glare simulation (2D Square facade system)

S/N	Shading State	Shading geometry	Annual Glare Simulation
1	2D square @ 90 open		
2	2D square @ 60 Half-open		
3	2D square @ 30 Half closed		
4	2D square @ 0 closed		

The 3D Square façade system was simulated for annual glare simulation. The shading states, shading geometries, and annual glare simulation are presented in Table 4.9. Shading state 1 slightly reduced the perceptible and intolerable glare. Shading states 2 and 3 eliminated perceptible glare and reduced the intolerable glare. Shading state 4 eliminated both the perceptible and the intolerable glare.

Table 4.9 Annual glare simulation (3D Square facade system)

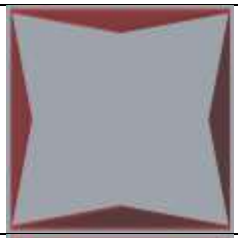
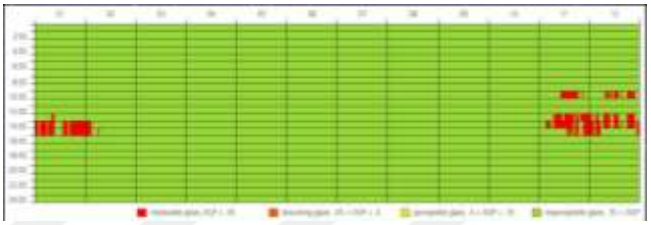
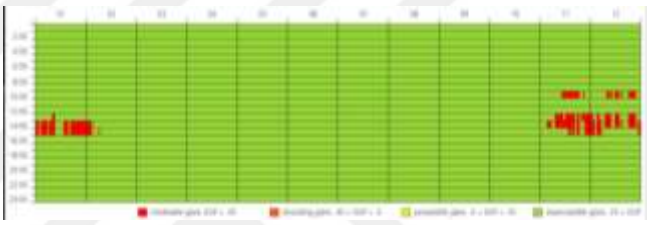
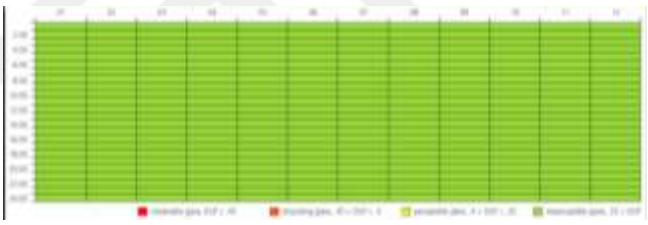
S/N	Shading State	Shading geometry	Annual Glare Simulation
1	3D square @ 45 open		
2	3D square @ 30 Half-open		
3	3D square @ 15 Half closed		
4	3D square @ 0 closed		

Table 4.10 presents the overall annual glare simulation results for all AFSs. The annual glare simulations from all the shading states of each AFS were combined into a annual glare shading simulation. These annual glare shading simulation results were used to generate the shading control as illustrated in Table 4.13. The annual glare simulation with shading results showed the performance of each AFS in glare management. 2D Circular AFS was able to reduce the 12.1 DGP recorded from the annual glare simulation of the base case model *(Reference office)* to 4.5 DGP. 2D Diamond and 3D Diamond AFS reduced the DGP to 3.7 and 3.4 respectively. the remaining AFSs (3D Circular, 2D Triangular, 3D Triangular, 2D Square, and 3D Square) successfully reduced the DGP to 0%. In regard to view, an important aspect of visual comfort, all AFSs recorded 77% of uninterrupted view i.e., the AFSs were open and allow for the office occupant's visibility of the outdoor environment.

Table 4.10. Annual Glare Simulation with Shading

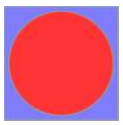
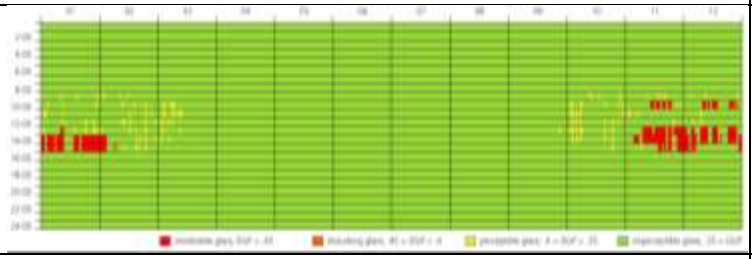
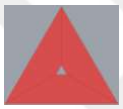
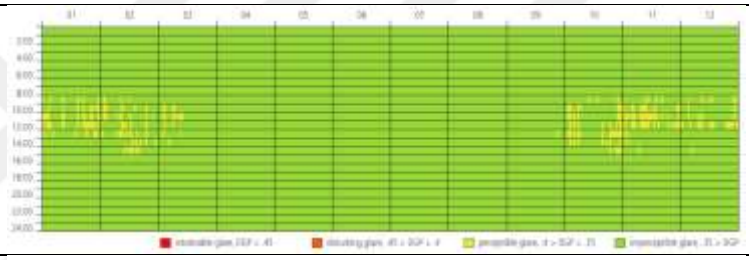
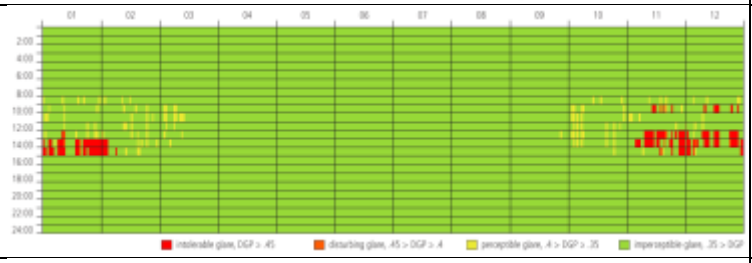
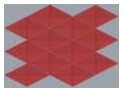
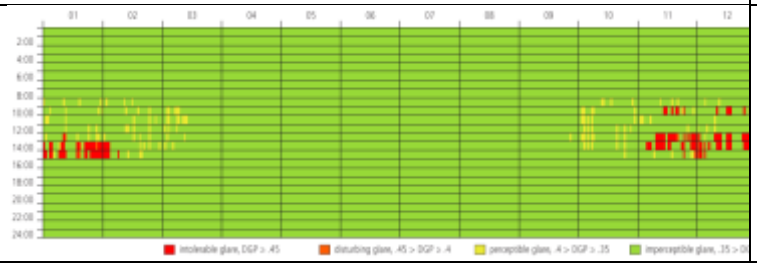
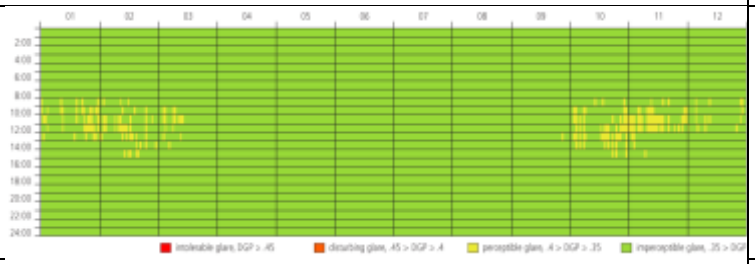
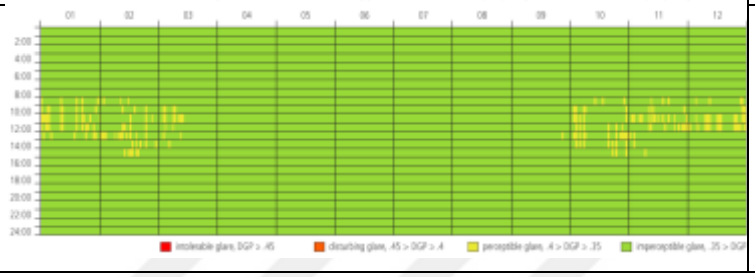
S/N	Shading State	Shading geometry	Annual Glare Simulation with Shading	DGP
1	2D Circular			4.5
2	3D Circular			0
3	2D Triangular			0
4	3D Triangular			0
5	2D Diamond			3.7
6	3D Diamond			3.4

Table 4.10. *continued*

S/N	Shading State	Shading geometry	Annual Glare Simulation with Shading	DGP
7	2D Square			0
8	3D Square			0

4.2. Daylight Autonomy Simulation Results

Daylight autonomy simulation was conducted for the base case model *(Reference office).* The sensors and calculation nodes for the office work plane were placed at a height of 0.9m. The distance between each calculation node was defined as 0.14m. The results from the simulation yielded a 46.29% of DA as presented in Figure 4.1.

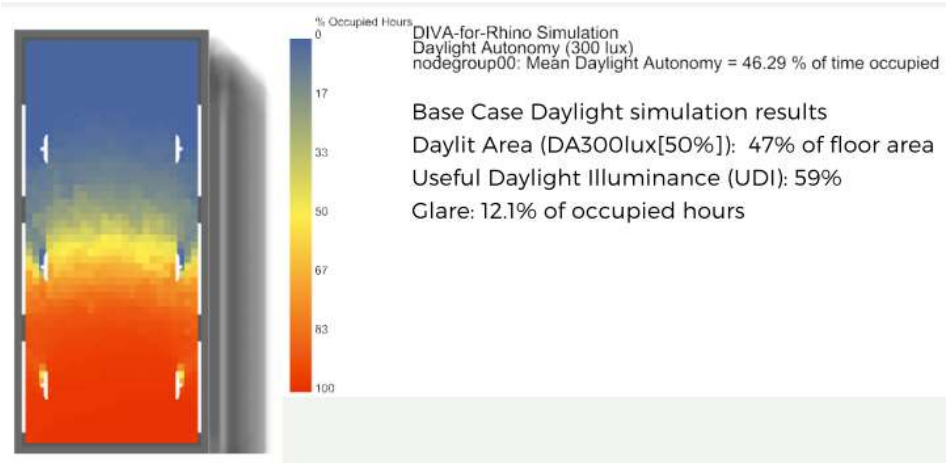


Figure 4.1. Base case (Reference office) Daylight autonomy simulation

Figure 4.2 represents the visualization of the base case model *(Reference office)* at a point in time showing the south window opening and occupant workstations. A false-color illuminance map was created to visualize the amount of illuminance in the interior space

(Figure 4.3). The DA simulation is a climate-based daylight metric simulation. The results analyzed in this study after the climate-based daylight metric simulations are; Daylight Autonomy, Daylit Area also known as Spatial Daylight Autonomy (sDA), and Useful Daylight Illuminance (UDI) all-inclusive in the DA simulation. Figure 4.1 also presents the results obtained after conducting a DA simulation on the base case model *(Reference office).* 47% of the floor area was daylit during 50% of the total occupied hours with a UDI and DA of 59% and 46.29% respectively.



Figure 4.2. Reference Office Point in time visualization

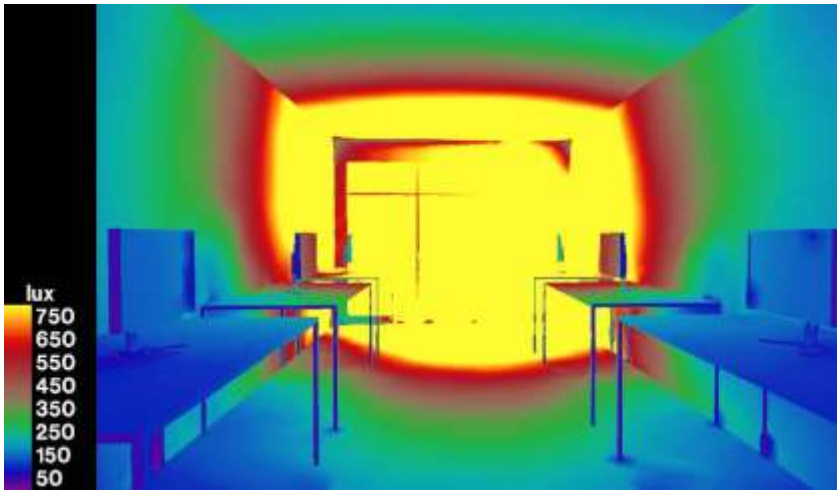


Figure 4.3. Reference Office false-color illuminance map

The DA simulations of the 2D and 3D AFSs were completed subsequent to the DGP simulations for each AFS and were presented in Section 4.1. Table 4.11 presents the results of the DA simulations, analyzed based on DA, sDA, and UDI. The 2D Circular AFS yielded

a 38.74% of DA, 42% of sDA, and a UDI of 52%. The 3D Circular AFS recorded a lower DA, and UDI of 34.22%, and 46% respectively in comparison to the 2D Circular AFS. The same sDA value of 42% was recorded for both the 2D and 3D Circular AFSs. The DA, sDA, and UDI results for the 2D Triangular AFS were 39.21%, 44%, and 53%, respectively. The DA of the 3D Triangular AFS was 39.61%, which was higher than the DA of the 2D Triangular AFS. The same result of sDA and UDI was recorded for both the 2D and 3D Triangular AFSs. DA of 38.41% was recorded for the 2D Diamond AFS. A value of 39.05% was recorded for the 3D Diamond AFS. The 2D Diamond recorded a higher UDI value of 50% compared to the 3D Diamond AFS with a UDI of 39%. Both 2D Diamond and 3D Diamond AFSs yielded the same value for sDA, 42%. 2D Square and 3D Square recorded the same values for sDA and UDI, which were 45% and 54% respectively. A DA of 40.41% was recorded for 3D Square AFS which was slightly higher than the 40.37% of DA for 2D Square AFS.

Table 4.11 Daylight Autonomy Simulations and Glare percentages

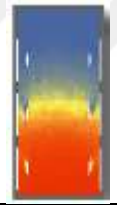
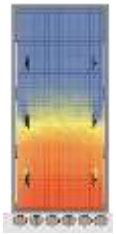
S/N	Shading state	DA	DA (%)	Daylit Area	UDI
1	Base Case		46.29	47	59
2	2D Circular		38.74	42	52
3	3D Circular		34.22	42	46
4	2D Triangular		39.21	44	53

Table 4.11. *continued*

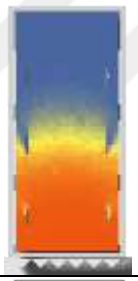
S/N	Shading state	DA	DA (%)	Daylit Area	UDI
5	3D Triangular		39.61	44	53
6	2D Diamond		38.41	42	50
7	3D Diamond		39.05	42	39
8	2D Square		40.37	45	54
9	3D Square		40.41	45	54

Figure 4.4 illustrates the compiled results from all the simulations conducted for the Base Case Model (*Reference Office*) and all the 2D and 3D AFSs.

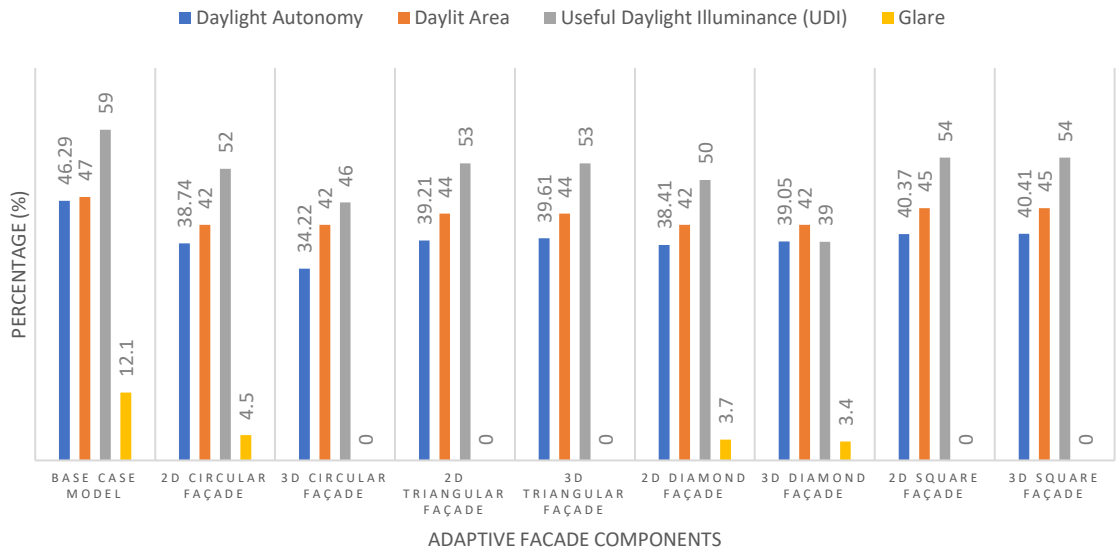


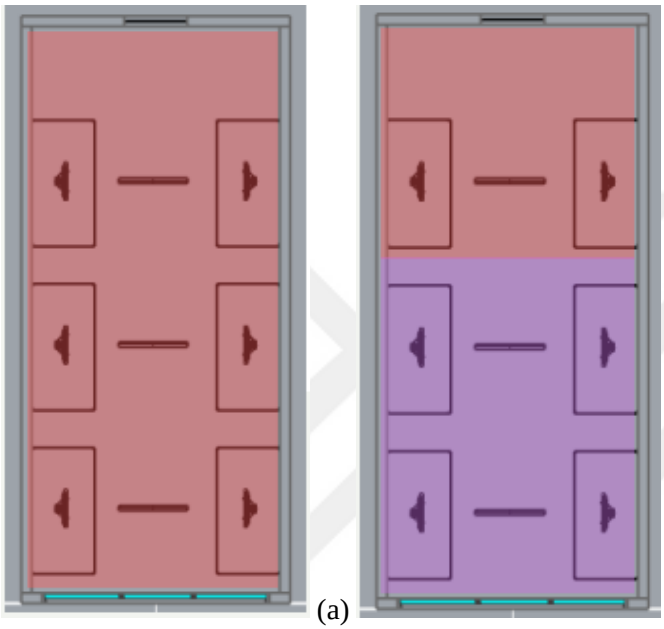
Figure 4.4. Compiled results of Daylight autonomy and glare simulations

4.3. Electric Lighting Simulation Results

The Reference office was simulated for Daylight Autonomy, the result shows that the work plane of users in the third row, farthest from the window (source of daylight) was underlit (no daylight). Such finding would be interpreted that occupants would refer to artificial lighting for visual comfort. The electric light (Figure 4.7) was introduced and was deemed necessary for the office space. The electric lights were placed at 3 intervals to illuminate the work planes in times of inadequate daylight or in the absence of it. A semi-direct light distribution fixture was selected for the lighting of the work planes as presented in Table 3.3. Surface-mounted light fixtures were selected for the hypothetical office space. Figure 4.8 presents the false-color illuminance map showing each workstation being fully illuminated by the artificial lighting at nighttime.

Light strategies were studied to generate a better electric lighting combination that will provide the required illuminance and be energy efficient for the office space. These strategies constitute various control systems and use photosensors to detect when the electric fixtures would switch on/off based on the occupancy schedule. The following light strategies were studied, and the selected strategy was based on the best performance for energy use:

Lighting strategy 1 - single group (Manual control_on/off switch): The single group lighting strategy (Figure 4.5 - a) was simulated for a year and the predicted annual electric lighting energy use is 318.2 kWh utilizing the manual control on/off switch. Figure 4.6 illustrates the manual control schedule for the lighting group 1. It shows that majority of the occupied period, the electric lighting fixtures are on and in use.



(a) (b)

Figure 4.5. Lighting strategies employed in the study, (a) single group lighting coverage, (b) split group lighting strategy

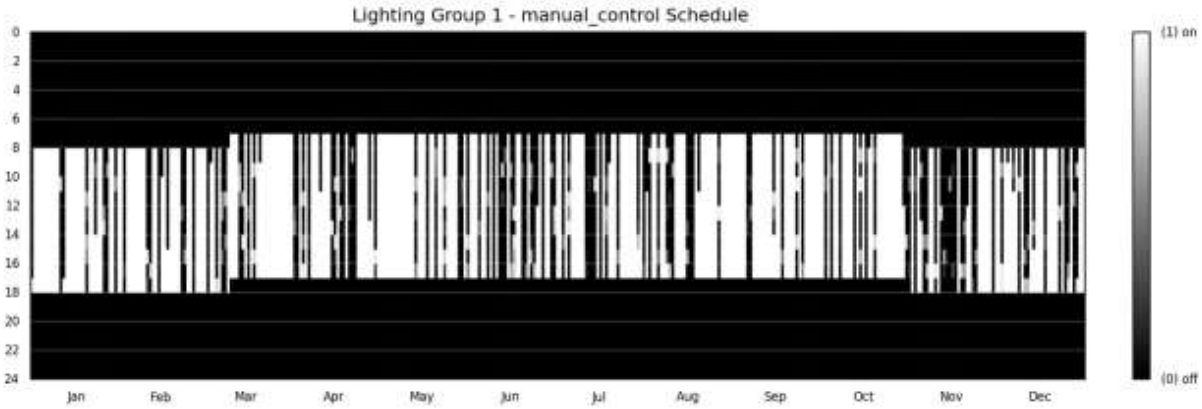


Figure 4.6. Manual control_on/off switch

Lighting strategy 2 - split group: The split group lighting strategy (Figure 4.5-b) utilizes two control systems to switch the lights on and off. The lighting fixtures of the first two rows of the work planes as colored in purple were controlled by occupancy sensors

combined with photosensors to dim the lights when the work planes were occupied, and the target illuminance level was acceptable. The work planes at the third row as colored in pink were controlled with an occupancy sensor to switch off when not occupied. Therefore, the predicted annual electric lighting energy use for the first two rows was 13.0 kWh, and the predicted annual electric lighting energy use for the Third row was 108.0 kWh. After simulating the lighting strategies, lighting strategy 1 consumed 318.2 kWh per annum, and lighting strategy 2 consumed 121.0 kWh. It is clear that lighting strategy 2 consumed less energy in comparison to lighting strategy 1. Therefore, lighting strategy 2 was adopted for the thermal simulation as it saved 62% of energy compared to lighting strategy 1.

Lighting strategy 2 was the suitable artificial lighting strategy for the present model and the results of the electric lighting simulations for the base case model *(Reference office)* and all the 2D and 3D AFSs were presented Table 4.12. Lighting group 2, with occupancy and photo sensors, consumed less electric energy for all cases (Table 4.12). Such finding was due to the utilization of daylight for most of the occupied office hours. Lighting group 1 presented higher energy consumption. This is due to the lack of daylight in that area of the office space. Lighting group 1 was assigned an occupancy sensor that detects when the work planes were not occupied and switches of the light. The base case consumed the least energy for artificial lighting. The most energy consumed for artificial lighting is the case of the 3D Circular AFS with energy use of 153.8 kWh compared to the 121.0 kWh energy use for artificial lighting of the base case model *(Reference office).*

Table 4.12. Electric lighting simulation results

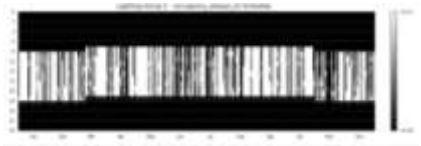
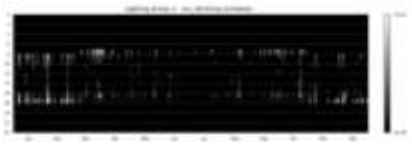
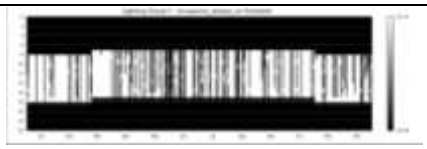
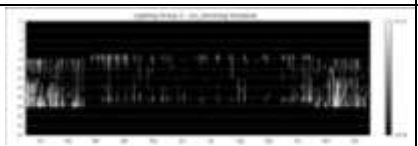
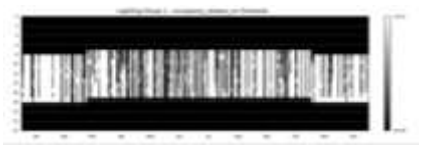
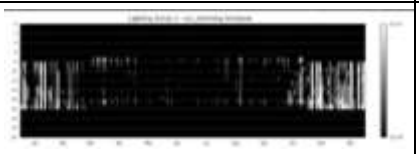
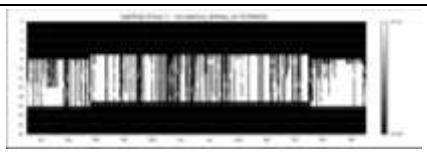
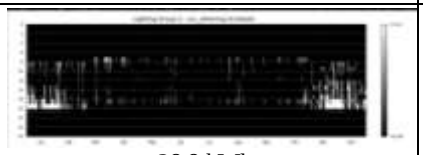
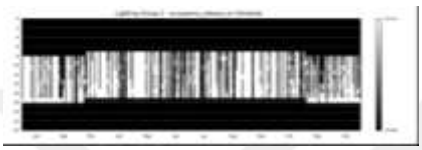
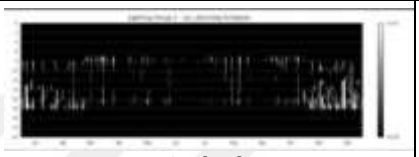
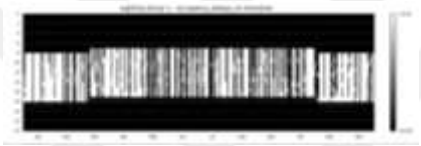
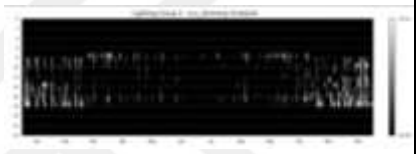
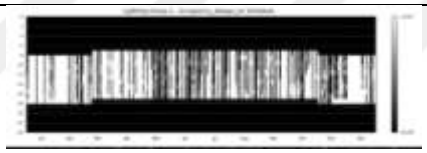
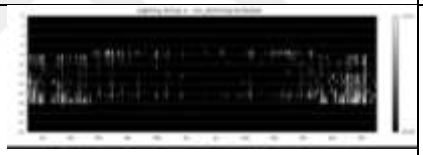
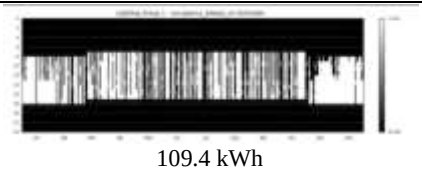
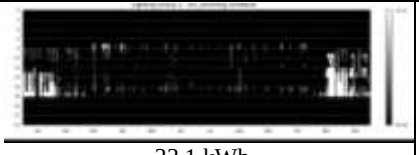
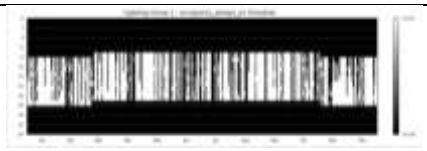
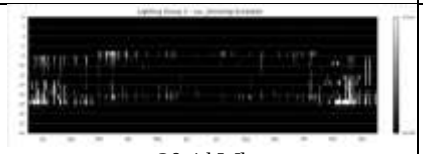
S/N	Shading State	Lighting group 1 (occupancy_always_on)	Lighting Group 2 (occ_dimming)	Energy Use per annum
1	Base case	 108.0 kWh	 13.0 kWh	121.0 kWh
2	2D Circular	 117.5 kWh	 31.1 kWh	148.6 kWh

Table 4.12. *continued*

S/N	Shading State	Lighting group 1 (occupancy_always_on)	Lighting Group 2 (occ_dimming)	Energy Use per annum
3	3D Circular	 110.6 kWh	 43.2 kWh	153.8 kWh
4	2D Triangular	 109.7 kWh	 28.8 kWh	138.5 kWh
5	3D Triangular	 108.5 kWh	 20.7 kWh	129.2 kWh
6	2D Diamond	 108.0 kWh	 22.5 kWh	130.5 kWh
7	3D Diamond	 109.0 kWh	 22.1 kWh	131.1 kWh
8	2D Square	 109.4 kWh	 33.1 kWh	142.5 kWh
9	3D Square	 110.3 kWh	 20.4 kWh	130.7 kWh

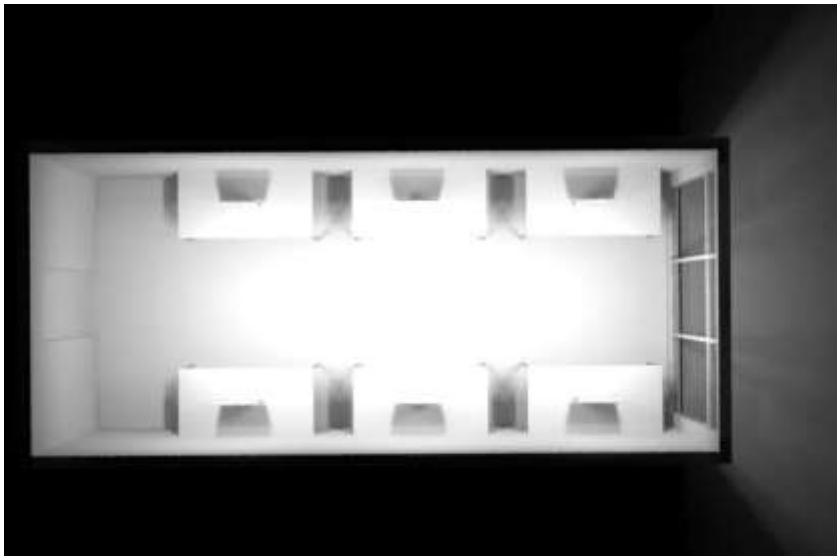


Figure 4.7. Office illumination through electric lights

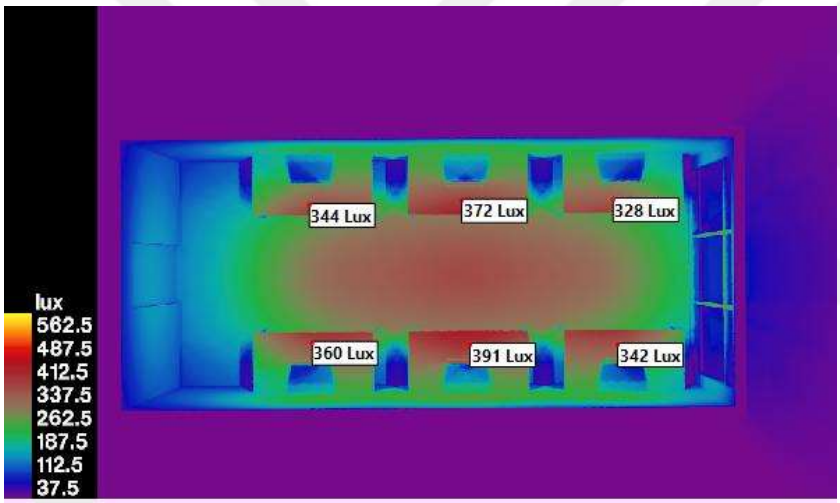
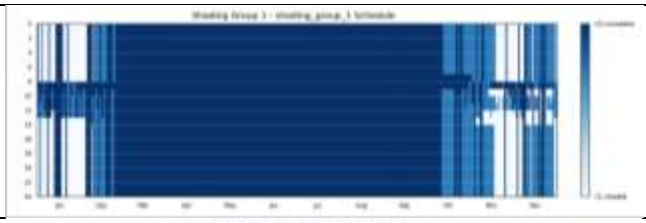
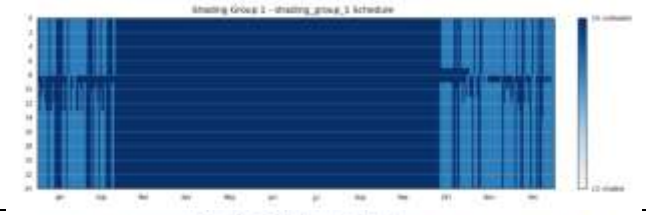
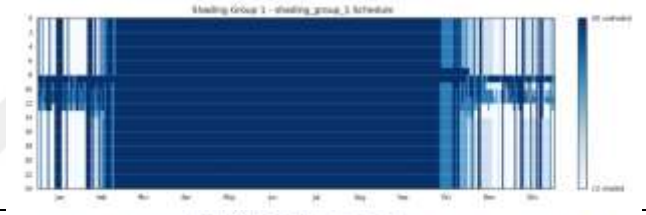
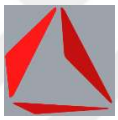
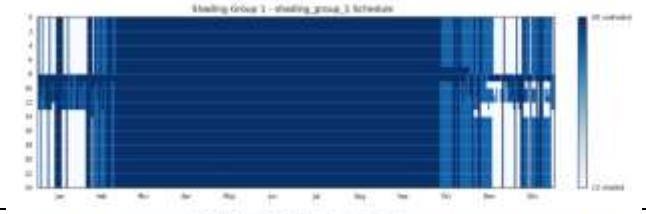
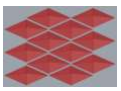
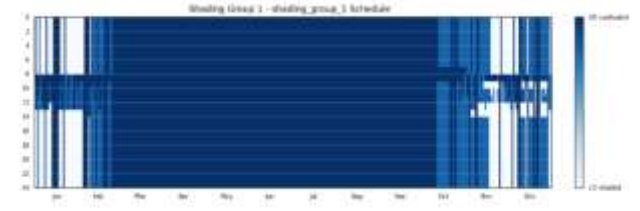
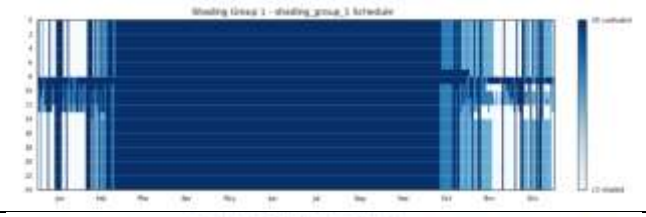
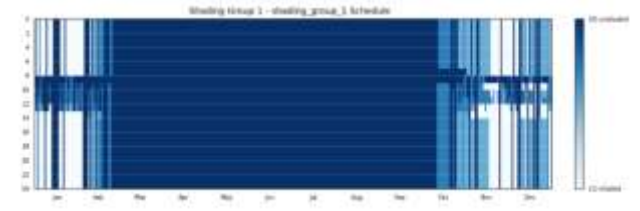


Figure 4.8. False color map of the office

4.4. Shading Control Results

The control shading control was simulated subsequent to the DGP and DA simulations for the base case and each AFSs. As illustrated in Table 4.13, the shading control schedule visualizes the shading states of each AFS, where dark blue refers to unshaded, white refers to shaded states. The hues between blue and white refers to a graduality in shading controls, where the shading state from unshaded to shaded was represented in the DIVA algorithm by (0) for unshaded and (1) for shaded.

Table 4.13 Shading Control Schedule

S/N	Shading State	Shading geometry	Shading Control Schedule
1	2D Circular		
2	3D Circular		
3	2D Triangular		
4	3D Triangular		
5	2D Diamond		
6	3D Diamond		
7	2D Square		
8	3D Square		

4.5. Thermal Simulation Results

The thermal simulations were conducted to investigate the total energy consumption for heating and cooling loads. The energy model was a simplified geometry processed in EnergyPlus for thermal simulation as shown in Figure 3.17. The base case model *(Reference office)* was modeled as an office unit within a large office building.

4.5.1. Monthly Energy Use

The monthly energy use describes the energy consumption in kWh and the monthly end-use result, the energy consumed for lighting, equipment, Heating, and cooling loads were described in end-uses. Table 4.14 presents the monthly energy use for all the cases. The Base case model *(Reference office)* consumed the highest energy for cooling as a result of excessive solar gains. The 2D AFSs performed well in reducing the cooling loads compared to the base case model *(Reference office)*. But the 3D AFSs reduced the energy consumption for cooling more compared to the 2D AFSs, as seen in Figure 4.10. However, the base case model *(Reference office)* consumed less energy for heating loads in comparison to the 2D and 3D AFSs. This is due to the fact that the solar gains are reduced with the adaptive solar shading elements thus the heating loads increased.

Due to the presence of the AFS's geometry on the office façade, the amount of daylight entering the space is reduced. This increased the amount of energy consumption for electric lighting (Table 4.10). In all cases, the most amount of energy consumption falls within the summer months and Autumn (June-September) with cooling energy as consuming the most energy.

Table 4.14. Monthly Energy Use

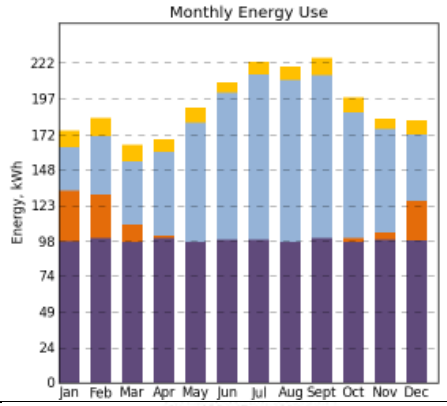
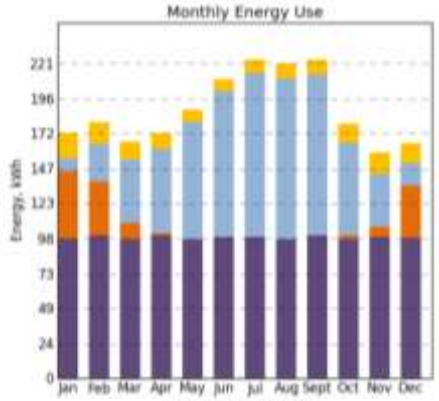
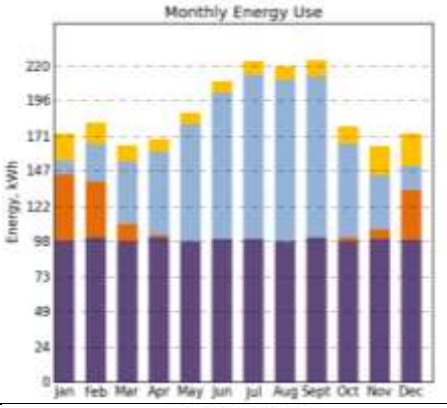
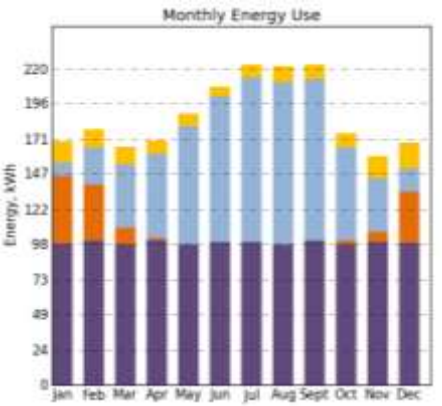
S/N	Shading State	Monthly Energy Use
		Legend: Equipment Energy, Heating Energy, Cooling Energy, Lighting Energy
1	Base case	
2	2D Circular	
3	3D Circular	
4	2D Triangular	

Table 4.14. *continued*

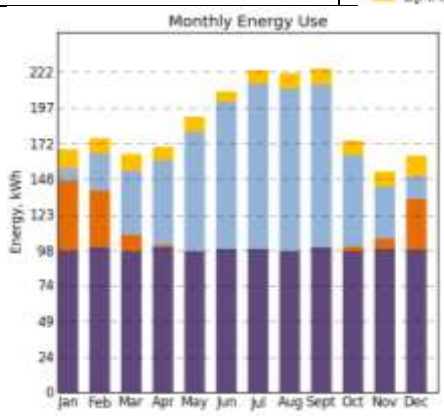
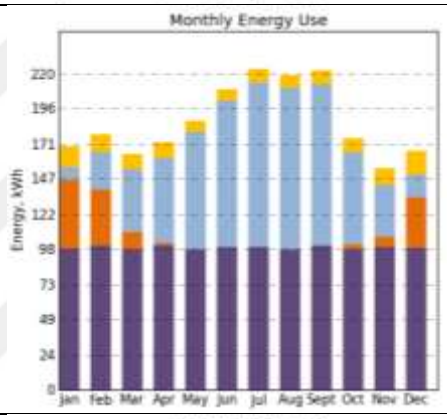
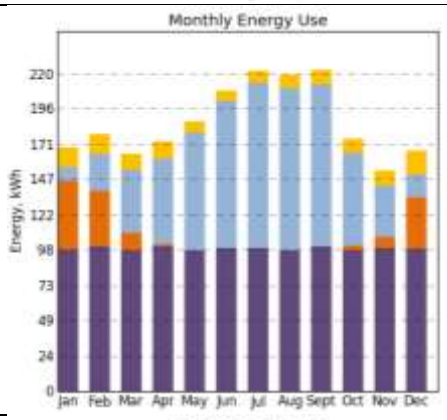
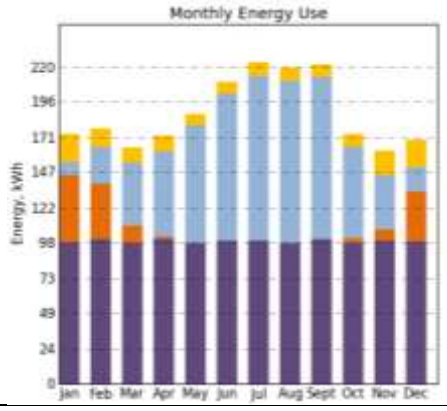
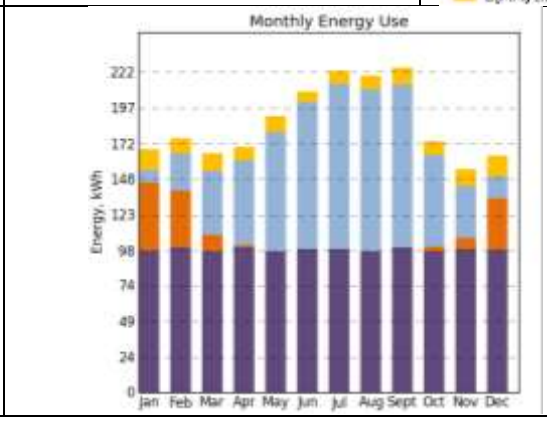
S/N	Shading State	Monthly Energy Use
		Legend
5	3D Triangular	
6	2D Diamond	
7	3D Diamond	
8	2D Square	

Table 4.14. *continued*

S/N	Shading State	Monthly Energy Use
		Legend
9	3D Square	

4.5.2. Heating and Cooling Energy Consumption

The heating and cooling energy consumption hourly maps (Table 4.15) present the annual energy consumed for heating and cooling. The colors depict the heating and cooling intensity, from red to blue which denotes heating and cooling, respectively. Furthermore, the graphs in Table 4.15 indicate that upon the occupancy of the office space, setpoint control system kicks in and consumption intensity could be observed from the map. Heating energy consumption for all cases was distinct between October and mid-April. The annual energy consumption for cooling the office space was higher compared to the energy used for heating in all cases. Figure 4.9 illustrates the reduction of annual cooling energy consumption of the base case model *(Reference office)* due to the introduction of the AFSs. Although, 2D and 3D AFSs both perform well in reducing the cooling load. The 3D AFSs perform better as described in Figure 4.9.

Table 4.15. Heating and cooling energy consumption

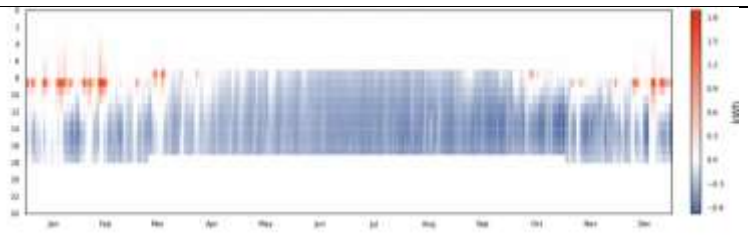
S/N	Shading State	Heating and Cooling Energy Consumption
1	Base case	

Table 4.15. *continued*

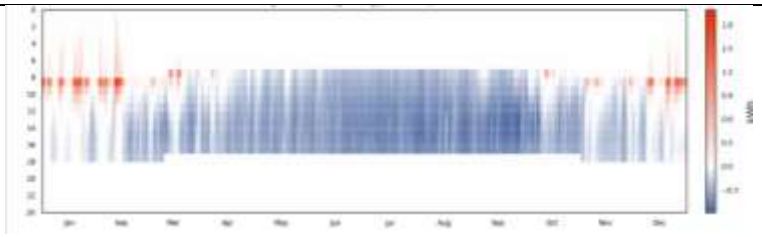
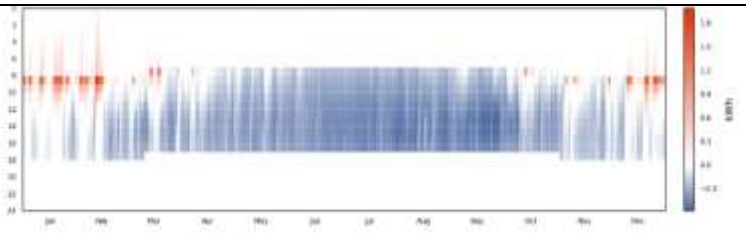
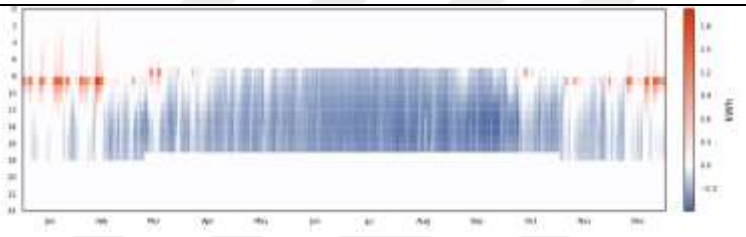
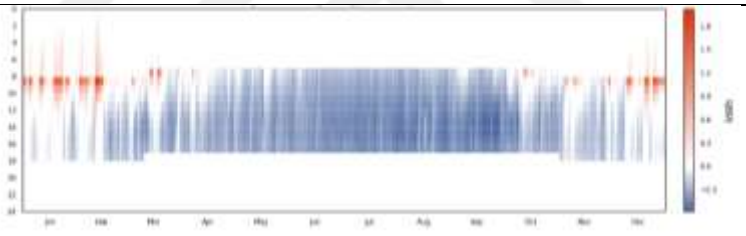
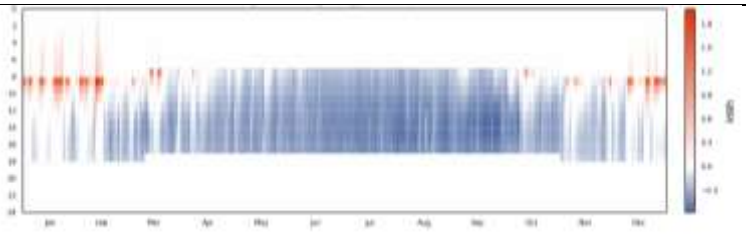
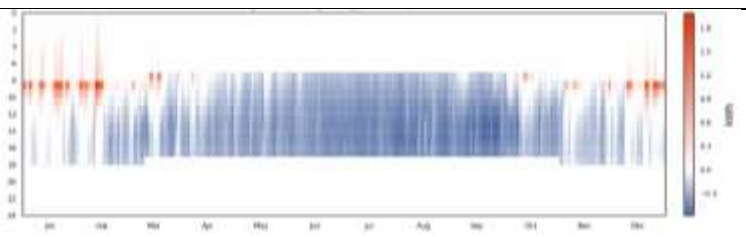
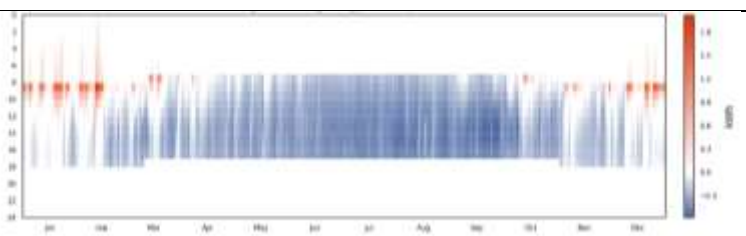
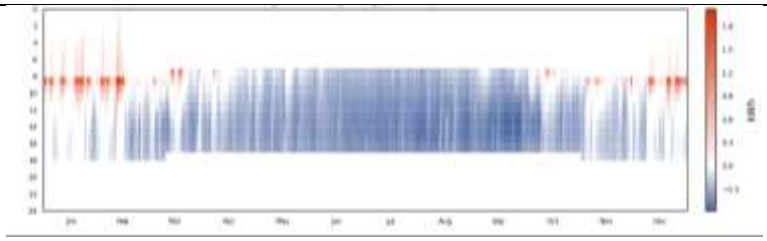
S/N	Shading State	Heating and Cooling Energy Consumption
2	2D Circular	
3	3D Circular	
4	2D Triangular	
5	3D Triangular	
6	2D Diamond	
7	3D Diamond	
8	2D Square	

Table 4.15. *continued*

S/N	Shading State	Heating and Cooling Energy Consumption
9	3D Square	

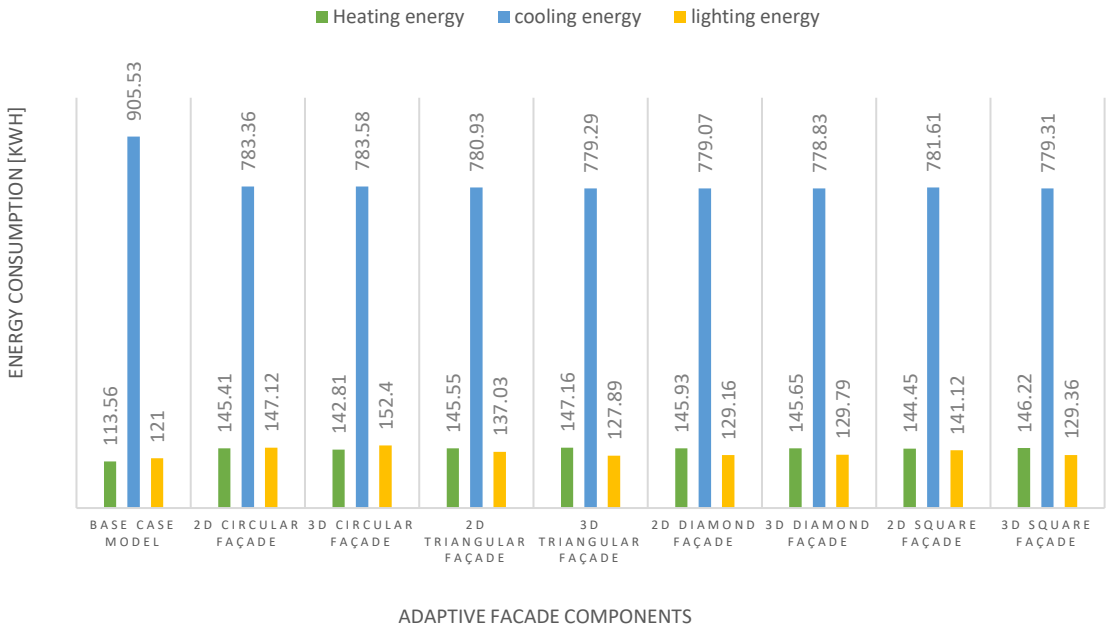


Figure 4.9. Heating, cooling, and lighting energy consumption

4.5.3. Energy use intensity (EUI)

EUI is the total annual building energy use divided by the gross floor area. the EUI may be expressed as a site energy EUI or a building energy EUI. Equation 4.1 was used to calculate the EUI of the Base case model (*Reference office*) and the 8 different AFS.

$$Energy\ Use\ Intensity\ (EUI) = \frac{total\ annual\ building\ energy\ (kWh)}{gross\ building\ area\ (m^2)} \qquad \text{Equation 4.1}$$

Accordingly, following results were obtained for:

Base case Model:

Interior Lights: Electricity [kWh](Hourly)	119.67
Interior Equipment: Electricity [kWh](Hourly)	1185.23
Heating: Energy Transfer [kWh](Hourly)	113.56
Cooling: Energy Transfer [kWh](Hourly)	905.53
Total annual building energy:	2323.99 kWh

$$\therefore\ EUI = \frac{2323.99\ kWh}{29.52\ m^2} = 78.73\ kWh/m^2/yr$$

2D Circular System:

Interior Lights: Electricity [kWh](Hourly)	147.12
Interior Equipment: Electricity [kWh](Hourly)	1185.23
Heating: Energy Transfer [kWh](Hourly)	145.41
Cooling: Energy Transfer [kWh](Hourly)	783.36
Total annual building energy:	2261.12 kWh

$$\therefore\ EUI = \frac{2261.12\ \ kWh}{29.52\ m^2} = 76.60\ kWh/m^2/yr$$

3D Circular System:

Interior Lights: Electricity [kWh](Hourly)	152.40
Interior Equipment: Electricity [kWh](Hourly)	1185.23
Heating: Energy Transfer [kWh](Hourly)	142.81
Cooling: Energy Transfer [kWh](Hourly)	783.58
Total annual building energy:	2264.02 kWh

$$\therefore\ EUI = \frac{2264.02\ \ kWh}{29.52\ m^2} = 76.70\ kWh/m^2/yr$$

2D Triangular System:

Interior Lights: Electricity [kWh](Hourly)	137.03
Interior Equipment: Electricity [kWh](Hourly)	1185.23
Heating: Energy Transfer [kWh](Hourly)	145.55
Cooling: Energy Transfer [kWh](Hourly)	780.93
Total annual building energy:	2248.74 kWh

$$\therefore\ EUI = \frac{2248.74\ \ kWh}{29.52\ m^2} = 76.20\ kWh/m^2/yr$$

3D Triangular System:

Interior Lights: Electricity [kWh](Hourly)	127.89
Interior Equipment: Electricity [kWh](Hourly)	1185.23
Heating: Energy Transfer [kWh](Hourly)	147.16
Cooling: Energy Transfer [kWh](Hourly)	779.29
Total annual building energy:	2239.57 kWh

$$\therefore\ EUI = \frac{2239.57\ \ kWh}{29.52\ m^2} = 75.90\ kWh/m^2/yr$$

2D Diamond System:

Interior Lights: Electricity [kWh](Hourly)	129.16
Interior Equipment: Electricity [kWh](Hourly)	1185.23
Heating: Energy Transfer [kWh](Hourly)	145.93
Cooling: Energy Transfer [kWh](Hourly)	779.07
Total annual building energy:	2239.40 kWh

$$\therefore\ EUI = \frac{2239.40\ \ kWh}{29.52\ m^2} = 75.90\ kWh/m^2/yr$$

3D Diamond System:

Interior Lights: Electricity [kWh](Hourly)	129.79
Interior Equipment: Electricity [kWh](Hourly)	1185.23
Heating: Energy Transfer [kWh](Hourly)	145.65
Cooling: Energy Transfer [kWh](Hourly)	778.83
Total annual building energy:	2239.50 kWh

$$\therefore\ EUI = \frac{2239.50\ \ kWh}{29.52\ m^2} = 75.90\ kWh/m^2/yr$$

2D Square System:

Interior Lights: Electricity [kWh](Hourly)	141.12
Interior Equipment: Electricity [kWh](Hourly)	1185.23
Heating: Energy Transfer [kWh](Hourly)	144.45
Cooling: Energy Transfer [kWh](Hourly)	781.61
Total annual building energy:	2252.41 kWh

$$\therefore\ EUI = \frac{2252.41\ \ kWh}{29.52\ m^2} = 76.30\ kWh/m^2/yr$$

3D Square System:

Interior Lights: Electricity [kWh](Hourly)	129.36
Interior Equipment: Electricity [kWh](Hourly)	1185.23
Heating: Energy Transfer [kWh](Hourly)	146.22
Cooling: Energy Transfer [kWh](Hourly)	779.31
Total annual building energy:	2240.12 kWh

$$\therefore\ EUI = \frac{2240.12\ kWh}{29.52\ m^2} = 75.90\ kWh/m^2/yr$$

Results from all the conducted simulations for the base case model *(Reference Office)* and all 2D and 3D AFSs were presented in Figure 4.11 indicated as the EUI. The EUI of the base case model *(Reference office)* was found to be 78.73 kWh/m^2 and this was the highest EUI among all simulated scenarios. The lowest EUI determined via simulation of the AFSs was 75.9 kWh/m^2. Three of the 3D AFS resulted with an EUI of 75.9 kWh/m^2 and only one 2D AFS yielded the same value. Once the 2D and 3D Circular AFS were compared, it was observed that the 2D AFS performed better with a difference of 0.11 kWh/m^2. The 3D Triangular AFS resulted with an EUI of 75.9 kWh/m^2, lower compared to the 76.2 kWh/m^2 EUI determined for the 2D AFS. for both the 2D and 3D Diamond AFSs an EUI of 75.9 kWh/m^2 EUI was identified. 3D Square AFS performed better compared to 2D Square AFS with a difference of 0.4 kWh/m^2 EUI.

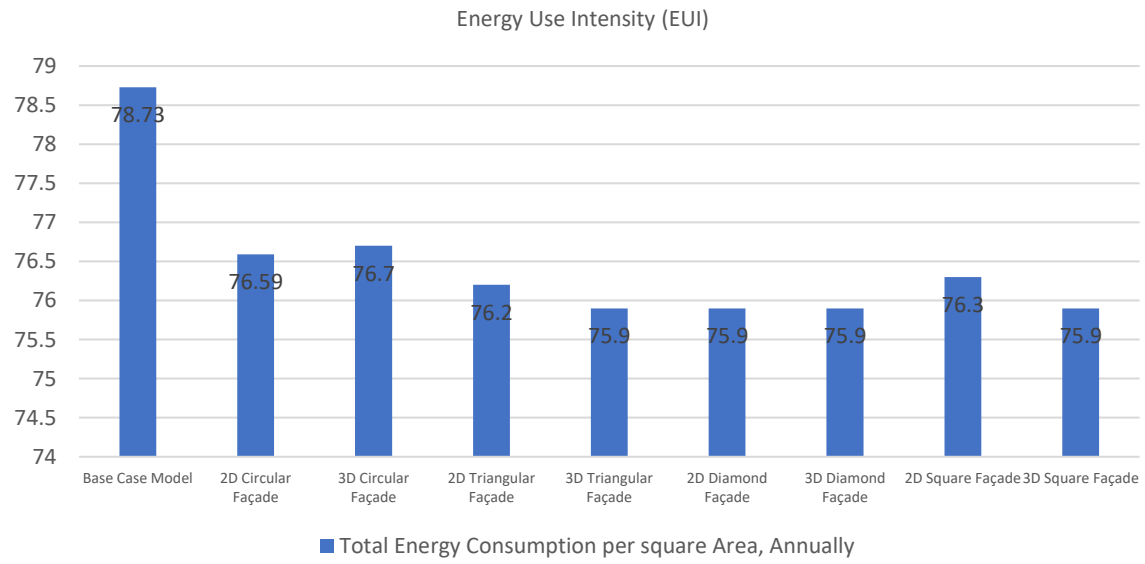


Figure 4.11. Energy Use Intensity (EUI) of the AFSs

5. CONCLUSION AND RECOMMENDATIONS

This study at its unset addressed the research questions outlined in the first chapter. The main research questions focused on evaluating the geometry and form of AFSs with respect to façade performance and the ability of AFSs to optimize visual and energy performance of buildings: “Does the geometry and form of an adaptive façade system affect the overall performance of a façade system” and “How can an AFS optimize the daylight levels, visual comfort, and reduce the solar gain of a building?”

The literature review informed the present thesis study with understanding the functions of a façade, the various typologies, purposes, technologies, and control systems of AFSs. Based on the knowledge gained due to the literature review, a design approach for AFSs was developed based on 2D and 3D AFSs to investigate their impact on daylight levels (DA, sDA, and UDI), visual comfort (View and glare), and energy performance (EUI).

The results as shown in Figure 4.4 illustrated Daylight levels for the modeled cases with adaptive façade systems (AFSs) on the south façade and the base case model *(Reference office)* without any shading devices. It was found that the AFSs affected the amount of daylight that penetrated the space and reduced solar gains. The main finding of the present study was outlined as, the 3D AFSs performed better compared to the 2D AFSs, except for the 3D Circular AFS in daylight availability (DA) simulations. Regarding glare (visual discomfort), all AFSs reduced the glare levels, except the 2D circular and both 2D and 3D Diamond AFSs. This is due to the presence of apertures between the components of the AFSs. The apertures could not successfully prevent direct sunlight from entering the office space. Furthermore, the entire AFSs reduced the EUI of the base case model *(Reference office)* as delineated in Figure 4.11.

Based on the second research question, which was formulated as: “How can an AFS optimize the daylight levels, visual comfort, and reduce the solar gain of a building?” it was found that AFSs were significantly beneficial various climates and building types. AFSs are

employed on buildings not just to respond to outdoor climatic fluctuations but also to control indoor comfort requirements. It is also important to state the benefits of conducting a building performance evaluation study for design projects at the initial stages. This can be time-saving, prevent errors and provide desirable results.

This study presented a research approach towards investigating the performance of AFSs in the optimization of daylight levels, visual comfort, and energy efficiency. It is expected that the study will contribute to the field of adaptive façades, daylighting designs and energy efficiency. Further studies might consider working with perforated and/or translucent materials and further examine daylight levels and glare studies for AFCs. Furthermore, to meet the European regulations and global reductions in energy consumption and carbon emission, incorporating energy generation features to adaptive façade components and systems is a notable research area for reducing the net energy consumption of buildings.

REFERENCES

Addington, D. M., and Schodek, D. L. (2005). *Smart materials and new technologies: for the architecture and design professions*: Routledge.

Addington, M. (2009). Contingent behaviours. *Architectural Design, 79*(3), 12-17.

Aelenei, L., Aelenei, D., Romano, R., Mazzucchelli, E., Marcin, B., and Rico-Martinez, J. M. (2018). *Case Studies - Adaptive Facade Network.*

Ahmed, M., Abdel-Rahman, A., Bady, M., and Mahrous, E. K. (2016). The thermal performance of residential building integrated with adaptive kinetic shading system. *International Energy Journal, 16*, 97-106.

Aizlewood, M., and Littlefair, P. (1994). Daylight prediction methods: A survey of their use.

Al-Ashwal, N. T., and Hassan, A. S. (2017). *The integration of daylighting with artificial lighting to enhance building energy performance.* Paper presented at the AIP Conference Proceedings.

Al-Obaidi, K. M., Ismail, M. A., and Abdul Rahman, A. M. (2015). Assessing the allowable daylight illuminance from skylights in single-storey buildings in Malaysia: a review. *International Journal of Sustainable Building Technology and Urban Development, 6*(4), 236-248.

Al-Obaidi, K. M., Ismail, M. A., and Abdul Rahman, A. M. (2016). Effective use of hybrid turbine ventilator to improve thermal performance in Malaysian tropical houses. *Building Services Engineering Research and Technology, 37*(6), 755-768.

Al-Obaidi, K. M., Ismail, M. A., Hussein, H., and Rahman, A. M. A. (2017). Biomimetic building skins: An adaptive approach. *An adaptive approach. Renewable and Sustainable Energy Reviews, 79*, 1472-1491.

Al Horr, Y., Arif, M., Kaushik, A., Mazroei, A., Katafygiotou, M., and Elsarrag, E. (2016). Occupant productivity and office indoor environment quality: A review of the literature. *Building and Environment, 105*, 369-389.

Alan, G. B. (2015). Henning Larsen's university building has a facade that moves in response to changing heat and light. Retrieved from https://www.dezeen.com/2015/07/14/henning-larsen-syddansk-universitet-sdu-kolding-campus-building-denmark-green-standards-university/

Ali, G., Bashir, M. K., and Ali, H. (2015). Housing valuation of different towns using the hedonic model: A case of Faisalabad city, Pakistan. *Habitat International, 50*, 240-249.

REFERENCES (continued)

Altomonte, S. (2008). Climate change and architecture: mitigation and adaptation strategies for a sustainable development. *Journal of Sustainable Development, 1*, 97-112.

Archdaily. (2010). BIX Light and Media Façade at MoMA. Retrieved from https://www.archdaily.com/89408/bix-light-and-media-facade-at-moma

Archdaily. (2012). Al Bahar Towers Responsive Facade / Aedas. Retrieved from https://www.archdaily.com/270592/al-bahar-towers-responsive-facade-aedas

Archdaily. (2013a). CH2 Melbourne City Council House 2 / DesignInc. Retrieved from https://www.archdaily.com/395131/ch2-melbourne-city-council-house-2-designinc

Archdaily. (2013b). Q1, ThyssenKrupp Quarter Essen / JSWD Architekten + Chaix and Morel et Associés. Retrieved from https://www.archdaily.com/326747/q1-thyssenkrupp-quarter-essen-jswd-architekten-chaix-morel-et-associes?ad_medium=gallery

Archilovers. (2018). Iconic Houses: Rietveld Schröder House. Retrieved from https://www.archilovers.com/stories/27133/iconic-houses-rietveld-schroder-house.html

Architecture Design, P. (2012). Flexibility vs. Polyvalence. *Desmystifying Architectural Design.* Retrieved from https://architecturedesignprimer.wordpress.com/2012/11/09/flexibility-vs-polyvalence/

Architecture, T. i. (2018). Homeostatic Facade. Retrieved from https://technologyinarchitecture.com/homeostatic-facade/

Architizer. (2007). Yale Sculpture Building and School of Art Gallery New Haven, CT, United States. Retrieved from https://architizer.com/projects/yale-sculpture-building-and-school-of-art-gallery/

Archtoolbox. (2021). Recommended Lighting Levels in Buildings. Retrieved from https://www.archtoolbox.com/materials-systems/electrical/recommended-lighting-levels-in-buildings.html

Aries, M. B., Veitch, J. A., and Newsham, G. R. (2010). Windows, view, and office characteristics predict physical and psychological discomfort. *Journal of environmental psychology, 30*(4), 533-541.

Ascione, F., Bellia, L., Mazzei, P., and Minichiello, F. (2010). Solar gain and building envelope: the surface factor. *Building Research and Information, 38*(2), 187-205.

REFERENCES (continued)

ASHRAE. (2010). *ASHRAE_STANDARD 90.1*. 1791 Tullie Circle NE Atlanta, GA 30329: Standing Standard Project Committee.

ASHRAE_211. (2018). *ASHRAE_STANDARD_211*. 1791 Tullie Circle NE Atlanta, GA 30329 Standing Standard Project Committee

Association Suisse des Electriciens. (1989). Éclairage intérieur par la lumičre du jour. *Association Suisse Des Electriciens, Swiss Norm SN 418911, Zurich*.

Athienitis, A., and Tzempelikos, A. (2002). A methodology for simulation of daylight room illuminance distribution and light dimming for a room with a controlled shading device. *Solar Energy, 72*(4), 271-281.

Ayoub, M. (2019). 100 Years of daylighting: A chronological review of daylight prediction and calculation methods. *Solar Energy, 194*, 360-390.

Birangal, G., Admane, D., and Shinde, S. S. (2015). Energy Efficiency Approach to Intelligent Building. *International Journal of Engineering Research, 4*, 389-393. doi:10.17950/ijer/v4s7/711

Bodart, M., and De Herde, A. (2002). Global energy savings in offices buildings by the use of daylighting. *Energy and Buildings, 34*(5), 421-429.

Boeke, J., Knaack, U., and Hemmerling, M. (2019). Superposition matrix for the assessment of performance-relevant adaptive façade functions. (2), 1-20%V 27. doi:10.7480/jfde.2019.2.2463

Böke, J., Knaack, U., and Hemmerling, M. (2019). State-of-the-art of intelligent building envelopes in the context of intelligent technical systems. *Intelligent buildings international, 11*(1), 27-45.

Böke, J., Knaack, U., and Hemmerling, M. (2020). Automated adaptive façade functions in practice-case studies on office buildings. *Automation in Construction, 113*, 103113.

Buğra, T. (2014). *Energy performance of smart buildings: simulating the impact of active systems and passive strategies.* (Masters Degree Practical), Middle East Technical University,The Graduate School Of Natural And Applied Sciences, Istanbul.

Bülow-Hübe, H. (2001). Energy-efficient window systems. Effects on energy use and daylight in buildings.

Carl, T., Schein, M., and Stepper, F. (2017). Sun Shades-About Designing Adaptable Solar Facades.

REFERENCES (continued)

Ćetković, A. J. T. A. (2012). Flexibility in architecture and its relevance for the ubiquitous house. *Technoetic Arts, 10*(2-3), 213-219.

CIBSE. (2005). Natural ventilation in non-domestic buildings. Applications Manual AM10:2005, London.

Climate Action Network, C. (2021, 22/03/2021). Revision of the Energy Performance of Buildings Directive. First input into the Commission's roadmap. Retrieved from https://caneurope.org/revision-energy-performance-buildings-directive/

Council, U. G. B. (2013). *LEED reference guide for building design and construction*: US Green Building Council.

Designing buildings. (2020). Solar gain in buildings. Retrieved from https://www.designingbuildings.co.uk/wiki/Solar_gain_in_buildings#:~:text=Solar%20gain%20is%20short%20wave,the%20fabric%20of%20the%20building.andtext=This%20results%20in%20heat%20accumulating,as%20the%20%27greenhouse%20effect%27.

Detail, I. (2011). Office Building in Cologne. Retrieved from https://inspiration.detail.de/office-building-in-cologne-108802.html?lang=en

Dienst, G. (2010). Cologne Oval Offices. Retrieved from https://structurae.net/en/media/161876-cologne-oval-offices

Dogan, T., and Reinhart, C. (2013). Automated conversion of architectural massing models into thermal 'shoebox'models. *Proceedings of BS*.

Dogan, T., and Reinhart, C. (2017). Shoeboxer: An algorithm for abstracted rapid multi-zone urban building energy model generation and simulation. *Energy and Buildings, 140*, 140-153.

EIA, U. E. I. A. (2017). Commercial buildings energy consumption survey. *EIA*.

Eisenbarth, C., Haase, W., Klett, Y., Blandini, L., and Sobek, W. (2021). Pneumatically Actuated Origami Sun Shading. *JOURNAL OF FACADE DESIGN and ENGINEERING, 9*(1), 16.

Elghazi, Y., Wagdy, A., and Abdalwahab, S. (2015). *Simulation driven design for kinetic system; optimize kaleidocycle façade configuration for daylighting adequacy in hot arid climates.* Paper presented at the Proceedings of BS2015: 14th Conference of International Building Performance Simulation Association.

REFERENCES (continued)

Elzeyadi, I. (2017). The impacts of dynamic façade shading typologies on building energy performance and occupant's multi-comfort. *Architectural Science Review, 60*(4), 316-324. doi:10.1080/00038628.2017.1337558

EN12665. (2011). *Light and lighting - Basic terms and criteria for specifying lighting requirements*. Brussel, Belgium.

EN. (2011). *Light and lighting - Lighting of work places - Part 1:Indoor work places. EN 12464- 1:2011*

Energy, U. D. O. (2011). Buildings energy data book. In: US Department of Energy.

EnergyPlus. (2020). Weather Data. Retrieved from https://energyplus.net/weather

Etheridge, D. (2010). Ventilation, air quality and airtightness in buildings. In *Materials for energy efficiency and thermal comfort in buildings* (pp. 77-100): Elsevier.

Favoino, F., Jin, Q., and Overend, M. (2014). Towards an ideal adaptive glazed façade for office buildings. *Energy Procedia, 62*, 289-298.

Ferguson, S., Siddiqi, A., Lewis, K., and de Weck, O. L. (2007). *Flexible and reconfigurable systems: Nomenclature and review*. Paper presented at the International Design Engineering Technical Conferences and Computers and Information in Engineering Conference.

Fiorito, F., Sauchelli, M., Arroyo, D., Pesenti, M., Imperadori, M., Masera, G., and Ranzi, G. (2016). Shape morphing solar shadings: A review. *Renewable and Sustainable Energy Reviews, 55*, 863-884.

Forty, A., and Forty, A. (2000). *Words and buildings: A vocabulary of modern architecture* (Vol. 268): Thames and Hudson London.

Frontczak, M., and Wargocki, P. (2011). Literature survey on how different factors influence human comfort in indoor environments. *Building and Environment, 46*(4), 922-937.

Furuto, A. (2012). Bloom / DO|SU Studio Architecture. Retrieved from https://www.archdaily.com/215280/bloom-dosu-studio-architecture?ad_source=searchandad_medium=search_result_all

Galasiu, A. D., Atif, M. R., and MacDonald, R. A. (2004). Impact of window blinds on daylight-linked dimming and automatic on/off lighting controls. *Solar Energy, 76*(5), 523-544.

REFERENCES (continued)

Galasiu, A. D., and Veitch, J. A. (2006). Occupant preferences and satisfaction with the luminous environment and control systems in daylit offices: a literature review. *Energy and Buildings, 38*(7), 728-742.

Goulthorpe, M. (2001). Aegis Hyposurface. *Routledge, New York*.

Group, U. E. R. (1994). Daylighting in Buildings Thermie.

Hansanuwat, R. (2010). *Kinetic facades as environmental control systems: using kinetic facades to increase energy efficiency and building performance in office buildings*: University of Southern California.

Hassan, A. S., and Al-Ashwal, N. T. (2015). Impact of building envelope modification on energy performance of high-rise apartments in Kuala Lumpur, Malaysia. *International Transaction Journal of Engineering, Management, and Applied Sciences and Technologies*, 91-105.

Hasselaar, B. L. H. (2013). *The Comfort Unit: Developed as Part of a Climate Adaptive Skin.* (Master of the Built Environment (Sustainable Development)), Technische Universiteit Delft,

Heidari Matin, N., and Eydgahi, A. (2019a). Factors affecting the design and development of responsive facades: a historical evolution. *Intelligent buildings international, 12*(4), 257-270.

Heidari Matin, N., and Eydgahi, A. (2019b). Technologies used in responsive facade systems: a comparative study. *Intelligent buildings international*, 1-20.

Heiselberg, P., Brohus, H., Hesselholt, A., Rasmussen, H., Seinre, E., and Thomas, S. (2009). Application of sensitivity analysis in design of sustainable buildings. *Renewable Energy, 34*(9), 2030-2036.

Hellinga, H. I. (2010). Daglicht en uitzicht. FACET. *Facade als Adaptief Comfortverhogend en Energiebesparend Toekomstconcept*.

Hensen, J. L., and Lamberts, R. (2012). *Building performance simulation for design and operation*: Routledge.

Hertzberger, H. (2005). *Lessons for students in architecture* (Vol. 1): 010 Publishers.

Hosseini, S. M., Ghiaci, M., Kulinich, S. A., Wunderlich, W., Monjezi, B. H., Ghorbani, Y., . . . Koupaei, A. J. (2020). Au-Pd nanoparticles enfolded in coil-like TiO2 immobilized on carbon fibers felt as recyclable nanocatalyst for benzene oxidation under mild conditions. *Applied Surface Science, 506*.

REFERENCES (continued)

Hosseini, S. M., Mohammadi, M., and Guerra-Santin, O. (2019). Interactive kinetic facade: Improving visual comfort based on dynamic daylight and occupant's positions by 2D and 3D shape changes. *Building and Environment, 165*.

Hövels, J. (2007). The Open Modular Façade Concept Master thesis. *TU Delft*, 128.

Howard, D. (1989). The future of ancient light. *Journal of Architectural and Planning Research, 6*(2), 132-153.

Hraska, J. (2018). Adaptive solar shading of buildings. *International Review of Applied Sciences and Engineering, 9*(2), 107-113.

Huovila, P. (2007). *Buildings and climate change: status, challenges, and opportunities*: UNEP/Earthprint.

IECC. (2021). 2021 International Energy Conservation Code (IECC). Retrieved from https://codes.iccsafe.org/content/IECC2021P1/chapter-4-ce-commercial-energy-efficiency#IECC2021P1_CE_Ch04_SecC405

Ihm, P., Nemri, A., and Krarti, M. (2009). Estimation of lighting energy savings from daylighting. *Building and Environment, 44*(3), 509-514.

Isenstadt, S., Petty, M. M., and Neumann, D. (2014). *Cities of light: Two centuries of urban illumination*: Routledge.

Jakubiec, J. A., and Reinhart, C. F. (2012). The 'adaptive zone'–A concept for assessing discomfort glare throughout daylit spaces. *Lighting Research and Technology, 44*(2), 149-170.

Kazanasmaz, T., Günaydin, M., and Binol, S. (2009). Artificial neural networks to predict daylight illuminance in office buildings. *Building and Environment, 44*(8), 1751-1757.

Kerr, R. (1865). *On ancient lights: and the evidence of surveyors thereon: with tables for the measurement of obstructions*: J. Murray.

Kevin, R. (2012). Appreciating Richard Neutra's Hall of Records. Retrieved from http://www.laobserved.com/archive/2012/08/appreciating_richard_neut.php

Kevin, V. D. W., and Alen, M. (2016). Annual Daylighting Performance Metrics, Explained. Retrieved from https://www.architectmagazine.com/technology/lighting/annual-daylighting-performance-metrics explained_o#:~:text=Spatial%20Daylight%20Autonomy%20(sDA)%20examines,on%20the%20horizontal%20work%20plane.

REFERENCES (continued)

Khajehzadeh, I., Vale, B. (2017). How New Zealanders distribute their daily time between home indoors, home outdoors and out of home. *Kōtuitui: New Zealand Journal of Social Sciences Online, 12*(1), 17-31.

Khoo, C. K., and Salim, F. D. (2013). *Lumina: a soft kinetic material for morphing architectural skins and organic user interfaces.* Paper presented at the Proceedings of the 2013 ACM international joint conference on Pervasive and ubiquitous computing.

Klein, T. (2013). Integral Facade Construction: Towards a new product architecture for curtain walls. 1-298.

Knaack, U., Klein, T., Bilow, M., and Auer, T. (2014). Principles of Construction. In *Façades* (pp. 1-133): Birkhäuser.

Knaack, U., Luible, A., Overend, M., Aelenei, L., Perino, M., Wellershof, F., and Brzezicki, M. (2015). *Adaptive facade network Europe.*

Knol, A., Kneepkens, S., and Zvironaite, K. (2014). Kinetica: A playful way through the world of moving facades. *Student working paper voor het vak AR0531 Innovation and Sustainability*.

Koene, F., Bakker, L., Lanceta, D., Narmsara, S., P, S., and Fraunhofer, I. (2014). Simplified building model of districts. *Proceedings of BauSIM*.

Koo, H.-J., and Velev, O. D. (2013). Regenerable photovoltaic devices with a hydrogel-embedded microvascular network. *Scientific reports, 3*(1), 1-6.

Košir, M. (2016). Adaptive building envelope: an integral approach to indoor environment control in buildings. *Automation and Control Trends, eds P. Ponce, AM Gutierrez, LM Ibarra (InTech)*, 121-148.

Krarti, M., Erickson, P. M., and Hillman, T. C. (2005). A simplified method to estimate energy savings of artificial lighting use from daylighting. *Building and Environment, 40*(6), 747-754.

Lechner, N. (2015). *HEATING, COOLING, LIGHTING Sustainable Design Methods for Architects*. Hoboken, New Jersey.Published simultaneously in Canada: John Wiley and Sons, Inc.

Leech, J. A., Nelson, W. C., Burnett, R. T., Aaron, S., and Raizenne, M. E. (2002). It's about time: a comparison of Canadian and American time–activity patterns. *Journal of Exposure Science and Environmental Epidemiology*, *12*(6), 427-432.

REFERENCES (continued)

Leupen, B. J. N. (2013). Polyvalence, a concept for the sustainable dwelling. *19*(3).

Li, D. H., and Lam, J. C. (2001). Evaluation of lighting performance in office buildings with daylighting controls. *Energy and Buildings, 33*(8), 793-803.

Li, D. H., and Lam, J. C. (2003). An investigation of daylighting performance and energy saving in a daylit corridor. *Energy and Buildings, 35*(4), 365-373.

Littlefair, P. (2001). Daylight, sunlight and solar gain in the urban environment. *Solar Energy, 70*(3), 177-185. doi:10.1016/S0038-092x(00)00099-2

Loonen, R., Rico-Martinez, J., Favoino, F., Brzezicki, M., Menezo, C., La Ferla, G., and Aelenei, L. (2015). *Design for façade adaptability–Towards a unified and systematic characterization.* Paper presented at the Proc. 10th Energy Forum-Advanced Building Skins, Bern, Switzerland.

Loonen, R., Trčka, M., Cóstola, D., and Hensen, J. L. M. (2013). Climate adaptive building shells: State-of-the-art and future challenges. *Renewable and Sustainable Energy Reviews, 25*, 483-493. doi:https://doi.org/10.1016/j.rser.2013.04.016

López, M., Rubio, R., Martín, S., and Croxford, B. (2017). How plants inspire façades. From plants to architecture: Biomimetic principles for the development of adaptive architectural envelopes. *Renewable and Sustainable Energy Reviews, 67*, 692-703.

Mahmoud, A. H. A., and Elghazi, Y. (2016). Parametric-based designs for kinetic facades to optimize daylight performance: Comparing rotation and translation kinetic motion for hexagonal facade patterns. *Solar Energy, 126*, 111-127. doi:10.1016/j.solener.2015.12.039

Mamoru, I. (2009). POLA GINZA FACADE TOKYO. Retrieved from https://www.hoberman.com/portfolio/pola-ginza-facade-tokyo/

Masoudi, S. (2018). *Adaptive Façade Design for the Regulation of Visual Comfort.* (MSc. Architecture, Urbanism and Building Sciences), Delft University of Technology,

McNeel, R. (2010). Grasshopper-Generative Modeling with Rhino, McNeel North America, Seattle, USA. In.

Michael, C., Baechler, T., L., G., Cole., P. C., Marye G., H., and Kathi, R. (2015). *Guide to Determining Climate Regions by County*. Washington, DC: Pacific Northwest National Laboratory Retrieved from https://www.energy.gov/eere/buildings/downloads/building-america-best-practices-series-volume-73-guide-determining-climate

REFERENCES (continued)

Moloney, J. (2011). Designing Kinetics for Architectural Facades: State Change. *Designing Kinetics for Architectural Facades: State Change*, 1-178.

Moon, P., and Spencer, D. (1942). Illumination from a non-uniform sky. *Illum. Engng, 37*, 707-726.

MVRDV. (2005). YPENBURG. Retrieved from https://www.mvrdv.nl/projects/152/ypenburg

Nabil, A., and Mardaljevic, J. (2005). Useful daylight illuminance: a new paradigm for assessing daylight in buildings. *Lighting Research and Technology, 37*(1), 41-57.

Nagy, Z., Svetozarevic, B., Jayathissa, P., Begle, M., Hofer, J., Lydon, G., . . . Schlueter, A. (2016). The Adaptive Solar Facade: From concept to prototypes. *Frontiers of Architectural Research, 5*(2), 143-156. doi:10.1016/j.foar.2016.03.002

Nejat, P., Jomehzadeh, F., Taheri, M. M., Gohari, M., and Majid, M. Z. A. (2015). A global review of energy consumption, CO2 emissions and policy in the residential sector (with an overview of the top ten CO2 emitting countries). *Renewable and Sustainable Energy Reviews, 43*, 843 - 862. doi:https://doi.org/10.1016/j.rser.2014.11.066

NWS, N. W. S. (2011). Summer2011Records. Retrieved from https://www.weather.gov/hgx/Summer2011Records

Ochoa, C. E., and Capeluto, I. G. (2008). Strategic decision-making for intelligent buildings: Comparative impact of passive design strategies and active features in a hot climate. *Building and Environment, 43*(11), 1829 - 1839. doi:https://doi.org/10.1016/j.buildenv.2007.10.018

Odeh, I., and Hussein, T. (2016). Activity pattern of urban adult students in an Eastern Mediterranean Society. *International journal of environmental research and public health, 13*(10), 960.

Oral, G. K., and Yilmaz, Z. (2003). Building form for cold climatic zones related to building envelope from heating energy conservation point of view. *Energy and Buildings, 35*(4), 383-388.

Parametrichouse. (2021). KAFD Spas Facade. Retrieved from https://parametrichouse.com/kafd-spas-facade/

Park, K.-W., and Athienitis, A. K. (2003). Workplane illuminance prediction method for daylighting control systems. *Solar Energy, 75*(4), 277-284.

REFERENCES (continued)

Pfeiffer, S. D. (1982). Ancient Lights: Legal Protection of Access to Solar Energy. *ABAJ, 68*, 288.

PTA. (2013). RMIT Design Hub. Retrieved from https://www.pta.com.au/projects/#s:education

Rawn, E. (2014). NBBJ Creates High Tech Shading System for Buildings. Retrieved from https://www.archdaily.com/540327/nbbj-creates-high-tech-shading-system-for-buildings?ad_medium=widgetandad_name=recommendation

Reinhart, C., and Davila, C. C. (2016). Urban building energy modeling–A review of a nascent field. *Building and Environment, 97*, 196-202.

Reinhart, C. F. (2014). *Daylight Handbook I*.

Reinhart, C. F., Jakubiec, J. A., and Ibarra, D. (2013). *DEFINITION OF A REFERENCE OFFICE FOR STANDARDIZED EVALUATIONS*.

Reinhart, C. F., Mardaljevic, J., and Rogers, Z. (2006). Dynamic daylight performance metrics for sustainable building design. *Leukos, 3*(1), 7-31.

Ring, A. L. (2017). "Polyvalent Adaptation": Design in a Temporal Context of Uncertain High-Risk Futures. *The Plan Journal, 2*(2), 185-209. doi: 10.15274/tpj.2017.02.02.19

Rogers, Z., and Goldman, D. (2006). Daylighting metric development using daylight autonomy calculations in the sensor placement optimization tool. *Boulder, Colorado, USA: Architectural Energy Corporation:*. Retrieved from http://www. archenergy. com/SPOT/SPOT_Daylight% 20Autonomy% 20Report. pdf.

Roth, L. (2015). IAAC student designs hydro-membrane textile for passive cooling. Retrieved from https://www.designboom.com/technology/hydro-membrane-luisa-roth-09-05-2015/

Sala, M., Gallo, C., and Sayigh, A. A. M. (1999). *Architecture - Comfort and Energy*: Elsevier Science.

Sargent, J. A., Niemasz, J., and Reinhart, C. F. (2011). *Shaderade: combining Rhinoceros and Energyplus for the design of static exterior shading devices.* Paper presented at the Proceedings of Building Simulation.

Scribd. (2021). Grasshopper. Retrieved from https://www.scribd.com/doc/251492246/Grasshoppert

REFERENCES (continued)

Smith, S. (2021). Articulated Cloud | Ned Kahn. Retrieved from https://www.arch2o.com/articulated-cloud-ned-kahn/

Solemma, L. (2020). DIVA-for-Rhino software version 4.0. Retrieved from https://www.solemma.com/diva

Solla, I. F. (2010, August 20). Facades: principles of construction - Ulrich Knaack. Retrieved from http://facadesconfidential.blogspot.com/2010/08/facades-principles-of-construction.html

Sullivan, R., Lee, E., and Selkowitz, S. (1992). A method of optimizing solar control and daylighting performance in commercial office buildings.

Trubiano, F. (2013). *Design and construction of high-performance homes: building envelopes, renewable energies and integrated practice*: Routledge.

Turan, I., Chegut, A., Fink, D., and Reinhart, C. (2020). The value of daylight in office spaces. *Building and Environment, 168*, 106503.

U.S., D. O. E. (2008). Energy efficiency trends in residential and commercial buildings. Retrieved from https://www1.eere.energy.gov/buildings/publications/pdfs/corporate/bt_stateindustry.pdf

U.S. General Services Administration. (2021). 6.15 Lighting. Retrieved from https://www.gsa.gov/node/82715

Velux. (2021). The many benefits of using daylight in buildings. Retrieved from https://www.velux.com/what-we-do/research-and-knowledge/deic-basic-book/daylight

Vinnitskaya, I. (2010). Kiefer Technic Showroom / Ernst Giselbrecht + Partner. Retrieved from https://www.archdaily.com/89270/kiefer-technic-showroom-ernst-giselbrecht-partner?ad_source=searchandad_medium=search_result_all

Visuallexicon. (2017). Arab World Institute – Jean Nouvel. Retrieved from https://visuallexicon.wordpress.com/2017/10/04/arab-world-institute-jean-nouvel/

Ward, G. J. (1994). *The RADIANCE lighting simulation and rendering system.* Paper presented at the Proceedings of the 21st annual conference on Computer graphics and interactive techniques.

REFERENCES (continued)

Waseef, A. A., and El-mowafy, B. N. (2017). *Towards a new classification for responsive kinetic facades.* Paper presented at the Proceedings of the memaryat international conference 'MIC.

WELL Certification. (2017). International WELL Building Institute.

WG1. (2018). WG1 Assessment. Retrieved from http://www.euroscitizen.eu/wg1-assessment/

WielAretsArchitects. (2014). Allianz Headquarters / Wiel Arets Architects. Retrieved from https://www.archdaily.com/489836/allianz-headquarters-wiel-arets-architects

Wigginton, M. (1996). *Glass in architecture*.

Willis, C. (1995). *Form follows finance: skyscrapers and skylines in New York and Chicago*: Princeton Architectural Press.

Wotton, E. (2000). *The IESNA Lighting Handbook and office lighting* (Vol. 14).

www.manfred-roeben.com. (2021). Duales System Deutschland AG. Retrieved from http://www.manfred-roeben.com/expo2000/exporeor.htm